

A STUDY OF ABIOTIC STRESS PROTECTING XYLOGLUCAN  
ENDOTRANSGLYCOSYLASE (XTH) GENES IN PLANTS



by  
Ezgi Türksever

Submitted to Graduate School of Natural and Applied Sciences  
in Partial Fulfillment of the Requirements  
for the Degree of Master of Science in  
Biotechnology

Yeditepe University  
2019

A STUDY OF ABIOTIC STRESS PROTECTING XYLOGLUCAN  
ENDOTRANSGLYCOSYLASE (XTH) GENES IN PLANTS

APPROVED BY:

Assist. Prof. Dr. Andrew John Harvey  
(Thesis Supervisor)  
(Yeditepe University)



Prof. Dr. Berna Sariyar Akbulut  
(Marmara University)



Assist. Prof. Dr. Bahar Soğutalmaz Özdemir  
(Yeditepe University)



DATE OF APPROVAL: .... / .... / 2019

## ACKNOWLEDGEMENTS

Firstly, I would like to express my special gratitude to my supervisor Assist. Prof. Andrew John Harvey for his invaluable assistance, support, guidance and patience. I was so lucky to involve in such a valuable project and work under a supervisor who always believed in me.

Secondly, I want to deeply thank to two person who were with me during this process. I would like to thank my dear project partner Dr. Burcu Gür for her friendship, great assistance and support during the project experiments and also a special thanks to Dr. Merve Seven who gave invaluable contributions to my academic knowledge and technical support during this process. Also, I want to thank Dr. Hülya Akdemir for her assistance during the experiments and her true friendship. I am appreciated for their help during the project. I would like to thank all my instructors and my fellows in Institute of Biotechnology for their instruction, advice and friendship.

Finally, I am sincerely grateful to my parents Leman Türksever and Tuna Türksever and my friend Erbil Bakır for their moral support during my thesis.

## ABSTRACT

### A STUDY OF ABIOTIC STRESS PROTECTING XYLOGLUCAN ENDOTRANSGLYCOSYLASE (XTH) GENES IN PLANTS

Xyloglucan endotransglycosylase/hydrolase (XTHs) enzymes which are found in the cell wall of all land plants, are recognized as cell-wall modifying enzymes having diverse roles during cell growth, maturation and response to external stresses. In many experiments, it was demonstrated that some of the *XTH* genes are upregulated during various abiotic stresses. In a recent work, it was shown that the heterologous over-expression of a hot pepper *XTH* gene increased the resistance to salt and drought stresses in *Arabidopsis* and tomato plants. This project aimed to examine a capsicum XTH enzyme (CaXTH2) at the genomic, transcriptomic and protein levels to get better insights about how those enzymes function and their roles under salt stress. Substrate specificity and enzyme characterization analyses show that unsubstituted xyloglucan was highly preferred by the CaXTH enzymes. CaXTH2 enzyme has shown the highest activity when tamarind seed xyloglucan (TXG) polysaccharide and XXXG (X7) oligosaccharide were used as donor-acceptor substrate couple. The next highest activity was shown when hydroxyethyl cellulose (HEC) was used as donor substrate with xyloglucan acceptor oligosaccharides. CaXTH2 enzyme gave activity with other oligosaccharides such as XT, CT, BB etc. with almost 0,1 percent of the TXG-XGO activity level, and this also supported that it had only low amounts of heterotransglycosylase activity. Different pepper varieties had been phenotypically observed and they showed susceptibility or tolerance under salt stress conditions. Genomic and transcriptomic analyses have demonstrated that *CaXTH2* gene was upregulated under salt stress conditions. However, *CaXTH2* does not seem to be directly responsible for the stress resistance. Nevertheless, this does not prove that *XTH* genes have no effect in stress tolerance under native promoters, but that they are likely to be part of a larger, more complex mechanism.

## ÖZET

### **BİTKİLERDE ABİYOTİK STRESE KARŞI KORUMA SAĞLAYAN KSİLOGLUKAN ENDOTRANSGLİKOSİLAZ (XTH) GENLERİ ÜZERİNE BİR ÇALIŞMA**

Tüm kara bitkilerinin hücre duvarında bulunan ksiloglukan endotransglükosilaz / hidrolaz (XTH) enzimleri, hücre büyümesi, olgunlaşması ve dış gerilmelere tepki de dahil olmak üzere çeşitli rollere sahip hücre duvarı değiştirici enzimler olarak kabul edilir. Birçok deneyde, bu *XTH* genlerinin bazılarının değişken abiyotik stresler sırasında indüklendiği gösterilmiştir. Yakın zamanda yapılan bir çalışmada, acı biber (*Capsicum annuum*) XTH geninin fazladan heterolog anlatımının, *Arabidopsis* ve domates bitkilerinde tuza ve kuraklık streslerine karşı direnci arttırdığı gösterilmiştir. Bu proje, bu enzimlerin nasıl çalıştığı ve tuz stresi altındaki rolleri hakkında daha iyi bilgi edinmek için genomik, transkriptomik ve protein seviyelerinde bir acı biber XTH enzimini (CaXTH2) incelemeyi amaçlamıştır. Substrat spesifikliği ve enzim karakterizasyonu analizleri, süstitüe edilmemiş ksiloglukanın XTH enzimleri tarafından oldukça tercih edildiğini göstermiştir. CaXTH2 enzimi, donor- alıcı substrat çifti olarak demirhindi tohumu ksiloglukan (TXG) polisakarit ve XXXG (X7) oligosakarit kullanıldığında en yüksek aktiviteyi göstermiştir. Bir sonraki en yüksek aktivite, hidroksietil selülozun (HEC) ksiloglukan alıcı oligosakaritlerle donör olarak kullanıldığı zaman gösterilmiştir. CaXTH2 enzimi, XT, CT, BB vb. gibi diğer oligosakaritler ile TXG-XGO aktivite seviyesi yüzde 100 olarak alındığında neredeyse yüzde 0,1 olan bir aktivite vermiş ve bu da heterotransglükosilaz aktivitesinin çok az ya da hiç olmadığını desteklemiştir. Farklı biber çeşitleri fenotipik olarak gözlenmiş ve tuz stresi koşullarında duyarlılık veya tolerans göstermişlerdir. Genomik ve transkriptomik analizler, *CaXTH2* geninin, tuz stresi koşulları altında anlatımının indüklendiğini göstermiştir. CaXTH2 enzimi stres direncinden doğrudan sorumlu görünmemektedir. Yine de, bu *XTH* genlerinin, yerli promotörler altında stres toleransı üzerinde bir etkisi olmadığını kanıtlamaz, fakat daha büyük ve daha karmaşık bir mekanizmanın parçası olma ihtimalleri yüksektir.

## TABLE OF CONTENTS

ACKNOWLEDGEMENTS.....	iii
ABSTRACT.....	iv
ÖZET .....	v
LIST OF FIGURES .....	viii
LIST OF TABLES.....	xii
LIST OF SYMBOLS/ABBREVIATIONS.....	xiv
1. INTRODUCTION.....	1
1.1. AIM OF THE THESIS.....	1
1.2. CAPSICUM ANNUUM .....	1
1.3. ABIOTIC STRESS .....	2
1.4. PLANT CELL WALLS .....	4
1.5. PLANT CELL WALL STRUCTURE.....	6
1.5.1. Cellulose .....	8
1.5.2. Pectins.....	9
1.5.3. Xylans .....	10
1.5.4. Mannans.....	11
1.5.5. Mixed- Linked $\beta$ -Glucans.....	12
1.5.6. Xyloglucans .....	13
1.6. XYLOGLUCAN ENDOTRANSGLYCOSYLASE/HYDROLASE ENZYMES	16
1.7. HETEROLOGOUS PROTEIN PRODUCTION AND PICHIA PASTORIS .....	22
2. MATERIALS AND METHODS .....	24
2.1. TARGET SELECTION FOR PROTEIN EXPRESSION, CODON OPTIMIZATION AND PRIMER DESIGN.....	24
2.2. HEAT SHOCK TRANSFORMATION AND PLASMID ISOLATION .....	25
2.3. TRANSFORMATION INTO YEAST .....	25
2.4. SELECTION OF THE ACTIVE ENZYME PRODUCING COLONIES.....	26
2.4.1. Selection of CaXTH2 Producing Colonies.....	26
2.4.2. TCA-Acetone Precipitation, SDS-PAGE, Western Blotting.....	26
2.5. DONOR AND ACCEPTOR SUBSTRATES.....	27

2.6.	HPLC ANALYSIS .....	28
2.7.	LARGE SCALE PROTEIN PRODUCTION AND PURIFICATION.....	28
2.8.	PH OPTIMIZATION .....	30
2.9.	ACTIVITY ANALYSES .....	30
2.10.	CAPSICUM PLANT GROWTH OPTIMIZATION STUDIES.....	31
2.11.	SALT STRESS APPLICATIONS .....	33
2.12.	RNA ISOLATION, cDNA SYNTHESIS AND QPCR.....	34
3.	RESULTS.....	37
3.1.	PROTEIN PRODUCTION AND ENZYME CHARACTERIZATION .....	37
3.1.1.	Target/Host Selection and Codon Optimization.....	37
3.1.2.	Selection of Active Enzyme Producing Colonies.....	38
3.1.3.	Large Scale Production .....	40
3.1.4.	pH Optimization .....	42
3.1.5.	Substrate Specificity and Enzyme Characterization.....	43
3.1.6.	Enzyme Kinetics .....	48
3.2.	CAPSICUM PLANT GROWTH TRIALS .....	51
3.3.	SALT STRESS.....	53
3.4.	RNA ISOLATION AND cDNA SYNTHESIS .....	66
3.5.	GENE EXPRESSION STUDIES .....	67
3.5.1.	Salt Stress Expression Levels for <i>CaXTH2</i> Gene.....	71
4.	DISCUSSION.....	78
5.	CONCLUSION .....	87
	REFERENCES .....	89

## LIST OF FIGURES

Figure 1.1. The representative structure of the primary cell wall.....	7
Figure 1.2. Structure of cellulose, $\beta$ -(1 $\rightarrow$ 4)- linked glucan chain. ....	8
Figure 1.3. The representative structure of glucuronoarabinoxylan (GAX).....	11
Figure 1.4. The representative structure of galactomannan.....	12
Figure 1.5. The representative structure of mixed- linkage (1 $\rightarrow$ 3; 1 $\rightarrow$ 4) $\beta$ -D-glucans. ....	13
Figure 1.6. Different side chain structures of xyloglucan and their one-letter-codes defined so far .....	14
Figure 1.7. A schematic representation of XET and XEH enzyme mechanisms .....	18
Figure 1.8. Representation of two different endotransglycosylation (XET) reactions; (a) Polysaccharide to polysaccharide ( $P\rightarrow P$ ) endotransglycosylation, (b) Polysaccharide to oligosaccharide ( $P\rightarrow O$ ) endotransglycosylation .....	19
Figure 1.9. The phylogenetic tree of GH16 enzymes based on their amino acid sequences .....	20
Figure 3.1. The SDS-PAGE image of TCA-acetone precipitated CaXTH2 proteins from small scale cultures .....	38
Figure 3.2. Western blotting results of TCA-acetone precipitated CaXTH2 proteins from small scale cultures .....	39
Figure 3.3. Size- exclusion HPLC chromatogram of CaXTH2 enzyme activity from different colonies using the TXG-XGO substrate couple.....	40



Figure 3.4. Silver stained SDS-PAGE gel image of CaXTH2-2 fractions 1 to 9 obtained from the size-exclusion polishing column .....	41
Figure 3.5. CaXTH2-2 fractions from 1 to 9 that were obtained after polishing step on 12 percent polyacrylamide gel and Western blotting using Anti-6xHis antibody.....	42
Figure 3.6. The optimization of pH for CaXTH2 enzyme using McIlvaine buffer ranging from pH 4.0 to 8.0.....	43
Figure 3.7. The graphs of CaXTH2 enzyme activity on TXG and HEC donor substrates with XGO, X7, XT and CT acceptor substrates based on incubation time and fluorescence (a. u.) value that shows the activity amount on HPLC analysis.....	45
Figure 3.8. The graphs of CaXTH2 enzyme activity on BBG, TXG and HEC donor substrates with BA, BB, BC, GM and LT acceptor substrates based on incubation time and fluorescence (a. u.) value that shows the activity amount on HPLC analysis.....	46
Figure 3.9. The graphs of CaXTH2 enzyme activity on BBG and HEC donor substrates with BA, BB, BC, LT and XGO acceptor substrates based on incubation time and fluorescence (a. u.) value that shows the activity amount on HPLC analysis.....	47
Figure 3.10. Michaelis- Menten (reaction rate ( $\mu\text{M}$ product/min) vs final X7 concentration ( $\mu\text{M}$ )) graph of CaXTH2 enzyme .....	50
Figure 3.11. Lineweaver- Burke (1/Reaction rate (min/ $\mu\text{M}$ product) vs final 1/X7 concentration (1/ $\mu\text{M}$ )) graph of CaXTH2 enzyme .....	50
Figure 3.12. Root and shoot length comparison of 11-day-old 'Erzurum' seedlings that were surface sterilized with 70 percent EtOH for 1.5 min .....	52

Figure 3.13. Phenotypic comparison of 11-day-old ‘Erzurum’ seedlings grown on 0.5 percent agar including sterile ultra-pure water medium.....	54
Figure 3.14. Phenotypic comparison of 11-day-old ‘Erzurum’ seedlings grown on 0.5 percent agar including sterile ultra-pure water medium .....	55
Figure 3.15. Comparison of root- shoot lengths and root numbers of 11-day-old ‘Erzurum’ seedlings.....	56
Figure 3.16. Phenotypic comparison of 11-day-old ‘Cila’ variety seedlings .....	59
Figure 3.17. Phenotypic comparison of 11-day-old ‘Samuray’ variety seedlings.....	60
Figure 3.18. Phenotypic comparison of 11-day-old ‘Aktör’ variety seedlings .....	61
Figure 3.19. Phenotypic comparison of 6-week-old ‘Çanakkale’ variety plants that the roots were soaked into 200 mM NaCl solution.....	64
Figure 3.20. Phenotypic comparison of 6-week-old ‘Kahramanmaraş’ variety plants that the roots were soaked into 200 mM NaCl solution.....	65
Figure 3.21. 1 percent (w/v) agarose gel electrophoresis results of RNA and cDNA samples obtained from 11-day old salt stress treated ‘Seki’ variety root tissue .....	67
Figure 3.22. The separation of the reference gene <i>CaActin</i> at 260 nm using Varian PLRP-S 1000A 5 µm 50x2.1 mm reverse phase column in HPLC .....	68
Figure 3.23. HPLC chromatogram image of the separated fragments of pUC19 which was digested with HpaII enzyme .....	69
Figure 3.24. Amplification curves of standards from $10^7$ copies/µl to $10^2$ copies/µl of <i>Caα-TUBULIN</i> formed by performing QPCR with reference gene primers .....	69

Figure 3.25. Melt curve analysis of standards from $10^7$ copies/ $\mu$ l to $10^2$ copies/ $\mu$ l of <i>Ca<math>\alpha</math>-TUBULIN</i> after performing QPCR with reference gene primers .....	70
Figure 3.26. cq vs. copy number graph of <i>CaXTH2</i> that was plotted after QPCR with gene specific primers and gene standards ( $10^2$ copies/ $\mu$ l- $10^9$ copies/ $\mu$ l) .....	70
Figure 3.27. Graphs showing the copy numbers of <i>CaXTH2</i> gene in root tissues of 11-day-old 0 mM- 25 mM and 50 mM NaCl containing MS medium grown (a) Aktör and (b) Seki variety .....	72
Figure 3.28. Graphs showing the copy numbers of <i>CaXTH2</i> gene in root tissues of 11-day-old 0 mM- 25 mM and 50 mM NaCl containing MS medium grown (a) Cila and (b) Samuray variety .....	73
Figure 3.29. Copy numbers of <i>CaXTH2</i> gene from (a) leaf and (b) root tissues of Çanakkale variety whose roots were soaked into 200 mM NaCl solution for 0 min as control, 10 min, 30 min and 120 min.....	75
Figure 3.30. Copy numbers of <i>CaXTH2</i> gene from (a) leaf and (b) root tissues of Kahramanmaraş variety whose roots were soaked into 200 mM NaCl solution for 0 min as control, 10 min, 30 min and 120 min.....	77

## LIST OF TABLES

Table 2.1. Forward and reverse primer sequences for <i>CaXTH2</i> gene for QPCR studies ....	25
Table 3.1. Selected <i>CaXTH2</i> gene for heterologous production .....	37
Table 3.2. Donors and acceptors which CaXTH2 enzyme showed activity.....	43
Table 3.3. The activity levels of CaXTH2 enzyme in picokatal/mg value on different substrate couples .....	48
Table 3.4. Comparison of root- shoot lengths, root number and germination percentage with Post-Hoc statistical analysis results of ‘Erzurum’ seedlings grown in MS agar medium .....	53
Table 3.5. Comparison of root- shoot lengths and root number and Post-Hoc statistical analysis results of ‘Erzurum’ seedlings that were grown on 0,5 percent agar including sterile ultra-pure water medium .....	54
Table 3.6. Comparison of root- shoot lengths and root number and Post-Hoc analysis results of ‘Erzurum’ seedlings that were grown on 0,5 percent agar including MS medium .....	57
Table 3.7. The average primary root- shoot lengths and germination rate percentages of 11-day-old ‘Cila’ variety seedlings in 0 mM NaCl, 25 mM NaCl and 50 mM NaCl concentration.....	62
Table 3.8. The average primary root- shoot lengths and germination rate percentages of 11-day-old ‘Samuray’ variety seedlings in 0 mM NaCl, 25 mM NaCl and 50 mM NaCl concentration.....	62

Table 3.9. The average primary root- shoot lengths and germination rate percentages of 11-day-old ‘Aktör’ variety seedlings in 0 mM NaCl, 25 mM NaCl and 50 mM NaCl concentration.....62

Table 3.10. The average primary root- shoot lengths and germination rate percentages of 11-day-old ‘Seki’ variety seedlings in 0 mM NaCl, 25 mM NaCl and 50 mM NaCl concentration.....63

Table 3.11. Copy numbers of *CaXTH2* gene in root tissues of Aktör, Seki, Cila and Samuray seedlings that were grown on MS agar containing 0 mM, 25 mM and 50 mM NaCl.....74

Table 3.12. Copy numbers of *CaXTH2* gene from the leaf and root tissues of 6-week-old Çanakkale seedlings whose roots were soaked into 200 mM NaCl solution for different time intervals (0 min as control-10 min-30 min-120 min) .....75

Table 3.13. Copy numbers of *CaXTH2* gene from the leaf and root tissues of 6-week-old Kahramanmaraş seedlings whose roots were soaked into 200 mM NaCl solution for different time intervals (0 min as control-10 min-30 min-120 min).....77

Table 4.1. CaXTH1, CaXTH2 and CaXTH3 enzymes as paired with substrates showing the highest activity.....80

Table 4.2. Kinetic parameters of CaXTH1, CaXTH2 and CaXTH3 enzymes.....81

## LIST OF SYMBOLS/ABBREVIATIONS

<i>Araf</i>	Arabinofuranose
AOX1	Alcohol oxidase 1 promoter
At	<i>Arabidopsis thaliana</i>
AX	Arabinoxylan
a. u.	Arbitrary unit
BA	Glucotetraose A
BB	Glucotetraose B
BBG	Barley $\beta$ -glucan
BC	Glucotetraose C
BMGY	Buffered glycerol-complex medium
BMMY	Buffered methanol-complex medium
bp	Base pair
BSA	Bovine serum albumin
Ca	<i>Capsicum annuum</i>
CAZy	Carbohydrate-active enzymes
cDNA	Complementary DNA
COR/LAE	Cold regulated/late embryogenesis-abundant
Cq	Quantification cycle
CSLC	Cellulose synthase- like family C
CT	Cellotetraose
DNA	Deoxyribonucleic acid
EG16	Endoglucanase family 16
EtOH	Ethanol
Fucp	Fucopyranose
Gal	Galactose
Galp	Galactopyranose
GAX	Glucuronoarabinoxylan
GH16	Glycoside hydrolase family 16
Glc	Glucose
GlcP	Glucopyranose

GlcA	Glucuronic acid
GM	Guar galactomannan
GX	Glucuronoxylan
HCl	Hydrochloric acid
HEC	Hydroxyethyl cellulose
HG	Homogalacturonan
HPLC	High pressure liquid chromatography
HSPs	Heat-shock proteins
kDa	Kilo Dalton
LB	Luria-Bertani
LT	Laminaritetraose
Man	Mannose
MCS	Multiple cloning site
<i>Mr</i>	Relative molecular mass
MS	Murashige and Skoog
MUR3	Galactosyltransferase enzyme
NaCl	Sodium chloride
NaOCl	Sodium hypochlorite
NF	Normalization factor
nm	Nanometer
OD	Optical density
PBS	Phosphate buffered saline
PCR	Polymerase chain reaction
QPCR	Quantitative polymerase chain reaction
RG	Rhamnogalacturonan
RNA	Ribonucleic acid
rpm	Revolutions per minute
rRNA	Ribosomal RNA
SDS-PAGE	Sodium dodecyl sulfate polyacrylamide gel electrophoresis
TBS-T	Tris buffered saline with Tween
TCA	Trichloroacetic acid
T <sub>m</sub>	Melting temperature
TXG	Tamarind seed xyloglucan

v/v	volume/volume
w/v	weight/volume
w/w	weight/weight
X7	Xyloglucan heptasaccharides
XEH	Xyloglucan hydrolase
XET	Xyloglucan endotransglycosylase
XGO	Xyloglucan oligosaccharide
XT	Xylotetraose
XTH	Xyloglucan endotransglycosylase/Hydrolase
Xyl	Xylose
Xylp	Xylopyranose
YPDS	Yeast extract peptone dextrose medium with sorbitol
6X-His	Polyhistidine-tag



# 1. INTRODUCTION

## 1.1. AIM OF THE THESIS

Cell wall is the most important part of the plants as it protects the plant from and interacts with its environment. In order to protect the plant from stresses and increase its yield, it is very crucial to understand the structure and function of the proteins and carbohydrates that exist in the plant cell wall. The modification of the cell wall is the major issue which allows cell expansion and growth by deposition and rearrangement of new wall polysaccharides. Xyloglucan endotransglycosylase/hydrolase (XTH) enzymes mediate the modifications by catalyzing the cleavage and rejoining of xyloglucan which is a major polysaccharide in the cell wall. It has been demonstrated that XTH enzymes are also capable of the transglycosylation of different cellulosic and non-cellulosic polysaccharides in the cell wall and they have important roles in many cell wall processes like expansion, elongation, signalling and response to several stress factors. Due to all those properties that XTH enzymes may function in, characterization of the enzymatic functions and examination of the roles of its gene products are highly desirable to contribute to the understanding of those enzymes. Although it is known that XTHs are stress responsive enzymes, their mechanisms and the reason of those changes during stress conditions are not really understood. In this study, it was aimed to examine the characterization of the Capsicum gene, *CaXTH2*, which is stress upregulated, in order to better understand the roles of this gene/enzyme in pepper plants under salt stress, its substrate specificity, enzyme kinetics and transcript data analysis were aimed to be performed.

## 1.2. CAPSICUM ANNUUM

Pepper (*Capsicum annuum L.*) is a well known and widely produced plant around the world due to its nutritious ingredients. The shape of the berry-like fruits of this plant can be in various colors, shapes and taste. Although pepper has been mainly cultivated in Asia, Africa and several Mediterranean countries, it was domesticated in North & South America. Pepper contains vitamin A, vitamin B, and high amount of vitamin C. Moreover,

the alkaloids and carotenoids that are present in its structure act as flavouring and coloring agents, mainly used in take-away foods [1]. Pepper also has a preservative effect on biological systems from oxidative stress by scavenging free radicals with beta-carotenoids, vitamin C and vitamin A [2]. Due to the alkaloids in its content, pepper fruit is pungent. In a study, it has been shown that the capsaicin, which is the leading alkaloid, may be used for the treatment of diabetic neuropathy, cluster headache, along with its anti-obesity and anti-cancer properties [3]. Approximate daily consumption amount has been determined to be 0.5 g / person per day in Europe. The highest pepper production in the world belongs to China (652510 hectares of dedicated area) followed by Indonesia, Nigeria and Turkey respectively. In Turkey, approximately 88000 hectares of land is committed to pepper production [4, 5].

It has been known that there are 25-30 defined species of capsicum and the most broadly grown species are *C. annuum-L.*, *C. frutescens-Mill.*, *C. baccatum-L.*, *C. chinense*, and *C. pubescens* with *Capsicum annuum* being the most common [6]. The Solanaceae family consists of nearly 2500 species and 102 genera. In a study it has been observed that the tomato and pepper genomic content was similar to each other and the capsicum sequences were complementary to tomato cDNA [7]. In the study of Choi and coworkers, abiotic stress inducible capsicum gene *CaXTH3* (*Capsicum annuum* endotransglycosylase 3) was over-expressed in tomato (*Solanum lycopersicum*) plants and it was found that transgenic tomato plants showed increased tolerance to salt and drought stresses and no phenotypic defects were observed. This may be explained by their genomic similarity [8].

### 1.3. ABIOTIC STRESS

Plants are affected by environmental changes more quickly than animals since they live in soil-plant-atmosphere continuum environment. They have to respond to the changes in environment for the sustainable survival. [9]. Environmental changes such as extreme temperatures, salinity level, waterlogging and drought are usually considered as abiotic stress factors which have negative effects of non-living elements on living organisms [10]. One of the most common stress factors is cold which causes a decrease in the number of reactions by changing the optimal enzyme working temperature and creates imbalanced metabolism by causing changes in the energy metabolism of the plant. Moreover, cold also

constricts water uptake which eventually leads to an increase in the deposition of cold-regulated late embryogenesis-abundant (COR/LEA) proteins. In a study conducted on *Festuca pratensis*, it has been observed that the rate of photosynthesis is directly related to the cold stress. Various studies have also shown the difference in down regulation of anabolic pathways and up regulation of catabolic pathways compared to plants that were grown in optimal temperature conditions. Heat stress is another factor that affects plant metabolism by leading to denaturation of intracellular proteins and protein misfolding. In the presence of heat stress, the heat-shock proteins (HSPs) has been released as they are chaperones. Another important stress factor is reduced water availability that induces drought which cause cellular dehydration. In the case of drought stress, the cell elongation in the shoot is inhibited due to the reduced water uptake. Therefore, roots continue to grow in order to reach water-rich areas in the soil that it has been planted. Different abiotic stresses might occur at the same time such as drought stress with high temperature. The decrease in water level might cause salinity issues and an increase of toxic compounds [10, 11].

When plants face environmental challenges, they need to respond and develop adaptive mechanisms. This response and adaptation processes has different stages. In the presence of a stress factor, the plant creates first a stress shock and non-acclimated plants become susceptible to the stress. Then, following the stress shock, the acclimation is initiated with increased plant tolerance and new homeostasis starts. If the plant has been exposed to stress too long, it goes to the exhaustion state in which it can not sustain the homeostasis anymore [10].

When the plants are exposed to stress, they activate stress inducible genes for the adaptation to the environmental changes. Those genes can be thought as two different groups depending on the proteins that they encode. First group of those genes directly translate their protein products to resist the stress conditions. Some of those proteins are osmotic regulatory proteins, LEA proteins and anti-freezing proteins. The other group of stress inducible genes translate proteins which have role in the signaling and the regulation of gene expression pathways such as transcriptional elements [9].

For the acclimation process after stress exposure, plant cells go through a lot of structural alterations such as growing of shoots during shading. In order to activate the cells for those kind of structural changes under stress, modification of the cell wall such as wall

elongation or expansion plays an important role. Cell wall is the barrier against pathogens or other stress conditions and cell wall proteins which take part in the cell wall modification processes are essential for stress response. It has been demonstrated that xyloglucan enzyme controls the growing and wall strengthening processes, therefore leading plant to relieve stress. Transglycosylase enzyme provides new xyloglucan chains that are transported to the cell wall in order to strengthen its structure [12].

Therefore it can be said that xyloglucan endotransglycosylase/hydrolase (XTH) enzymes are responsible from the re-modelling of the cell wall structure which is also important for stress response. In a study conducted on hot pepper plants, it has been shown that under various abiotic stress conditions (drought, high salinity, cold) the level of isolated cDNA clones (*pCaXTH1*, *pCaXTH2* and *pCaXTH3*) was increased and after that it was observed that *35S-CaXTH3* transgenic *Arabidopsis thaliana* plants showed increased tolerance to drought and salinity stress. However despite the stress tolerance, abnormal morphology was observed on plant leaves. *35S-CaXTH3* transgenic *Arabidopsis* leaves increased small size cells leading to high amount of mesophyll cells with limited amount of starch. That results showed that *CaXTH3* in *Arabidopsis* changed the construction of the cell wall as a response to stress [13]. In another study, *CaXTH3* gene which is commonly used to improve the stress tolerance of crop plants was used this time to obtain transgenic tomato (*Solanum lycopersicum*) plants. *35S:CaXTH3* transgenic tomato plants showed increased tolerance to drought and salinity stress. There were no morphological changes on plants even after 2 weeks of drought exposure and they were still green and unwithered. The changes in the construction of the cell wall such as closure of the stomatas helped the plants to develop tolerance to stress conditions and these studies showed that cell wall modification enzymes such as XTH enzymes have important roles in defense mechanisms to abiotic stresses [8].

#### **1.4. PLANT CELL WALLS**

The most important structure giving shape to the plants is the plant cell wall that is located at the outer surface of the plasma membrane. The properties of many different plant types on the planet and their physical appearance are mainly determined by the composition of their plant cell walls. According to type of plant cells, their cell wall characteristics, shape,

size and position can display alterations. In the early stages of plant cells, the plant cell wall which is a thin flexible layer composed of various polysaccharides and structural proteins is an active compartment since cell division is rapid and organogenesis starts. Meristem tissues comprised of tiny stem cells that initiates the organogenesis whereas the xylem vessels that are responsible for water transport composed of huge cell walls. Although cell wall is known as a thin layer – between 0.1- 1  $\mu\text{m}$ - in most of the plant cells, it is the major component which gives shape to the protoplast (cytoplasm and nucleus) within and rigidity to the plant. The cell wall structure has important roles on many of the physical traits of plants such as their robustness to variety of stresses or their ability to grow to huge sizes. [14].

The plant cells are found cemented together by their cell walls, so cell migration is impossible for them. For this reason, cell growth is managed by controlled cell division and cell- specific enlargement which the cell wall contributes. During the growth of a cell its flexible wall is under stress due to the resistance of stretching wall polymers to the cell turgor pressure. This stress provides the required mechanical energy for the extension of the cell wall. Wall extension is achieved by a controlled polymer creep/loosening mechanism which is a controlled irreversible and time- dependent extension that the cellulose microfibrils and matrix- polysaccharides slide within the wall and increase the surface area of the wall. This process is controlled by the selective wall loosening and shifting of cellulose microfibril linkages. Wall loosening is a modification for the extension of the cell wall in response to the wall stress [14].

Cell wall consists mainly of polysaccharides, lignins and proteins. Beside the polysaccharides that constitute the wall matrix, cell wall has structural proteins and the proteins that work as enzymes for the remodeling of the cell wall [15].

Plant cell wall not only gives strength to the plants and contributes to cell growth but also have other major roles. Due to its location, it plays role in cell communication between adjacent cells and also in plant- microbe interactions. They produce defense responses to possible pathogens and protect the cells from inflammation [16]. It is also used as animal and human nutrition. Polysaccharides in the cell wall matrix are essential dietary fibers and the source of textile and paper industries [15].

## 1.5. PLANT CELL WALL STRUCTURE

Plant cell wall contains mainly cellulose which consists of  $\beta$ -(1 $\rightarrow$ 4)-linked glucan chains. They are bound each other via hydrogen bonds and form the crystalline cellulose microfibrils which are made at the plasma membrane. In addition to these microfibrils, it includes different matrix polysaccharides which are bound tightly to those microfibrils by hydrogen bonding and have major role in building the cell wall structure [16, 17].

Generally, cell wall structure is divided into two as primary cell wall and secondary cell wall. Primary cell wall consists mainly from cellulose microfibrils that are embedded into non-cellulosic  $\beta$ -linked polysaccharides (hemicelluloses) and pectins. Those matrix polysaccharides are grouped as hemicellulosic (xyloglucans, xylans, glucomannans and mixed-linked glucans) and pectic (homogalacturonan and rhamnogalacturonan I and II) polysaccharides which are synthesized in Golgi cisternae and transported by secretory vesicles to the wall of the cell and forms the primary cell wall structure. Whereas cellulose is synthesized at the plasma membrane and impregnated into a matrix composed of other polysaccharides, glycoproteins and structural proteins that have roles in recognition and signaling events and enzymes that participate in wall remodeling. The composition of the cell wall varies among different plants or even different tissues of the same plant. Primary cell wall has important role in cell growth and expansion. For that reason, it is deposited throughout the cell growth and it is extensible to allow the expansion of the cell without rupturing cells under turgor pressure [15, 16].

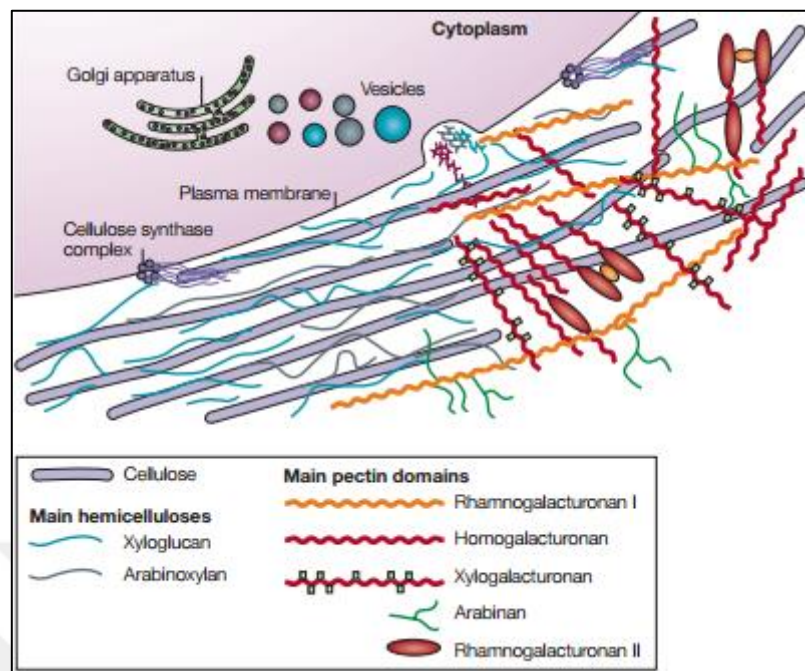


Figure 1.1. The representative structure of the primary cell wall [14].

Hemicelluloses form significant non-covalent associations with cellulose such as xyloglucan- cellulose network in type I primary cell wall. Xyloglucan is interlocking molecule and the proportion of xyloglucans are equal to cellulose microfibrils in type I primary cell wall [18]. Those polysaccharides are neutral molecules that are extracted from the cell wall with alkali and they constitute about 30 percent (by weight) of the cell wall which is even greater than thick secondary walls. Their molecular structure compose of linear  $\beta$ - (1 $\rightarrow$ 4)- linked backbone including single residue and side branches. Cellulose and xyloglucan constitute 50 percent of the total cell wall polysaccharides in primary cell wall. Xyloglucans bind the surface of the cellulose microfibrils and fill the gaps between microfibrils which creates the cellulose-xyloglucan matrix [19, 20].

There are three main polysaccharide domains in primary cell wall which are cellulose-xyloglucan matrix, pectin and structural proteins. While the xyloglucan- cellulose matrix consists 50 percent (by weight) of the cell wall mass, pectin consists 35 percent (by weight) of the total cell wall mass for type I in dicots and less portion of type II in monocots. In the type I primary cell wall of dicots, xyloglucans comprise the 25 percent (by weight) of the cell wall mass while in type II cell walls of grasses this percentage drops to 2 percent- 10 percent (by weight) [20].

Pectins are acidic molecules and they consist of different structural domains which the level of those domains vary in pectins in different plants. The most important domain of pectins are homogalacturonan (HG) and rhamnogalacturonan I (RGI) which are found in most of the primary cell wall structural models. In those cell wall models, pectins generate a gel-like network by the cross-linkage between calcium ions and homogalacturonan from their junction zones [19].

Primary cell wall is deposited at the extracellular surface of the plasma membrane and after the cell growth in certain cell types which are exposed to mechanical stress, additional cell wall synthesis occurs and it is deposited as secondary cell wall, interior to the primary cell wall. Secondary cell wall includes lignins except primary cell wall polysaccharides and it is deposited after the completion of cell growth to give mechanical stability by surrounding the vessel or fiber elements in woody plants [14, 15, 17].

### 1.5.1. Cellulose

Cellulose is the most commonly found biopolymer in nature with major role in primary cell wall structure of plants. It acts as a scaffold allows other wall components to bind it through. Cellulose does not exist as a single chained structure in nature. It is an insoluble molecule in water due to it's highly stable molecular structure [21]. Its structure consists of  $\beta$ - (1 $\rightarrow$ 4)- linked glucose residues that composed as unbranched fibrils and every second glucosyl residue in those fibrils is found rotated 180° on the chains longitudinal axis (Figure 1.2). It can also be said that cellulose consists of repeating units of cellobiose (a disaccharide including two  $\beta$ -(1 $\rightarrow$ 4)- linked glucose molecules) [22].

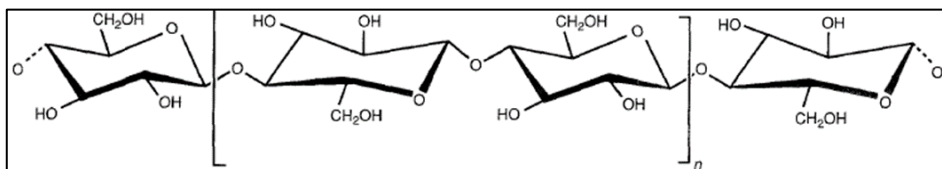


Figure 1.2. Structure of cellulose,  $\beta$ -(1 $\rightarrow$ 4)- linked glucan chain. Cellobiose is indicated in brackets [22].



In nature, starting from the synthesis, cellulose is composed of frequent chains that are called as microfibrils. It is generated at the apoplastic side of the plasma membrane and consists of unbranched 36 parallel hydrogen bonded  $\beta$ -(1 $\rightarrow$ 4)-D-glucan chains that assembles into paracrystalline microfibrils. It has been observed that the microfibril sizes might differ depending on the specie and the type of the plant. The width of these chains varies between 5 to 15 nm and placed 20-40 nm far from each other [23]. The Van der Waals bonds and hydrogen bonds are responsible from the structure of polymeric glucosyl chains that are linked together. Therefore, they causes the crystallization of cellulose at some regions through microfibril. These crystallized regions are having a strict phenotype and spaced by amorphous areas that are less likely to crystallize. This tight crystal alignment protects containing glycosidic bonds from a probable enzymatic attack. Moreover, the pectin and cellulosic  $\beta$ -linked polysaccharides increase the robustness of the plant against enzymatic attack by improving the structure of cell walls [24].

They are found in both primary and secondary cell wall and by cross- linking tightly with the other non- cellulosic  $\beta$ -linked polysaccharides together they build the cell wall architecture. This architecture and composition of the cell wall is not uniform during the growth and differentiation of the plant cells. While the older materials are pushed outward from the wall, new wall materials are laid down [16]. According to some studies, the cross-links between cellulose and other polysaccharides weakens the mechanical strength of the cell wall by preventing the aggregation of cellulose while facilitating the expansion of the cell wall [17].

### **1.5.2. Pectins**

Pectins are the most interesting compounds among other polysaccharides with their complex structure and multi-tasking abilities [14, 25]. They are proposed to be important for porosity control and ionic environment control of the cell wall. They are responsible for the adhesion of adjoining cells in an adhesive layer called middle lamella and form gel-like structures that push microfibrils apart and ease their slippage during cell growth [14, 17]. Approximately 35 percent of primary cell wall is composed of pectins in dicots and non-graminaceous monocots [26]. They are structurally complex and acidic macromolecules which consist of different structural domains varying in pectins from different plants.

Homogalacturonan (HG) and rhamnogalacturonan I (RGI) are the most important pectic domains found mostly in current cell wall structure models. The homogalacturonan (HG) domain consists of linear  $\alpha$ -(1 $\rightarrow$ 4)- linked D-galacturonan backbone which is methyl esterified from its variable segments. Homogalacturonan domains of pectin forms gel-like network by cross linking with the calcium ions from its unesterified segments. Rhamnogalacturonan I (RGI) consists of galacturonan backbone interrupted by  $\alpha$ -L-rhamnosyl residues. Rhamnogalacturonan II (RGII) which is found quantitatively minor but structurally complex has function as binding the trace element boron. Borate-diester cross-links between RGII molecules and apiose residues are important for strengthening of the cell wall [17, 19].

### 1.5.3. Xylans

Xylans are the main non-cellulosic  $\beta$ - linked polysaccharides found in secondary cell wall of dicots (~20 % (w/w)) generally in the form of glucuronoxylan (GX) and also found as glucuronoarabinoxylan (GAX) in all type of walls of commelinid monocots. They are abundant in endosperm tissue of cereal grains as storage polysaccharides. They are mainly responsible for tissue development and tissue strengthening process [27].

Xylans compose of D-xylose units with  $\beta$ -(1 $\rightarrow$ 4) linkage and are substituted differently based on the tissue type and plant species. If the xylan backbone is substituted with  $\alpha$ -(1 $\rightarrow$ 2)- linked D-glucuronic acid (GlcAp) or 4-O-methyl-glucuronic acid, glucuronoxylan (GX) polymers are formed. Xylan backbone can be *O*-acetylated especially in grasses. If the *O*-acetylated xylan backbone is substituted with  $\alpha$ -(1 $\rightarrow$ 3) or  $\alpha$ -(1 $\rightarrow$ 2)- linked  $\alpha$ -L-arabinofuranosyl (Araf) and  $\alpha$ -(1 $\rightarrow$ 2)- linked D-glucuronic acid or 4-O-methyl-glucuronic acid, the new polymer is called glucuronoarabinoxylan (GAX). If the xylose backbone is substituted only with  $\alpha$ -L-arabinofuranosyl (Araf) and acetyl substituents without  $\alpha$ -(1 $\rightarrow$ 2)- linked glucuronic acid or 4-O-methyl-glucuronic acid, it is called arabinoxylan (AX). The L-arabinose residue may be further substituted with ferulate substituent at the C-5 position and heteroxylans can be linked to lignins from there (Figure 1.3) [27, 28].

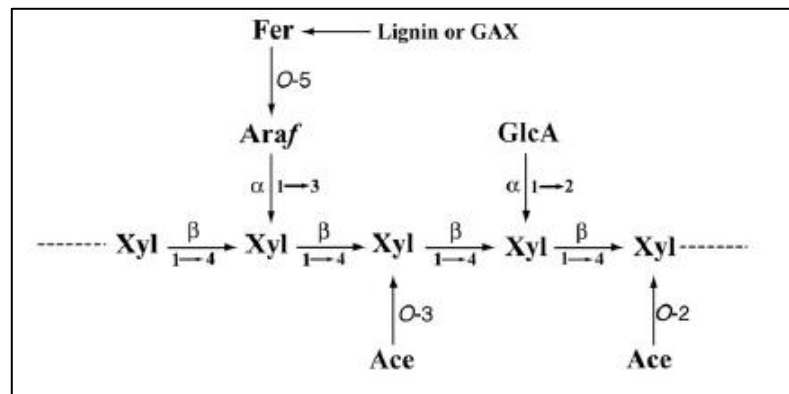


Figure 1.3. The representative structure of glucuronoarabinoxylan (GAX). The  $\beta$ -(1 $\rightarrow$ 4)-linked xylopyranosyl (Xylp) backbone is substituted with *O*-acetylation from *O*-2 and *O*-3 position,  $\alpha$ -(1 $\rightarrow$ 2) and  $\alpha$ -(1 $\rightarrow$ 3)- linked arabinofuranosyl (Araf) residues and ferulate residues [28].

#### 1.5.4. Mannans

Mannans are thought to be the most ancient non-cellulosic  $\beta$ - linked polysaccharides since they are found in some algae species. They are the major polysaccharides found in secondary wall of gymnosperms and also few of them (up to 5 percent) found in cell walls of spermatophytes. They have important roles in providing cell wall rigidity and responsible for storage of seeds. Also, they take part in wall signaling, tissue differentiation and embryogenesis [27]. Their backbone generally consists of linear chains of  $\beta$ -(1 $\rightarrow$ 4)- linked D-mannosyl residues. According to their backbone and side chain compositions, they are divided into four groups as mannan, glucomannan, galactomannan and glucogalactomannan. When the polysaccharide backbone consists of  $\beta$ -(1 $\rightarrow$ 4)- linked D-mannosyl and D-glucosyl residues in 3:1 ratio with up to 18 percent acetylation, it is called glucomannan. In galactomannan, mannan residues are substituted with  $\beta$ -(1 $\rightarrow$ 6)-linked galactosyl residues (Figure 1.4) and in glucogalactomannan,  $\beta$ -(1 $\rightarrow$ 6)- linked galactosyl residue is linked to glucomannan backbone. The existence of substitution increases the solubility of the polymers. Mannosyl residues have the potential for being *O*-acetylated from *O*-2 or *O*-3 position in glucogalactomannans [27, 28].

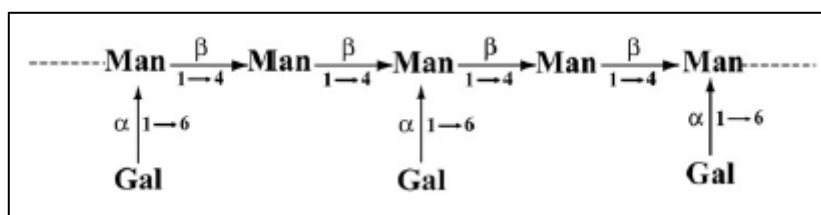


Figure 1.4. The representative structure of galactomannan.  $\beta$ -(1 $\rightarrow$ 4)- linked mannosyl (Man) backbone is substituted with  $\alpha$ -(1 $\rightarrow$ 6)- linked galactosyl (Gal) side chains [28].

Linear mannan and glucomannan backbones protect the seeds from mechanical damage. Since they are insoluble in water, they are durable after exposure to water. They show crystalline polymorphism as cellulose and divided into two groups as mannan I which has highly crystalline structure or mannan II which shows less crystallinity and includes water molecules.  $\alpha$ -(1 $\rightarrow$ 6)- linked D-galactose substitution makes mannan soluble in water via preventing the interactions between adjacent molecules and increases water retaining capacity that is important during the plant growth in dry conditions [29].

### 1.5.5. Mixed- Linked $\beta$ -Glucans

The mixed linked  $\beta$ - glucans are found mainly in grasses than other land plants. They are seen in the cell walls of starchy endosperm and in aleurones of Poaceae especially barley (*Hordeum vulgare*), oat (*Avena sativa*) and rye grains (*Secale cereale*) [30]. They have been discovered in the ancient plant *Equisetum* even though they are only found in the grasses. It has been also found in liverworts, green and red algae species. Mixed-linked  $\beta$ -glucans are storage polymers for the energy required for cell elongation. They are also found in mature rice stem tissues even though they are less in wheat, rice and maize [27].

The mixed-linked  $\beta$ -glucans are non-substituted linear glucan backbone- based polysaccharides. They composed of D-glucofuranosyl residues (Glc<sub>f</sub>) which are linked together by  $\beta$ -(1 $\rightarrow$ 4) and  $\beta$ -(1 $\rightarrow$ 3) linkages. The  $\beta$ -(1 $\rightarrow$ 4)- linked sequential oligoglucosyl units in the form of cellotriosyl or cellotetriosyl are connected via  $\beta$ -(1 $\rightarrow$ 3) linkages (Figure 1.5). Especially in barley and in most of other grasses,  $\beta$ -(1 $\rightarrow$ 3)- linked glycosyl residue occurs as a single residue between  $\beta$ -(1 $\rightarrow$ 4)- linked oligoglucosyl units and there is

no adjacent  $\beta$ -(1 $\rightarrow$ 3)- linked glycosyl residue. Their (1 $\rightarrow$ 4) to (1 $\rightarrow$ 3) linkage ratio in barley varies from 2.2: 1 to 2.6: 1 [31].

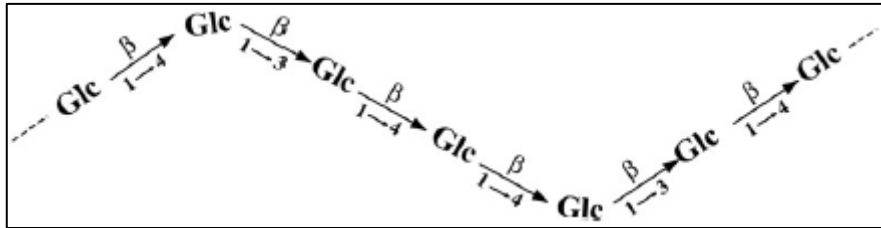


Figure 1.5. The representative structure of mixed- linkage (1 $\rightarrow$ 3; 1 $\rightarrow$ 4)  $\beta$ -D-glucans. More than two adjacent  $\beta$ -(1 $\rightarrow$ 4)- linked glucosyl residues have a  $\beta$ -(1 $\rightarrow$ 3)- linked glucosyl residue in between [28].

### 1.5.6. Xyloglucans

Xyloglucan is one of the main non- cellulosic  $\beta$ - linked polysaccharides that is found in the primary cell wall of higher plants. It functions as a load- bearing component of the cell wall forming an extensible network by making direct tether or indirect link between cellulose microfibrils. It is also known that xyloglucan is linked to pectin polysaccharides covalently [14, 27, 32]. It behaves as a spacer polymer preventing the cellulosic aggregates and also as an adapter molecule enabling cellulose to interface with other matrix polysaccharides. Xyloglucan can also act as storage polysaccharides in seeds and cotyledons. In some dicot plants such as *Tamarindus indica*, *Tropaeolum majus* or *Hymenaea stigonocarpa*, it is deposited during seedling and used as storage polymer [27].

Xyloglucan is a highly substituted polysaccharide with lots of repeating subunit structures. Nineteen side chain structures have been found so far and single letter codes according to the residue type is commonly used for each different structure.  $\beta$ - D glucan backbone which is connected via  $\beta$ -(1 $\rightarrow$ 4) glycosidic linkages without further substitution is abbreviated as 'G'. If xylosyl ( $\alpha$ -D-Xylp) residue is linked to glycosyl backbone via  $\alpha$ -(1 $\rightarrow$ 6) glycosidic bond, the side chain structure is abbreviated as 'X'. When galactosyl ( $\beta$ -D-Galp) residue is linked to xylosyl ( $\alpha$ -D-Xylp) residue by  $\beta$ -(1 $\rightarrow$ 2) linkage, it is abbreviated as 'L'. When fucosyl ( $\alpha$ -L-Fucp) residue is linked to galactosyl (L) via  $\alpha$ -

(1→2) linkage, it is abbreviated as ‘F’. In most plants, the structures of xyloglucan polymers that are represented with G, X, L and F letters are found but there are also some other scarce residues resulting in different side chain structures. If arabinofuranosyl ( $\alpha$ -L-Araf) which is linked via  $\alpha$ -(1→2) linkage instead of  $\beta$ -(1→2)- linked galactosyl and additional xylosyl residue ( $\beta$ -D-Xylp) which is linked via  $\beta$ -(1→2) linkage are attached to xylosyl residues, the side chain structures are abbreviated as ‘S’ and ‘U’, respectively. If a second arabinofuranosyl ( $\beta$ -L-Araf) residue is added to ‘S’ by  $\beta$ -(1→3) linkage, it is abbreviated as ‘T’. If another galactosyl ( $\alpha$ -D-Galp) residue is added onto ‘L’ side chain structure by  $\alpha$ -(1→2) linkage, it is abbreviated as ‘J’ [20, 33, 34, 35].

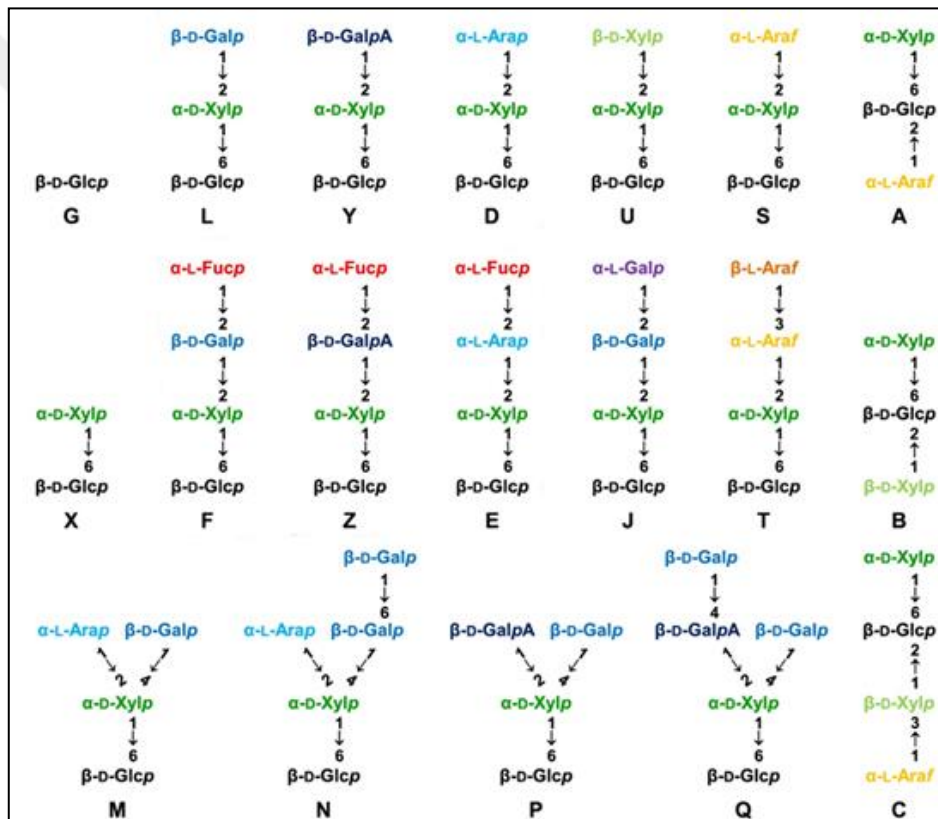


Figure 1.6. Different side chain structures of xyloglucan and their one-letter-codes defined so far [35].

Xyloglucan consists of glycosyl backbone which is usually substituted with xylosyl ( $\alpha$ -D-Xylp) residue with  $\alpha$ -(1→6) linkage at three out of four glucosyl residues in dicot and non-graminaceous monocot plants, leading to an XXXG-type xyloglucan. In other monocots and Solanales, it is found substituted with xylosyl ( $\alpha$ -D-Xylp) residue in only two out of

four glycosyl residues, resulting in the XXGG-type xloglucan. It has also been observed that, there are some plant xyloglucan having higher degree of backbone xylosylation such as four xylosyl substituents per five glycosyl residues (XXXXG-type) or more. The XXXG-type xyloglucan is often galactosylated or fucosylated forming the fucogalactoxyloglucan in most dicot plants while XXGG-type xyloglucan is *O*-acetylated on glucan backbone resulting in the acetoxylloglucan in many tissues of grasses [20, 27]. Most of the higher plants have XXXG-type xyloglucan chain which can be substituted with other sugar residues. For instance; when a galactosyl residue is added to the xylosyl residue XXLG, XLXG or XLLG xyloglucan oligosaccharides can be observed according to the position of the xylosyl residue and when a fucosyl residue is added to that galactosyl residue at the third position, XLFG or XXFG xyloglucan oligosaccharides can be observed [34]. Also, *O*- acetyl substituent can be present in xyloglucan chains at various positions in different plants. For example, in *Arabidopsis thaliana*, *O*- acetylation occurs on galactosyl residue while in grasses and Solanales, it occurs on glucosyl residue as it was mentioned before [27]. According to some studies, it is believed that fucosylated xyloglucan serves as the source of signal molecules that control the auxin- mediated expansion and also fucosylation may facilitate xyloglucan- cellulose interactions by supporting planar conformation of the xyloglucan backbone [15].

As the other non- cellulosic polysaccharides, xyloglucans are synthesized in Golgi apparatus and then transported to the cell wall. The cellulose synthase- like family C (CSLC) genes are responsible for the synthesis of the glucan backbone of xyloglucan. They are integral enzymes with multiple transmembrane domains. It is predicted that the catalytic domain of the enzyme is located on the cytosol site which enables to use cytosolic UDP- glucose for the glucan backbone synthesis [36]. For instance, in *Arabidopsis thaliana*, AtCSLC4 which is a member of CSLC family is responsible for glucan backbone of the xyloglucan chain and for the other subunits;  $\alpha$ - 1,6- xylosyltransferases (XXT1, XXT2 and XXT5),  $\alpha$ - fucosyltransferase and  $\beta$ - 1,2- galactosyltransferase (MUR3) enzymes are responsible [27].

In order to analyze the oligosaccharides, the xyloglucan polysaccharides are fragmented using endo-1, 4- $\beta$ -glucanase enzyme which makes endohydrolysis reaction of the  $\beta$ -(1 $\rightarrow$ 4) glycosidic linkages between D-glucosyl residues. The substrates of this enzyme are cellulose and xyloglucan and the enzyme digests the non-crystalline regions of cellulose. It

contributes to the cell wall loosening by releasing xyloglucans between cellulose microfibrils. The interactions between xyloglucan and cellulose have important roles in cell wall growth and mechanics [14].

The storage and structural role of xyloglucan and its branching positions influence its binding capacity to cellulose. For example, fucose residue in xyloglucan gives planar conformation to the saccharide and affects its binding to cellulose. According to an experiment with fucosylated pea and unfucosylated *Tamarindus indica*; it was suggested that fucose increase the adsorption affinity of xyloglucan to cellulose. However, after it was shown that if the molecular weight of the unfucosylated saccharide is similar with the fucosylated one, its binding capacity can be improved. Also, the presence of high amounts of galactosyl residue also influence its interaction with cellulose [32].

#### **1.6. XYLOGLUCAN ENDOTRANSGLYCOSYLASE/HYDROLASE ENZYMES**

The plant cell wall which is an active compartment of the cell takes part in a variety of dynamic processes to provide the interaction with the outer environment such as response to abiotic stresses and pathogens. It also takes part in the adjustment of the cell size and cell to cell adhesion [37]. Cell wall modification is the major issue in plant biology which allows cell expansion and growth by deposition and rearrangement of new wall polysaccharides. The changes in cell wall extensibility enable turgor-dependent cell expansion while the addition of new saccharides ensures the persistence of wall thickness. The expansion occurs in a directional way and cause morphological effects at tissues of the plant. During the expansion, new cell wall saccharides must be synthesized and added into the wall to maintain the mechanical and functional features. In other words, while the disassembly and remodeling of the wall occurs, the integration and deposition of the cell wall polymers occurs at the same time during cell growth and development. The main purpose of the cell wall here is to maintain controlled growth while keeping the cell intact [17, 38].

Xyloglucan is an important polysaccharide that tethers the cellulose microfibrils and forms the load-bearing structure of the cell wall. The cellulose microfibrils should separate from each other during the cell elongation and expansion process and this requires the modification of the xyloglucan chains. All those processes are achieved by the action of



modifying enzymes that affect the xyloglucan molecules by cleavage upon xyloglucan addition or hydrolysis of xyloglucan chains [39]. The xyloglucan endotransglycosylase/hydrolase (XTHs) (EC 2.4.1.207) enzymes have the potential to cause transient cleavage of the matrix and provide a mechanism for turgor-driven expansion of the cell wall [40]. They mediate this modifications by catalyzing the cleavage and rejoining of the xyloglucan chains via xyloglucan endotransglycosylase (XET) activity or they hydrolyze the xyloglucan via xyloglucan endohydrolase (XEH) activity. XTH enzymes that are researched so far display both XET and XEH activity or one of them [41].

The enzymatic mechanism of XETs occurs in two steps; first XET cleaves the  $\beta$ -(1 $\rightarrow$ 4)-linked D-glucosyl backbone and the reducing end product remains attached to the surface of the enzyme and then XET transfers the reducing part of the xyloglucan onto another non-reducing xyloglucan molecule. The xyloglucan that is cleaved at the beginning is called donor substrate and the other xyloglucan which the cleaved portion is transferred is called acceptor substrate. Sometimes instead of transferring another acceptor xyloglucan molecule after cleavage of donor xyloglucan, the XEH enzymes attach a H<sub>2</sub>O molecule to the cleaved site and the chain is shortened irreversibly (Figure 1.7). XEH activity has been observed in diverse plants such as nasturtium seeds, pea stems, ripening tomatoes and azuki bean stem cells. It was observed that even in the presence of XGOs there was no XET activity in azuki bean stem cells instead, XEH activity was exhibited [39].

XETs use disproportionation reaction mechanism and change the molecular masses of xyloglucans so that some will decrease in mass while some other will increase. The enzyme cleaves the donor polysaccharide from a site close to the reducing end and then transfers the acceptor oligosaccharide which has lower *Mr* (relative molecular mass) [42].

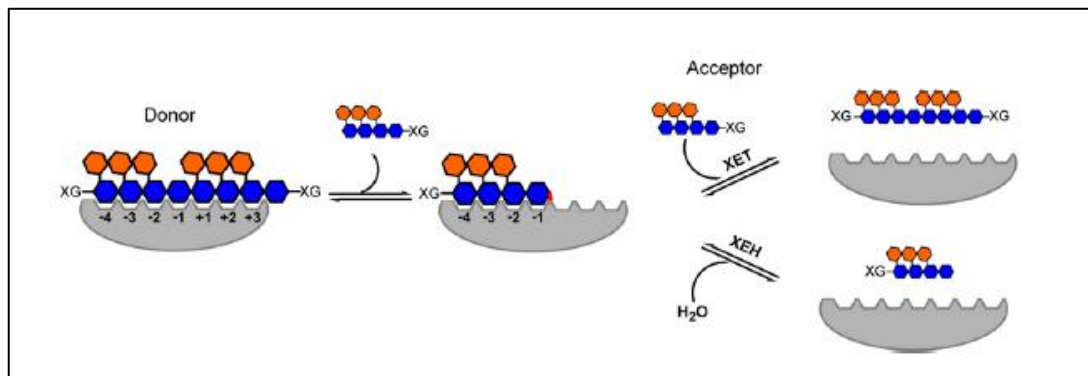


Figure 1.7. A schematic representation of XET and XEH enzyme mechanisms. On the left, donor xyloglucan binds to the XET/XEH enzyme and it is cleaved by the enzyme resulting in covalently linked glycosyl-enzyme intermediate. On the right, this intermediate is broken down by an acceptor either water (XEH) or non-reducing xyloglucan molecule (XET) [40].

It has been shown that plant cell growth is controlled by how the xyloglucans are integrated into the wall and the molecular size of the free xyloglucans. This integration occurs in two ways; first the synthesized and secreted xyloglucans encounter nascent cellulose microfibrils at the plasma membrane surface and anchor its terminus into the microfibrils. Secondly, the xyloglucans secreted into the cell wall is transglycosylated by the XETs that are found in apoplastic space. The molecular size of the xyloglucan which is a tether between cellulose microfibrils can be decreased when xyloglucan oligosaccharide (XXXG) is added into the wall. XET bound to the xyloglucan cleaves and transfer the reducing end to XXXG non-reducing end and cause the cleavage of the tether [43].

Endotransglycosylation occurs in two ways; between two xyloglucan polysaccharides ( $P \rightarrow P$ ) or between a xyloglucan polysaccharide and a xyloglucan oligosaccharide ( $P \rightarrow O$ ) (Figure 1.8). When the reducing end of the xyloglucan acceptor is <sup>3</sup>H-labelled (radioactive) and is transglycosylated to the donor xyloglucan molecule which is non-radioactive and so higher molecular weight xyloglucan chain is produced. Also, the acceptor oligosaccharide (XGO) is fluorescently labeled with sulphorhodamine and it is transglycosylated to the donor xyloglucan which has higher molecular weight. In this case, XGO-sulphorhodamine acceptor substrate is used in high- throughput screening of XET activity. Xyloglucan oligosaccharides as acceptor substrates are more preferable than polysaccharides due to

their favorable kinetics. There is also oligosaccharide- oligosaccharide transglycosylation but small donors are not preferred [39].

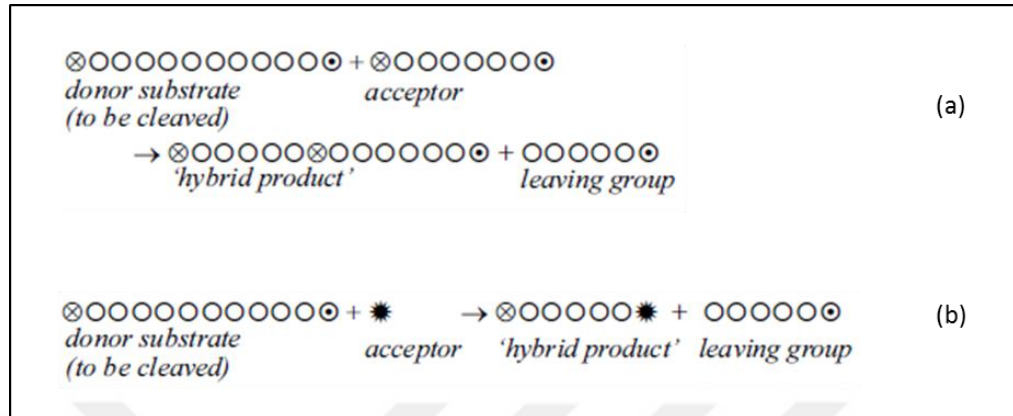


Figure 1.8. Representation of two different endotransglycosylation (XET) reactions; (a) Polysaccharide to polysaccharide ( $P \rightarrow P$ ) endotransglycosylation, (b) Polysaccharide to oligosaccharide ( $P \rightarrow O$ ) endotransglycosylation. The empty circles refer to one  $\text{Glc}_4$ -based xyloglucan oligosaccharide and the circles with dots refer to the reducing sugars. The acceptor circle refers to fluorescently or radioactively labelled oligosaccharide [39].

The xyloglucan polysaccharides are the main donor molecules for XTHs which can show greater or lesser reaction rates with fucose residue containing xyloglucans. For example, XTH from tomato plant gives priority to solanaceous xyloglucan that has no fucose residue instead of other xyloglucans. XGOs (xyloglucan oligosaccharides) are used as acceptor molecules for XET activity. It was shown that the reducing terminus is not essential unlike the Xyl/Glc-rich backbone which is essential for acceptor function. The possible residues such as fucose or galactose are not important for this function, however they may influence the enzyme- substrate interactions [44].

XTH enzymes are found in apoplast and optimal pH for this place is between 5 and 6. The amino acid sequence of the XTH enzyme active sites is DEIDFEFLG which is conserved in most of the enzymes [39]. They belong to the subfamily glycoside hydrolases GH16 (Glycoside Hydrolase family 16) group of enzymes in CAZy (Carbohydrate- active enzymes) classification [45]. GH16 enzymes show diverse substrate specificities with members that cleave  $\beta$ -(1 $\rightarrow$ 3) or  $\beta$ -(1 $\rightarrow$ 4) bonds in glucans and galactan chains. In GH16 family, XTH gene products are closely related with bacterial  $\beta$ -(1 $\rightarrow$ 3) ;  $\beta$ -(1 $\rightarrow$ 4)- glucan

hydrolases [40]. Phylogenetic analysis revealed that XTH enzyme families of different species are classified into three main groups as I, II and III based on their amino acid sequences with Group III is further divided into sub-groups as Group IIIA and Group IIIB [39]. Newly added fourth group that includes small number of XTH enzymes are called as Ancestral Group. Also another group called EG16 Group was added to the classification which has at least one endo-glucanase enzyme [39, 46] (Figure 1.9).

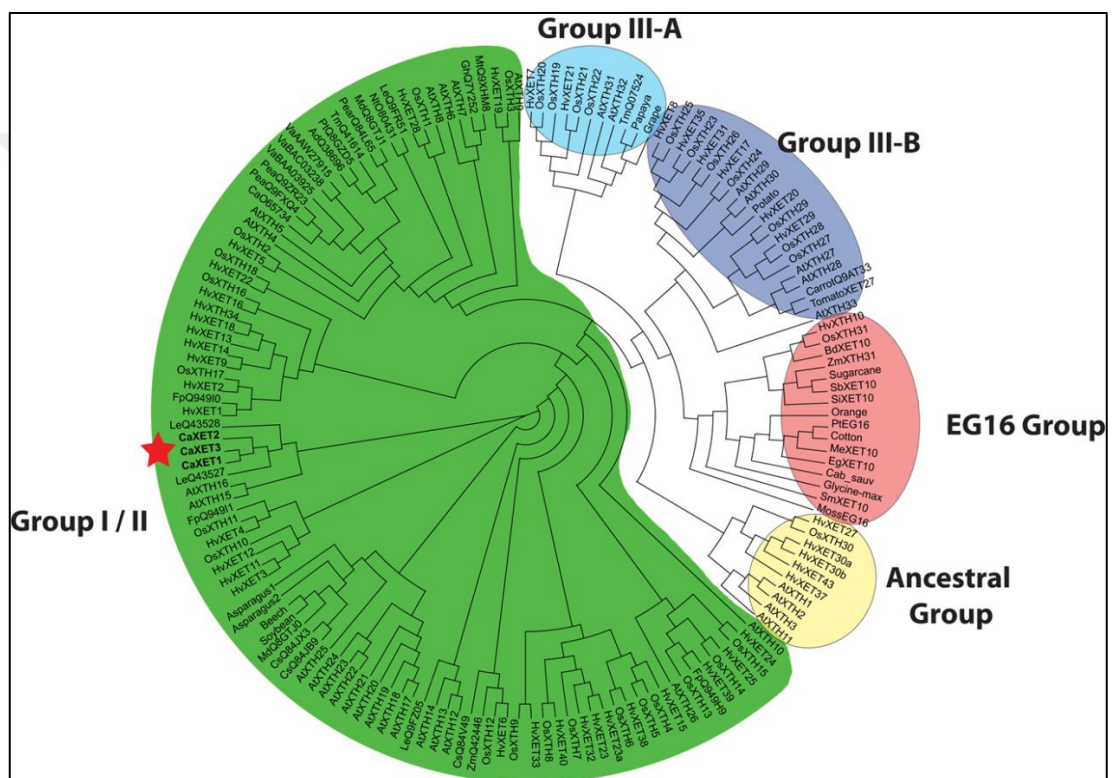


Figure 1.9. The phylogenetic tree of GH16 enzymes based on their amino acid sequences.

Group I, II IIIA and IIIB contain XET enzymes. The red star indicates the enzymes included in abiotic stress studies.

XTH enzymes are encoded by large multigene families in higher plants. While the model organism, *Arabidopsis thaliana* contains 33 genes, the other land plants from vascular and non-vascular to monocots and dicots have 20- 60 genes for XTH enzyme. The abundance of those genes brings to mind that XTH enzymes show tissue specificities and also specific properties. They exhibit different expression patterns based on different environmental and developmental stimuli. XTHs have been correlated with the formation of aerenchyma,

generation of tracheary elements, ripening of the fruits, responding to harsh environmental conditions such as wind or touch, elongation in epicotyls, protecting against parasites and weakening of the endosperm cap during seed germination [41] suggesting that, XTHs have also important function catalyzing the depolymerization or solubilization of xyloglucan during wall disassembly [39]. According to the expression studies with *Arabidopsis thaliana*, specific XTH enzymes were determined in division, differentiation or elongation regions of the roots including different tissues such as root hairs and vascular tissues. For instance, *AtXTH12*, *AtXTH13* and *AtXTH14* generated by gene duplication process are expressed especially in roots. Difference of optimal pH and temperature values for diverse XTH enzymes also support the idea of specificity in enzymic activities [41].

Different *XTH* genes are responsible for different morphological changes in plants. For instance; in *Arabidopsis thaliana*, *AtXTH22* gene is induced when facing mechanical stresses such as wind or touch and its expression resulted in shorter phenotypes. *XTH* genes also show variable responses to different hormones and biotic and abiotic stresses and undergo upregulated expression especially, in response to growth promoting hormones such as auxins, gibberellic acid or brassinosteroids [39]. The expression of *CaXTH 3* gene that belongs to *Capsicum annuum* hot pepper plants is induced by abiotic stresses such as high salinity, drought and cold temperature. They were transformed into tomato plants to enhance their tolerance to those stresses and their stress resistance was increased [8].

Rice (*Oryza sativa*) and *Arabidopsis thaliana* have similar number of gene families and members. In *Oryza sativa*, 29 (*OsXTH*) *XTH* genes are present while in *Arabidopsis thaliana*, there are 33 (*AtXTH*) *XTH* genes. It is significant because xyloglucans are found in much lesser amount in *Oryza sativa* than in *Arabidopsis thaliana*. XTHs are highly conserved in all land plants with strong conservation of the XET domain with only one amino acid variation on catalytic site. For example, in *AtXTH9* and *AtXTH11* genes, some amino acid alterations were observed at their catalytic domain. They also appear in monocots which are lack of abundant xyloglucans [38] and this situation supports the interpretation that XTHs also act as heterotransglycosylating enzymes that links different polysaccharides [31].

## 1.7. HETEROLOGOUS PROTEIN PRODUCTION AND PICHIA PASTORIS

For the structure of the plant and characterization of proteins they should be obtained in a purified state and observed at different time intervals to see its effects. This process is time-consuming on living organisms and purifying a specific target protein among similar proteins is very difficult. Another technique, heterologous expression of the genes encoding the target proteins in a host is developed and began to be widely used. By this method, recombinant plant proteins can be produced in active form and at adequate levels for their structural and biochemical characterization [47].

The methylotrophic yeast *Pichia pastoris* has become one of the mostly used hosts for heterologous expression of eukaryotic genes thanks to its ease of usage for genetic modifications due to the high gene targeting and high transformation rate abilities. Also, high levels of protein production can be achieved by *Pichia pastoris* expression system. Most importantly, this eukaryotic system has the ability to mediate post-translational modifications including glycosylation, cleavage of newly produced proteins and forming disulphide bonds etc. which allows for production of soluble and correctly folded proteins. Linearized DNA is inserted into host genome via homologous recombination to generate stable transgenic lines. Also it is known that *P. pastoris* secretes low level of non-recombinant proteins that supports downstream purification [47, 48, 49].

Heterologous protein production in *Pichia pastoris* system has multiple stages that needs to be considered. The target DNA sequence is cloned into a vector with suitable promoter and transcription terminator sequence. The vector that has the protein coding DNA sequence is transformed to the yeast to provide the stability. Then, heterologous expression of the protein of interest into an appropriate culture environment and obtaining the pure and concentrated protein of interest [49].

Another benefit of *P. pastoris* system is the availability of strong promoters for the expression of foreign genes of interest and production of target proteins at large amounts with ease and low cost. This system gives chance to choose from various *P. pastoris* strains and vectors with a wide promoters, selectable markers and secretion signal choices. In order to control the heterologous protein production and reduce the selection of the cells which do not express the protein of interest, an inducible promoter is needed [50]. The

*AOX1* (alcohol oxidase 1) promoter is considered as an effective promoter which can be induced by methanol [48]. In order to clone a foreign protein into the vector, vector has to include a multiple cloning site (MCS) for cloning of the gene of interest that encodes the protein with a transcription termination sequence and also a selection marker gene for the selection of transformant cells.

Although *P.pastoris* is a suitable host for heterologous expression, it has also some disadvantages. During the secretion of newly expressed proteins into the medium proteins might be degraded. In order to prevent the degradation, optimum media conditions might be provided by arranging the pH and temperature and also protease deficient strains can be used as host [51]. The SMD1168 strain of *P. pastoris* which is protease-deficient and so more suitable for expression of certain heterologous proteins [50].

## 2. MATERIALS AND METHODS

### 2.1. TARGET SELECTION FOR PROTEIN EXPRESSION, CODON OPTIMIZATION AND PRIMER DESIGN

It has been known from the literature that Xyloglucan endotransglycosylase/hydrolase (*XTH*) genes increase tolerance to abiotic stresses and increased expression of pepper (*Capsicum annuum*) *XTH* genes in *Arabidopsis thaliana* and tomato plants provide resistance to drought and salt stresses. Based on those research, pepper CaXTH2 enzyme was chosen for salt stress studies of this project. For the heterologous expression in *P.pastoris*, plant gene sequence was modified according to the host organism. Since the preference of the codons representing different amino acids may vary from organism to organism, codon optimization of the plant gene was performed according to *P.pastoris* and also signal peptide coding region of gene sequence was removed by GenScript company. *CaXTH2* gene was obtained in pPicZ $\alpha$ -C yeast expression vector from the company. Since this vector contains 6 Histidine amino acid codon in its cloning region, expressed protein will contain 6-His tag at C terminal end and this will facilitate the detection and purification of the protein.

Gene specific primers for *CaXTH2* were designed and ordered from Centromer DNA company (Table 2.1). Primers were designed using Primer 3 program and validated using 'NetPrimer' program. Since *XTH* genes in pepper plants are homologous to each other BLAST program used to prevent any matching sequences and unique primer couple sequences were designed. For further QPCR studies, 6 different housekeeping genes *CaACTIN*, *CaUBIQUITIN*, *CaGAPDH*, *CaEIF5A2*, *Ca $\alpha$ -TUBULIN* and *Ca $\beta$ -TUBULIN* were chosen as reference genes since they are all expressed in every cell and their expression levels are the same despite changing conditions and their primers were ordered. Optimization studies were performed for those 6 housekeeping genes using their primers and as a result of the studies *CaACTIN*, *CaEIF5A2* and *Ca $\alpha$ -TUBULIN* which give the best results were chosen as reference genes for further QPCR analysis.



Table 2.1. Forward and reverse primer sequences for *CaXTH2* gene for QPCR studies.

	Forward Primer Sequence	Reverse Primer Sequence
<i>CaXTH2</i>	ATGCAAGCGTTCAAGGTTCT	AAAACAATTCATTCTATTTC AAGATTAC

## 2.2. HEAT SHOCK TRANSFORMATION AND PLASMID ISOLATION

Lyophilized pPicZ $\alpha$ -C plasmids containing *CaXTH* gene were dissolved in ddH<sub>2</sub>O and heat shock transformation to *E.coli* DH5 $\alpha$  was carried out [52]. Competent cell preparation was done before transformation [53]. Transformed bacteria cells were grown in 5 ml Low Salt LB broth media containing zeocin at 200 rpm 37 °C overnight as recommended by “EasySelect *Pichia* Expression Kit Manual, Invitrogen, CA”. The next day, plasmid isolation was performed using “Nucleospin Plasmid Isolation Kit” (Cat no:740588). 30 percent glycerol stock of DH5 $\alpha$  cells containing *CaXTH2* gene in pPicZ $\alpha$ -C plasmid was prepared and kept at -80°C.

## 2.3. TRANSFORMATION INTO YEAST

In order to linearize the pPicZ $\alpha$ -C plasmids including *CaXTH2* gene, digestion reaction was performed for 10 $\mu$ g of plasmid using *DraI* restriction enzyme. In this way, linearized plasmids were ready to be transformed into yeast *Pichia pastoris* SMD1168H cells by electroporation method [54]. For this transformation method, “Bio-Rad Gene Pulser” device with 1,5 kV, 25  $\mu$ F and 200  $\Omega$  values were used. After electroporation, samples were resuspended in 1M sorbitol and YPD containing tube and incubated in the shaker at 30 °C for 2 hours. In order to determine the transformed colonies, streaking on YPDS agar plates containing zeocin was performed according to the instructions of “Invitrogen, EasySelect *Pichia* Expression Kit Manual” (K1740-01).

## **2.4. SELECTION OF THE ACTIVE ENZYME PRODUCING COLONIES**

### **2.4.1. Selection of CaXTH2 Producing Colonies**

Selection of transformant colonies were performed according to Invitrogen, EasySelect Pichia Expression Kit Manual” as described before. Transformant colonies from CaXTH2 (10 colonies) were inoculated into 10 ml BMGY medium in falcon tubes to start culture and grown at 30 °C and 170 rpm overnight until the OD<sub>600</sub> values reached between 2 to 6. Next day after OD<sub>600</sub> measurements, samples in falcon tubes were precipitated by centrifugation (8 minutes at 3220 x g) and resuspended in 10 ml BMMY medium to make the OD<sub>600</sub> value of 1. Samples then were incubated in shaker at 22 °C 170 rpm for 5 days and once a day induction by methanol addition (1 percent of medium) was performed. At the end of 5 days incubation, cells were precipitated by centrifugation for 10 minutes at 10000 x g and supernatant was used for further analysis.

### **2.4.2. TCA-Acetone Precipitation, SDS-PAGE, Western Blotting**

Since protein concentration is low in supernatant, TCA- acetone precipitation method was performed to precipitate and obtain proteins. 900 µl of supernatant was mixed with 100 µl of TCA (100 percent) and incubated on ice for an hour. Then, proteins were precipitated by centrifugation at +4 °C, 12000 x g for 10 minutes. 800 µl acetone (-20 °C , HPLC grade) was added onto the pellet and tubes were incubated overnight at -20 °C. Centrifugation at +4 °C, 6500 x g for 10 minutes was carried out to pellet undissolved proteins. Washing with acetone step was repeated twice with 30 minutes time intervals. After final centrifugation acetone was discarded, tubes were kept on the bench until pellet was completely dried and then it was dissolved in ultrapure water. For screening of the proteins of interest, SDS-PAGE gel electrophoresis was performed using Hoefer Minigel System bound to Bio-Rad Universal power source. In order to prepare samples for loading to the gel, 2x Laemmli Sample Buffer was mixed with samples and samples were first boiled at 95 °C for 8 minutes, then centrifugation was carried out at 5000 x g for 3 minutes in order to avoid any reduction of sample because of boiling. Proteins were separated in 12 percent polyacrylamide gel and for visualization of the gel Coomassie Brilliant Blue

method was performed. The gel was stained using Coomassie Brilliant Blue dye by incubating in it for 45 minutes on shaking platform and then destaining was done by washing with ultrapure water on shaking platform same as in staining. Another 12 percent polyacrylamide gel was prepared and Western blotting was performed using “Thermo Pierce Power Blotter” (25 V, 30 min) and “Trans Blot Turbo Transfer Pack” 0,2  $\mu\text{m}$  nitrocellulose membrane in order to control the protein expressions. After transfer, membrane was incubated in blocking solution (5 percent non-fat milk) overnight. After discarding blocking solution, membrane was treated with “Abcam Anti-6X His” antibody in TBS-T solution for an hour at RT and then washed twice with TBS-T, each time for 5 minutes and once with PBS for 10 minutes. “Amersham ECL Prime Western Blotting Detection Reagents” (GE Healthcare Cat. No. Rpn232) were mixed with PBS and added onto the membrane in dark and images were taken by Image Lab software immediately after that.

2  $\mu\text{l}$  aliquot of each culture sample was used for activity testing on HPLC. Enzyme reactions were prepared with 10  $\mu\text{l}$  of 0,4 percent (w/v) donor substrate, 1  $\mu\text{l}$  of 50  $\mu\text{M}$  sulforhodamine-tagged acceptor substrate and 2  $\mu\text{l}$  of culture sample and incubated at 30  $^{\circ}\text{C}$  for 24 hours in PCR device to avoid any contamination. At the end of 24 hours, reactions were stopped by 6  $\mu\text{l}$  of 90 percent formic acid. Screening of proteins and enzyme activity results were compared to approve active enzyme producing colony and to start large-scale enzyme production from that single colony.

## **2.5. DONOR AND ACCEPTOR SUBSTRATES**

For activity analysis of the CaXTH2 enzyme, donor and acceptor substrates were used for reactions. All acceptors and donors were obtained from Megazyme International, Ireland company except hydroxyethyl cellulose (HEC) which was bought from Fluka (Sigma-Aldrich). As acceptor oligosaccharides; xyloglucan oligosaccharides (XGOs), xyloglucan heptasaccharides (X7), (1 $\rightarrow$ 4)- $\beta$ -D-xylotetraose (XT), (1 $\rightarrow$ 4)- $\beta$ -cellotetraose (CT), (1 $\rightarrow$ 3);(1 $\rightarrow$ 4)- $\beta$ -glucotetraose A (BA), (1 $\rightarrow$ 3);(1 $\rightarrow$ 4)- $\beta$ -glucotetraose B (BB), (1 $\rightarrow$ 3);(1 $\rightarrow$ 4)- $\beta$ -glucotetraose C (BC), laminaritetraose (LT), galactosyl mannotriose (GM) were used. Acceptor oligosaccharides were tagged with sulforhodamine B fluorescent dye. The stocks of oligosaccharides were kept at -20  $^{\circ}\text{C}$  and aliquoted for use by diluting them

with ultrapure water to 50 $\mu$ M concentration and kept at +4 °C. As donor polysaccharides; tamarind seed xyloglucan (TXG), barley  $\beta$ -glucan (BBG), hydroxyethyl cellulose (HEC) were used. All donor polysaccharides were prepared at 0,8 percent (w/v) concentration and diluted to 0,4 percent with 0,2M ammonium acetate with 1:1 ratio. The pH value of ammonium acetate used for dilution was determined depending on enzyme's working pH value.

## **2.6. HPLC ANALYSIS**

For activity analysis of the enzyme "Agilent 1100 Series" high pressure liquid chromatography (HPLC) system including FLD fluorescent detector was used. It was known that Sulforhodamine B fluorescent dye excites light at 570 nm wavelength and emits light at 590 nm wavelength. The reactions that were run on HPLC system was analyzed with the separation of donor and fluorescent tagged acceptor substrates using a BioSep-SEC 4000 column, 75x7,80 mm (Phenomenex, Torrance, CA) with a mobile phase comprised of 0,1 M 80 percent ammonium acetate at pH 6.0 and 20 percent acetonitrile in 0,5 ml/min flow rate. Then, the evaluation of reaction results were done using ChemStation software program (Agilent Technologies, Palo Alto, CA). 19  $\mu$ l volume of the reaction was completed to 30  $\mu$ l by adding 11  $\mu$ l of ultrapure water into reaction tubes and 15  $\mu$ l of it was injected by the device.

## **2.7. LARGE SCALE PROTEIN PRODUCTION AND PURIFICATION**

Active enzyme producing colony which is the CaXTH2-2 was selected according to the results of the activity analysis on HPLC and screening. By using that single colony (2<sup>nd</sup> colony) large- scale protein production was performed as it was explained before on Section 2.4. Production was started with small-scale (400 ml) BMGY culture and after obtaining desired OD<sub>600</sub> values culture medium changed to BMMY (2L) for large-scale production of the protein. Starting from the 3<sup>rd</sup> day of methanol induction to the cells in BMMY medium, everyday one enzyme activity reaction was prepared (20 hours incubation at 30 °C) and run on HPLC. After 5 days of methanol induction was completed, *P. pastoris* cells and BMMY medium were removed by centrifugation at 10000 x g for 10

minutes and all supernatant was filtered with 0,2  $\mu\text{m}$  RC Filter (Sartorius AG, Germany) and transferred to new clean bottles. Ammonium sulphate protein precipitation method was performed by adding ammonium sulphate solution slowly onto the supernatant solution at +4  $^{\circ}\text{C}$  until ammonium sulphate was dissolved completely and its concentration reached to 85 percent (w/v). Culture proteins were divided into falcon tubes and precipitated by centrifugation at 12000 x g, +4  $^{\circ}\text{C}$  for 20 minutes and the supernatant was discarded. Protein pellet in falcons were dissolved in 10ml 20mM sodium phosphate buffer solution with pH 7.4 and collected into one bottle. The next day, remaining ammonium sulphate in protein solution was removed by dialysis method. All protein solution was transferred into 4 different cellulose dialysis membranes and membranes were soaked into 15 ml 20mM sodium phosphate buffer solution (pH 7.4) containing tanks which were at +4  $^{\circ}\text{C}$  cold room. Sodium phosphate buffer was refreshed after 3 hours incubation and kept overnight. Next day, proteins which were heterologously produced with 6XHis-tag were purified by affinity chromatography using “AKTAprime Plus (GE Healthcare)” system. Proteins were purified via 5 ml volume HisTrap FF (GE Healthcare) column according to manual instructions. Elution of the protein was carried out with 0,5 M imidazole containing elution buffer. Then, buffer exchange to 0,1 M ammonium acetate (pH 6.0) was carried out using “HiPrep 26/10 Desalting column” (GE Life Sciences). Purified protein solution in ammonium acetate buffer was concentrated to 5 ml by centrifugation at 3220 x g, +4  $^{\circ}\text{C}$  with “Millipore Centrifugal Units (Amicon Ultra-15 Centrifugal Filter Unit, Cat. No. UFC900324, MWCO 3000)” for around 30 minutes. For concentrated proteins, further purification step-polishing- was performed by passing the enzyme through “HiPrep Sephacryl S200 HR” column using the AKTAprime Plus (GE Healthcare) system”. First of all the column was conditioned with 0,1 M ammonium acetate and the protein was separated based on their size and collected into falcon tubes (fractions between 26-74) which was called fractionation. Since there were 50 fractions of proteins, they were combined as triplicates to make SDS-PAGE method easier and concentrated using Millipore Centrifugal Units at 3220 x g, +4 $^{\circ}\text{C}$  for 40 minutes as before until the volume was around 250- 500  $\mu\text{l}$ . In order to find out which fractions contained the protein of interest, fraction triplets were loaded to 12 percent polyacrylamide gel and stained with Silver nitrate solution. Also, Western blotting was performed as in small-scale production before by transferring separated proteins to “TransBlot Turbo Transfer Pack” 0,2  $\mu\text{m}$  nitrocellulose membrane and treated with “Abcam Anti- 6X His” antibody. Meanwhile,

activity analysis was done by running enzyme reaction of each triplet fractions on HPLC. According to the screening image results, fractions which gave protein bands on gel were combined (fractions between 38-50) and concentrated to around 2 ml volume. Enzyme that purified completely was kept at +4 °C to be used for enzyme activity analyses.

In order to determine the concentration of purified CaXTH2-2 enzyme, Bradford assay was performed. Different concentrations of BSA standards were prepared (0,125 mg/ml BSA, 0,25 mg/ml BSA, 0,5 mg/ml BSA, 0,75 mg/ml BSA, 1 mg/ml BSA, 1,25 mg/ml BSA, 1,5 mg/ml BSA) and incubated with Bradford reagent and the samples at room temperature for 5 minutes in dark. Then, Bradford measurements were taken at 590 nm wavelength to plot a standard curve and the concentration of CaXTH2-2 enzyme was calculated using the equation of the curve.

## **2.8. PH OPTIMIZATION**

The optimum pH value for activity can vary from enzyme to enzyme. In order to determine the optimum pH value that CaXTH2-2 enzyme worked best, enzyme reactions were prepared at different pH. For those activity tests, TXG donor substrate stocks which were diluted with McIlvaine buffer solution with 1:1 ratio (v/v) to obtain different pH values between pH 4.0 and pH 8.0 and XGO acceptor substrate was used. Also, different enzyme dilutions were tested and 1/2000 diluted enzyme determined as the best working concentration for the enzyme. Enzyme reactions were prepared and incubated at 30 °C for 1 hour. HPLC system was used for detection of the activity.

## **2.9. ACTIVITY ANALYSES**

Purified and concentrated CaXTH2-2 enzyme was used for activity analysis on different substrate couples. Donors and sulforhodamine-tagged acceptors were used as substrate couples to determine which substrates the enzyme was active on. Then, the substrate couple which the enzyme showed the best activity was used for further enzyme kinetic studies. First reactions were set with each substrate couple for 24 hours at 30°C. Then, for each couple, generally 4 time points were determined including the 0. hour according to the activity level of the enzyme. The product formation was detected in fluorescence (a.u.)

by the area under the curve values for each time interval on HPLC image and using that values linear graphs were plotted (fluorescence (a.u.) vs. time) for the calculation of enzyme activity in picokatal/mg units. After the enzyme activity levels in picokatal/mg units were determined for each substrate couple, the relative activity values in picokatal/mg were compared with each other as percentage when TXG-XGO couple activity level was taken as 100 percent.

In addition to enzyme activity analysis, enzyme kinetic studies were carried out with donor TXG and acceptor X7 substrates which CaXTH2-2 enzyme showed the highest activity among others. Enzyme reactions that were prepared with different TXG and X7 concentrations were incubated at 30 °C for 1 hour and the reactions were analyzed via HPLC system as in activity analysis. In order to determine the optimum TXG substrate concentration that the enzyme showed the highest activity, X7 concentration was kept constant at 50 µM and different TXG concentrations between 0,05- 0,08 percent (w/v) were prepared for kinetic reactions. Then, optimum TXG concentration was kept constant and this time different X7 concentrations (1 µM, 5 µM, 10 µM, 15 µM, 20 µM, 30 µM, 50 µM, 70 µM, 100 µM, 150 µM, 200 µM, 250 µM, 300 µM, 400 µM and 500 µM) were used for enzyme reactions. By using those activity results, Michaelis-Menten and Lineweaver- Burke graphs were plotted and  $V_{max}$ ,  $K_m$  and  $K_{cat}$  values were calculated.

## **2.10. CAPSICUM PLANT GROWTH OPTIMIZATION STUDIES**

For salt stress applications and QPCR studies, different varieties of *Capsicum annuum* pepper plants were used in this project. In order to test their germination and growth rate, they were subjected to different methods using different media and environment. For seed germination and growth optimization studies, ultra-pure water with agar, MS (Murashige and Skoog) medium and soil were used. As soon as the seeds were obtained, their germination rate was observed by germinating different types of pepper seeds in the greenhouse. Germination trials were done in soil at 22°C and 16-hour light/8-hour dark photo-period conditions.

After determining the optimum temperature and photo-period conditions, seed germination optimization trials for salt stress applications were performed in *in-vitro* conditions. Before starting germination, seeds were subjected to seed imbibition process in order to wake the

dormant seed up and activate the biochemistry of the embryo by incubating seeds in a tube on a rotater with sterile ultra-pure water for ~ 20 hours. First of all, sterile ultra-pure water containing 0,5 percent agar with pH 5.8 was used as medium for seed germination in laboratory [55]. Before adding 0,5 percent agar, the pH of the ultra-pure water was adjusted to pH 5.8 using 1M HCl and then autoclaved with the agar. Seeds were germinated in 50 ml of sterile ultra-pure water agar with pH 5.8 medium in magenta boxes in plant growth cabinet (Digitech DG1200) adjusted to 22 °C temperature and 55 percent humidity in dark for 5 days. For further seed germination and salt stress trials, MS (Murashige and Skoog) medium was also used as it has been considered as one of the richest plant growth medium composed of macro and micro-nutrients, vitamins and organic compounds. MS medium was purchased as powder and after adding sucrose (20 g/l), all were dissolved in ultra-pure water and its pH was adjusted to 5.8. Then, 0,5 percent agar was also added into the medium before sterilization with autoclave. For pepper plant seed germination, 50 ml of MS agar medium was added to magenta boxes and same growth conditions were used as before. On 5<sup>th</sup> day, after germination magenta boxes were taken to 16-hour light/8-hour dark photo-period conditions in growth cabinet for 6 more days for salt stress applications. Those growth trials were performed and 11-day-old seedlings were used for phenotypic tests and further QPCR studies.

Contamination problem had occurred in most of the magenta boxes since MS medium is one of the richest plant growth media and it is open to any possible microorganism contamination. In order to prevent contamination, surface sterilization optimization experiments were performed on pepper varieties to determine the most efficient surface sterilization method. Seeds were subjected to various sterilization experiments with 70 percent ethanol and different concentration amounts of sodium hypochlorite (NaOCl) (4 percent stock, Merck) with different time periods and the most efficient surface sterilization protocol was decided after statistical analysis (Post Hoc) multiple comparison test as 70 percent EtOH for 1.5 minutes and 25 percent NaOCl (4 percent stock, Merck) for 15 minutes. After surface sterilization method was optimized, seeds were used for further germination studies on MS medium.

In order to obtain more mature pepper plants and apply them different salt stress application such as soaking in NaCl solution on different time intervals, seed germination studies were performed using wet perlite as medium and seeds were kept in dark for first



couple of days and then kept in 16 hour light/8 hour dark photo-period conditions with the temperature between 23 °C- 28 °C, ~ 50 percent humidity in the greenhouse for 3 weeks and then germinated seeds were transferred to soil-peat mixture for another 2-4 weeks for plant growth and salt applications were applied to those plants.

## **2.11. SALT STRESS APPLICATIONS**

As it was mentioned on plant growth optimization section, ultra-pure water with 0,5 percent agar, MS medium with 0,5 percent agar in laboratory and soil in greenhouse were used as different media for salt stress application studies. Salt stress application protocol in Cho et al. (2006) article was mimicked and after seed imbibition and surface sterilization “Erzurum” pepper seeds were germinated in 50 ml of sterile ultra-pure water agar with pH 5.8 medium in magenta boxes in plant growth cabinet (Digitech DG1200) adjusted to 22 °C temperature and 55 percent humidity in dark for 5 days. Then germinated seeds were transferred into 0 mM (control), 50 mM, 100 mM NaCl containing 50 ml of ultra-pure water agar with pH 5.8 medium in magenta boxes and grown 6 days more in 16 hour-light/8-hour dark photo-period. At the end of incubation process, root and shoot lengths were measured and their growth and germination rate were statistically analyzed by “Post Hoc” multiple comparison test. Based on the results of this trial, another salt stress application test was performed with lower NaCl salt concentrations. Erzurum variety seeds were germinated in ultrapure water agar pH 5.8 medium for 5 days as mentioned before and then germinated seeds were transferred on to 5 mM, 10 mM, 20 mM, 30 mM and 40 mM NaCl containing ultrapure water agar pH 5.8 medium for 6 days more in 16-hour light/8-hour dark photo-period. The root and shoot lengths of 11-day old Erzurum variety seedlings were measured.

Using Aktör, Seki, Cila and Samuray varieties salt stress trials on MS agar medium were performed. Seeds were germinated on pH 5.8 MS agar medium for 5 days in dark as mentioned before and then transferred to 0 mM (control), 25 mM and 50 mM NaCl containing MS agar medium in magenta boxes for 6 days more in plant growth cabinets. After measuring their root and shoot lengths, ~100 mg of root samples were taken, washed with ultra-pure water and frozen in liquid nitrogen before they were kept in – 80 °C for

further QPCR analysis. Experiments done in ultra-pure water agar and MS agar medium were in duplicates and for each salt concentration ~20 seeds were germinated.

In addition to previously tested salt stress applications, other optimization methods were tested with more mature seedlings such as spraying the leaves with NaCl solution or watering the pots with NaCl containing water. Upon optimizing the process, plants were grown in soil-peat mixture with watering different concentrations of NaCl (0 mM (control), 30mM, 50 mM, 100 mM, 200 mM and 300 mM). In order to obtain more mature plants, Çanakkale and Kahramanmaraş seeds were germinated on wet perlite in the greenhouse at temperature between 23 °C- 28 °C, ~ 50 percent humidity and 16-hour light/8-hour dark photo-period for 3 weeks. Then, germinated seeds were transferred into pots containing soil-peat mixture and grown for 3 weeks more in greenhouse conditions. 6-week old plants were taken out from pots and roots were washed with water and then soaked into 200 mM NaCl solution for different time intervals (0 minutes (control), 10 minutes, 30 minutes and 120 minutes). Experiments were done with duplicates including control for both varieties and 2 seedlings were used for each time interval. After incubation in salt solution root and leaf samples were collected and frozen in liquid nitrogen and stored in -80 °C for further QPCR analysis.

## **2.12. RNA ISOLATION, cDNA SYNTHESIS AND QPCR**

RNA isolation was performed from the samples of stress treated and non-stress treated pepper plants using “iNtRON Biotechnology easy-spin (DNA free) Total RNA Extraction Kit”. The concentration of eluted RNA samples were measured by “NanoDrop 2000 spectrophotometer (ThermoFisher)” and using measured concentration values (in ng/μl) required RNA template amount for cDNA synthesis reaction was calculated. 5 μg of aliquoted RNA sample was used for cDNA synthesis using “SuperScript® IV First-Strand Synthesis System” (Cat no: 18091050). Isolated RNA samples and synthesized cDNA samples were aliquoted (4-5 μl) after performing each protocol for their quality check via 1 percent (w/v) agarose gel electrophoresis for 45 minutes at 90V. While isolated RNA samples were kept at -80 °C, synthesized cDNA samples which were used as template for QPCR analysis were kept at -20 °C.

In order to determine which housekeeping genes were going to be used for their expression stability under different conditions for QPCR analysis and to determine the optimum  $T_m$  values of those reference gene's primers, gradient PCR studies were performed using "Maximo Taq DNA Polymerase (Geneon)" enzyme. After each gradient PCR protocol, product samples were checked via 1 percent (w/v) agarose gel electrophoresis. Three out of six reference housekeeping genes which showed clear and sharp bands at correct sizes were chosen for QPCR analysis and optimum  $T_m$  values which belonged to those clearest bands were determined. *CaACTIN*, *CaEIF5A2* and *Caa-TUBULIN* were chosen as reference genes. The same optimization studies were performed for *CaXTH2* gene and optimum  $T_m$  temperature was determined based on gel electrophoresis results.

After  $T_m$  values were determined traditional PCR method was performed to bulk up the *CaXTH2* gene products to create calibration curve using copy numbers of gene from  $10^9$  copies/ $\mu$ l to  $10^2$  copies/ $\mu$ l and corresponding cq values. At the end of traditional PCR, products were checked via 2 percent (w/v) agarose gel electrophoresis and reactions containing same gene products were combined in one tube. Bulk up reactions containing *CaXTH2* gene products were then run on "Agilent Tech. 1260 Infinite" HPLC machine with "PLRP-S 1000A 5  $\mu$ M" reverse phase column. In this way, unwanted impurities such as primer dimers, buffer salts, non-specific products were removed and pure gene products were quantified. According to the peak structures given on HPLC, gene products were collected and area under the curve was calculated manually and recorded. After collecting the pure gene product, pUC19 vector (500 ng/ $\mu$ l) was digested with HpaII restriction enzyme to be used as a reference in order to find how many copies of the gene was included in collected amount of product. Reaction containing digested pUC19 vector was run on HPLC machine with "PLRP-S 1000A 5  $\mu$ M" reverse phase column. The peak images on chromatogram were matched with each digested fragment and area under their curve values were calculated. Since it was known that pUC19 was digested into 10-11 fragments with known size of base pairs with HpaII enzyme, exact size of digested fragments corresponding area under the curve values were determined. Since 1  $\mu$ g weight of pUC19 vector was used and it's molecular weight was known from pUC19 vector datasheet (N3041S, lot no:0371209, NEB), mole number in digestion reaction was calculated and the weight of each fragment was calculated in nanograms. The weight of fragments were proportioned to area under the curve values of the fragments and using this

ratio and area under the curve value of collected *CaXTH2* gene, the weight of product was calculated in nanograms. The mole amount of collected *CaXTH2* product was calculated based on its molecular weight. Then, the mole amount of the product was multiplied with Avogadro's number and double strand DNA copy number of collected product was determined. Then, the solution containing *CaXTH2* gene product was evaporated using "Eppendorf Concentrator 5301" and then concentrated product was resuspended in calculated amount of double distilled DNase-free water to obtain  $10^{11}$  DNA strand/ $\mu$ l standard concentration. Using this solution, serial dilution was performed to obtain standards from  $10^9$  copies/ $\mu$ l to  $10^2$  copies/ $\mu$ l. Those standards were used as template and QPCR reactions were set with gene specific primers and using QPCR data cq vs. copy number graphs were plotted for *CaXTH2*. Then, this graph was used for the calculation of gene expression levels of stress-treated and non-treated control leaf and root tissues [56].

After synthesizing cDNAs of control and stress-treated tissues, real QPCR analysis were done. cDNAs were used as template and reactions were set up with housekeeping primers and *CaXTH2* gene specific primers using "Bio-Rad iTero Universal SYBR Green Supermix kit" and reactions were run with 96-well plates in "Bio-Rad CFX96TM Real-Time System" machine. Then, the results were analyzed with "Biorad CFX Manager" program. Normalization studies were carried out with cq values of standardized reference genes and by using "GeNorm" program Normalization factors (NF) were calculated for each sample. In order to prevent any variations that might have occurred during RNA isolation or cDNA synthesis, NF values were applied to the cq values of the samples and normalized cq values were then used to be applied to the equation of the *CaXTH2* gene's calibration curve. From this curve, the double strand DNA copy number of *CaXTH2* gene in tissues were calculated.

### 3. RESULTS

#### 3.1. PROTEIN PRODUCTION AND ENZYME CHARACTERIZATION

##### 3.1.1. Target/Host Selection and Codon Optimization

One of the Capsicum genes, *CaXTH2*, was chosen for this study. After bioinformatic studies were performed with the gene, its signal peptide sequence, start and stop codon sequences were removed in order to make the gene ready to be cloned into the expression vector pPicZ $\alpha$ . The  $\alpha$ -peptide coding sequence, including the start codon, are part of the expression vector pPicZ $\alpha$ -C, whilst 6xHis tag is also present at the 3' end and become part of the *CaXTH2* gene coding region. Expected sequence length (bp) and protein weight of *CaXTH2* gene were determined after codon optimization (Table 3.1). Gene sequence which was prepared for cloning and transformation was delivered in the pPicZ $\alpha$ -C expression vector from GenScript (GenScript, NJ, USA).

Table 3.1. Selected *CaXTH2* gene for heterologous production.

Name of the gene	Plant origin	GeneBank accession number	Length (bp) after optimization	Molecular weight after optimization (kDa)
<i>CaXTH2</i>	<i>Capsicum annuum</i>	DQ439861.1	822	33,88

pPicZ $\alpha$ -*CaXTH2* vector was first transformed into DH5- $\alpha$  *E.coli* cells to increase the amount of plasmid for yeast transformation. Electroporation method which was found as the most efficient technique was used for transformation to *P. pastoris*. In order to select the transformant colonies, YPDS agar medium including zeocin antibiotic was used.

### 3.1.2. Selection of Active Enzyme Producing Colonies

Ten different zeocin resistant *P.pastoris* SMD1168H colonies expected to be expressing, and extracellularly secreting, CaXTH2 enzyme were cultured, and screening for active enzyme was performed. After selection on zeocin-containing plates, grown colonies were picked and inoculated into liquid cultures. After 5 days of methanol induction, supernatants were precipitated by TCA- acetone precipitation method since the enzyme concentration in supernatant was low for screening of CaXTH2 enzyme. SDS-PAGE method was performed for the screening of the proteins by loading them to 12 percent polyacrylamide gel and visualization of the protein bands on the gel was carried out using Coomassie staining, followed by Western blotting. A Coomassie stained SDS-PAGE gel image of the 10 different colonies of CaXTH2 enzyme appeared to show expressed CaXTH2 protein. The strongest looking protein band belonged to the 2<sup>nd</sup> colony of CaXTH2 enzyme at ~40 kDa weight (Figure 3.1).

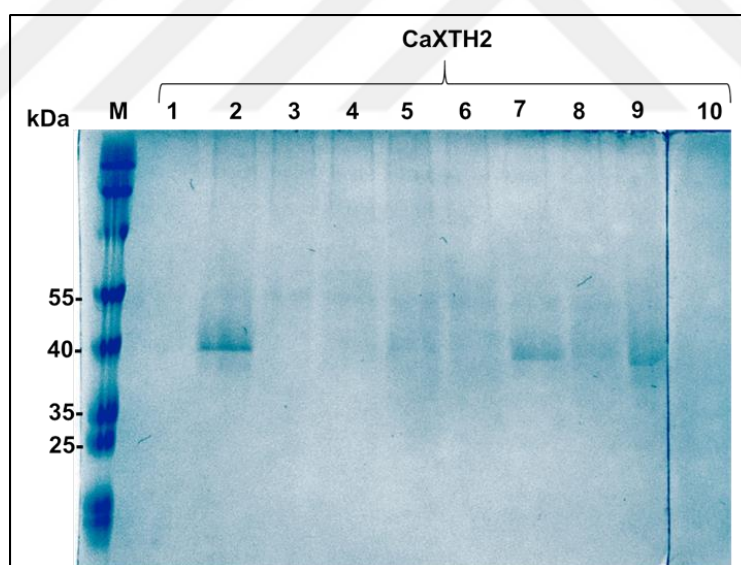


Figure 3.1. The SDS-PAGE image of TCA-acetone precipitated CaXTH2 proteins from small scale cultures of 10 different colonies on a 12 percent polyacrylamide gel. Marker-PageRuler Prestained Protein Ladder (Thermo Fisher).

Western blotted gel image showed the same 10 colonies confirmed by the SDS-PAGE results (Figure 3.2). However, other than 2<sup>nd</sup> colony, there were protein bands on other colonies which were looking less intense. This supported the idea that those colonies did

not produce as much protein as the 2<sup>nd</sup> colony for CaXTH2. At the same time, smear-like banding patterns for the labelled protein bands observed for all colonies supported the idea that those patterns might be due to the differential glycosylation of the proteins. Comparing SDS-PAGE and Western blot results confirmed that the 2<sup>nd</sup> colony producing the highest protein amount. The predicted size of the CaXTH2 protein was ~33,88 kDa including the 6xHis tag and c-myc epitope, but the protein band size of the 2<sup>nd</sup> colony was ~35-40 kDa. This difference is most likely because of the glycosylation of the protein, and the fact that XTH proteins have larger than usual numbers of hydrophobic amino acids which affects their mobility on SDS-PAGE gels.

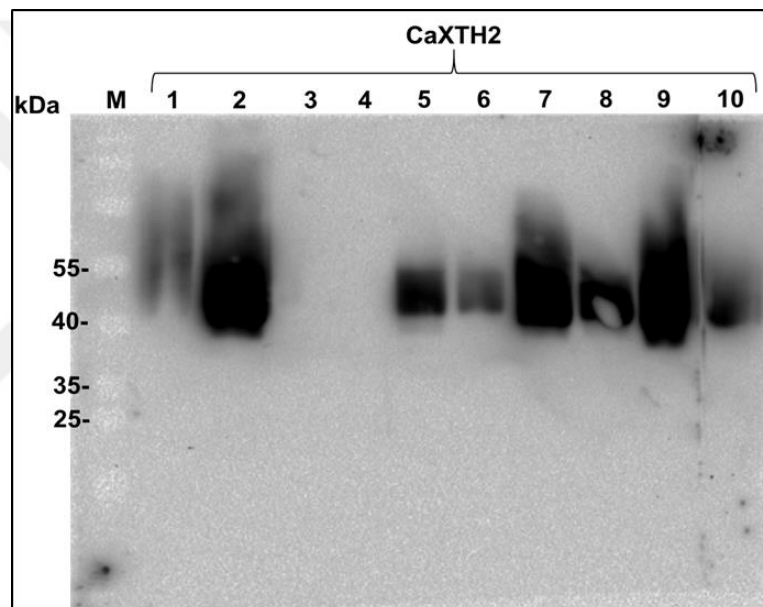


Figure 3.2. Western blotting results of TCA-acetone precipitated CaXTH2 proteins from small scale cultures of 10 different colonies on 12 percent polyacrylamide gel. Marker (M): PageRuler Prestained Protein Ladder.

Selection of transformant active enzyme producing colonies was done via screening of YPDS + zeocin plates and enzyme activity analysis using the HPLC method. According to the HPLC results, more than one colony were found to produce the active protein as in screening results. For CaXTH2 enzyme, the 2<sup>nd</sup> colony was chosen as the most active enzyme producing colony and further large scale production and purification was carried out with CaXTH2-2 (Figure 3.3). Since the larger molecules were detected faster according to the size exclusion principle, the first peak which formed at 2,8 minutes on HPLC

chromatogram was the TXG-XGO transglycosylation products and the area under the curve showed the product amount at the end of the reaction. The peak around 6 minutes represents the sulforhodamine-tagged oligosaccharides which reduces in height as the oligosaccharide is transferred onto the donor molecules. The highest peak at around 2,8 minutes belonged to the most active enzyme producing colony.

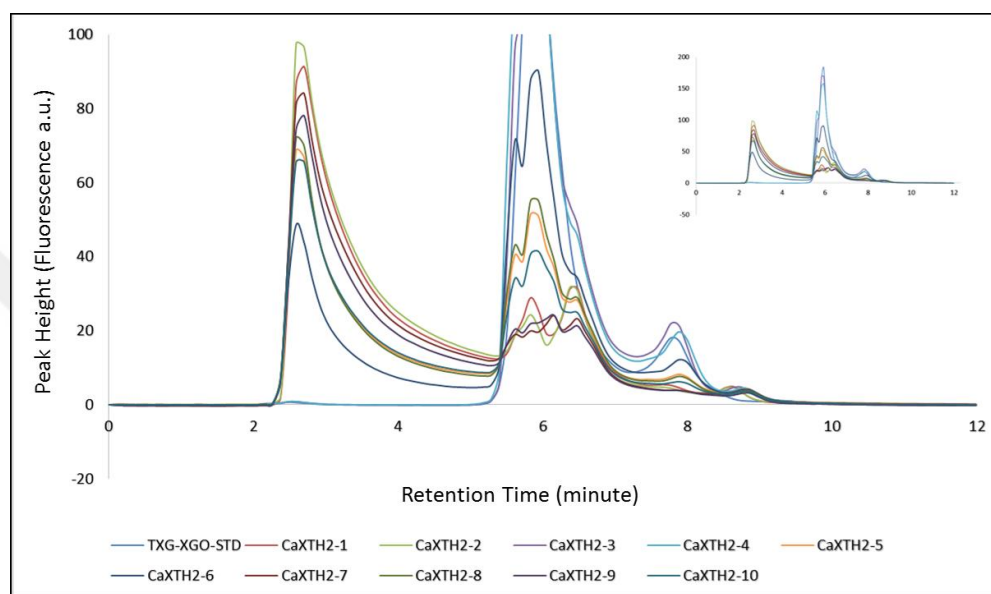


Figure 3.3. Size- exclusion HPLC chromatogram of CaXTH2 enzyme activity from different colonies using the TXG-XGO substrate couple.

### 3.1.3. Large Scale Production

Large scale protein production was carried out with a total of 2L culture medium, followed by an initial ammonium sulphate precipitation. Further purification was carried out via affinity chromatography and after buffer exchange to 0,1 M pH 6 ammonium acetate buffer and concentration of proteins to 5 mL volume, a final purification was carried out by passing the concentrated protein solution through a “HiPrep Sephacryl S200 HR” column which used the size exclusion principle. Fractionation was performed as the larger molecules would be in early fractions and fractions between 26-75 which were showing peak on chromatogram were collected. Since there were a lot of fractions, they were combined in triplets to reduce to 17 fractions and concentrated to ~250-500  $\mu$ l volume



using “Millipore Centrifugal Units”. Then, those concentrated 17 fractions were subjected to Silver staining and Western blotting procedures in order to determine the purest protein of interest including fractions. SDS-PAGE and Western blotting results showed protein bands only in first 9 fraction triplets. The 1<sup>st</sup> fraction triplet did not show any protein bands in any procedure. Starting from the 2<sup>nd</sup> fraction triplet protein bands on variable sizes which might include contaminated proteins started to appear. Pure protein of interest started to be observed with the 5<sup>th</sup> fraction triplet until the 9<sup>th</sup> fraction triplet even if the 9<sup>th</sup> one on Silver stained gel image had very weak protein band (Figure 3.4). However, after Western blotting there was an intense protein band also on 9<sup>th</sup> fraction thanks to the specificity of Western blotting procedure (Figure 3.5).

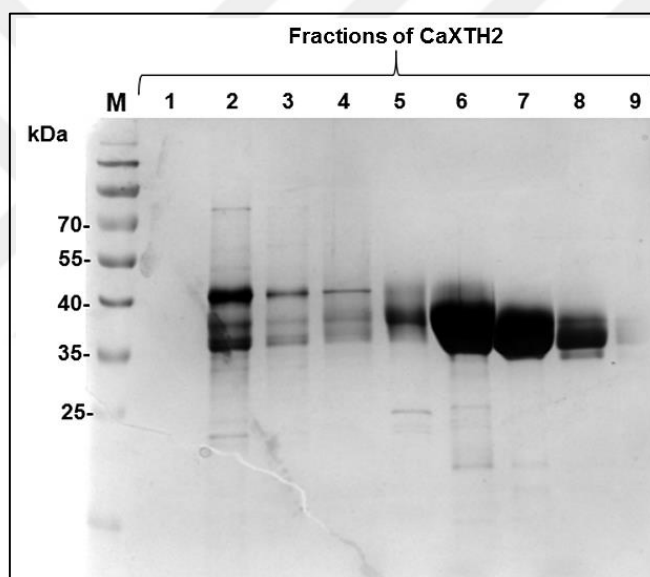


Figure 3.4. Silver stained SDS-PAGE gel image of CaXTH2-2 fractions 1 to 9 obtained from the size-exclusion polishing column. Marker (M): PageRuler Prestained Protein Ladder.

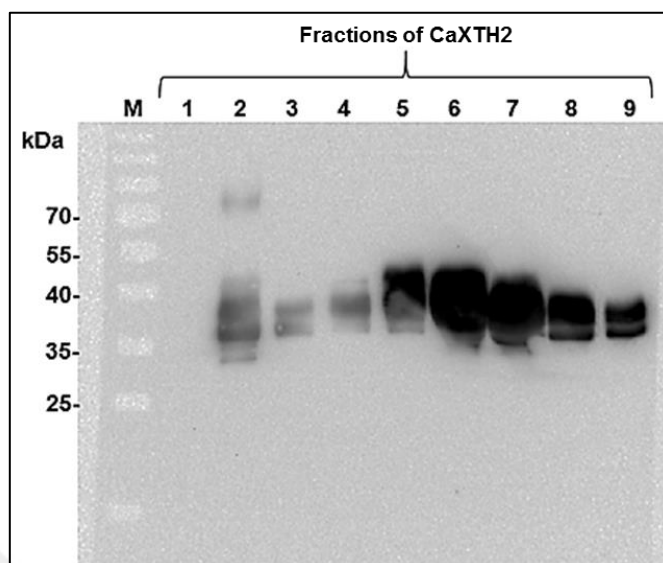


Figure 3.5. CaXTH2-2 fractions from 1 to 9 that were obtained after polishing step on 12 percent polyacrylamide gel and Western blotting using Anti-6xHis antibody. Marker (M): PageRuler Prestained Protein Ladder.

As a result of both detection procedures, the fraction triplets 5, 6, 7, 8 and 9 (fractions between 38-50) which had pure CaXTH2-2 were combined and concentrated to ~2 ml volume. Bradford Assay method was performed to measure the concentration of the protein. The concentration of CaXTH2-2 protein was calculated as 2,723 mg/ml.

#### 3.1.4. pH Optimization

The optimum working pH value that the enzyme showing the highest activity was determined before CaXTH2 enzyme activity analysis. The enzyme was incubated with TXG donor substrate dissolved in McIlvaine buffers that were prepared at different pH values and XGO acceptor substrate for 1 hour at 30°C. Then, the reactions were run on HPLC and the analysis were performed to match the activity levels with pH values. The pH values of TXG-XGO substrate couple ranged from pH 4.0 to 8.0. The CaXTH2 enzyme seemed to be working best between pH 5.5 and 6.5. The enzyme showed the highest activity at pH 6.3 and the activity level seemed to drop after 6.5 but there was still activity even after pH 7 (Figure 3.6). For further enzyme characterization studies, the substrates were prepared at pH 6.3 which was optimum for highest enzyme activity.

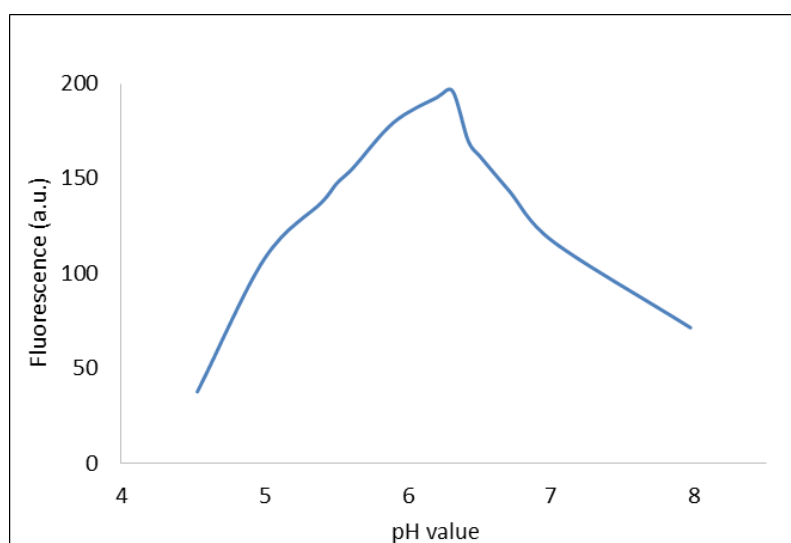


Figure 3.6. The optimization of pH for CaXTH2 enzyme using McIlvaine buffer ranging from pH 4.0 to 8.0.

### 3.1.5. Substrate Specificity and Enzyme Characterization

After optimizing the working pH, the activity of CaXTH2 enzyme was tested on different donor- acceptor substrate couples. TXG, HEC and BBG were used as donor substrates while XGO, X7, XT, CT, BA, BB, BC, LT and GM sulforhodamine-tagged oligosaccharides were used as acceptor substrates. The pH of the ammonium acetate buffers including donor substrates was arranged to 6.3 and enzyme activity was tested on different substrate couples by setting up 24 hour reactions for HPLC analysis. Then, the substrates that the enzyme showed activity on were listed on below table (Table 3.2).

Table 3.2. Donors and acceptors which CaXTH2 enzyme showed activity.

Donors	Acceptors								
<b>TXG</b>	XGO	X7	XT	CT	LT	BA	BB	BC	GM
<b>BBG</b>	XGO		XT	CT	LT	BA	BB	BC	
<b>HEC</b>	XGO	X7	XT	CT	LT		BB	BC	

Further enzyme activity reactions were performed using the donor and acceptor substrate couples on Table 3.2 which the CaXTH2 enzyme was active on. Linear product formation

(fluorescence (a. u.)) vs incubation time graphs were generated for each substrate couple by optimization of the dilution factor of the enzyme and the time intervals that the enzyme worked at its highest performance (Figure 3.7). After determining the time intervals that the enzyme would work the best, the fluorescence (a. u.) values representing the product amounts in this time interval were also determined. Then, the specific activity levels in picokatal/mg values were calculated using those fluorescence (a. u.) and time interval values determined for each substrate couple and a table was drawn (Table 3.3). The activity level of the enzyme was different on each substrate couple and as the activity of the enzyme increased, higher dilution factor and/or shorter incubation times were required to create linear graphs. For each substrate couple, at least 3 different time intervals were determined varying from 10 minutes to 4 hours and each reaction was repeated at least 3 times. According to the Table 3.3, the CaXTH2 enzyme activity levels in picokatal/mg were significantly the highest for TXG-XGO and TXG-X7 substrate couples compared to other substrate couples. Although, the activity level on TXG-XGO was almost half of the activity level on TXG-X7, as 2026,9 picokatal/mg, it was still two to four orders of magnitude higher than the other substrate couples. When HEC was used as donor substrate, the following highest activities belonged to the substrate couples with the same acceptor oligosaccharides XGO and X7 and when HEC-X7 was 11,76 picokatal/mg, HEC-XGO was 11,67 picokatal/mg. The enzyme activity levels were the highest when BA, BB and BC acceptor oligosaccharides were coupled with TXG donor substrate. The highest activity was observed with the TXG-BB substrate couple as 3,008 picokatal/mg and the following was TXG-BA with 2,164 picokatal/mg activity and then TXG-BC with 1,654 picokatal/mg. The activity level with TXG-BB substrate couple was very similar to the activity level with TXG-XT substrate couple which was 3,254 picokatal/mg. There were no detected enzyme activity with HEC-BA substrate couple, and HEC-BB and HEC-BC were very similar to each other with 1,534 picokatal/mg and 1,504 picokatal/mg. Compared to TXG and HEC donor substrates, the enzyme activity levels with BBG donor substrate were the lowest. Also, the activity with LT and GM acceptor substrates were the lowest, when coupled with TXG substrate still highest compared to HEC and BBG. GM acceptor oligosaccharide showed activity only with TXG donor substrate.

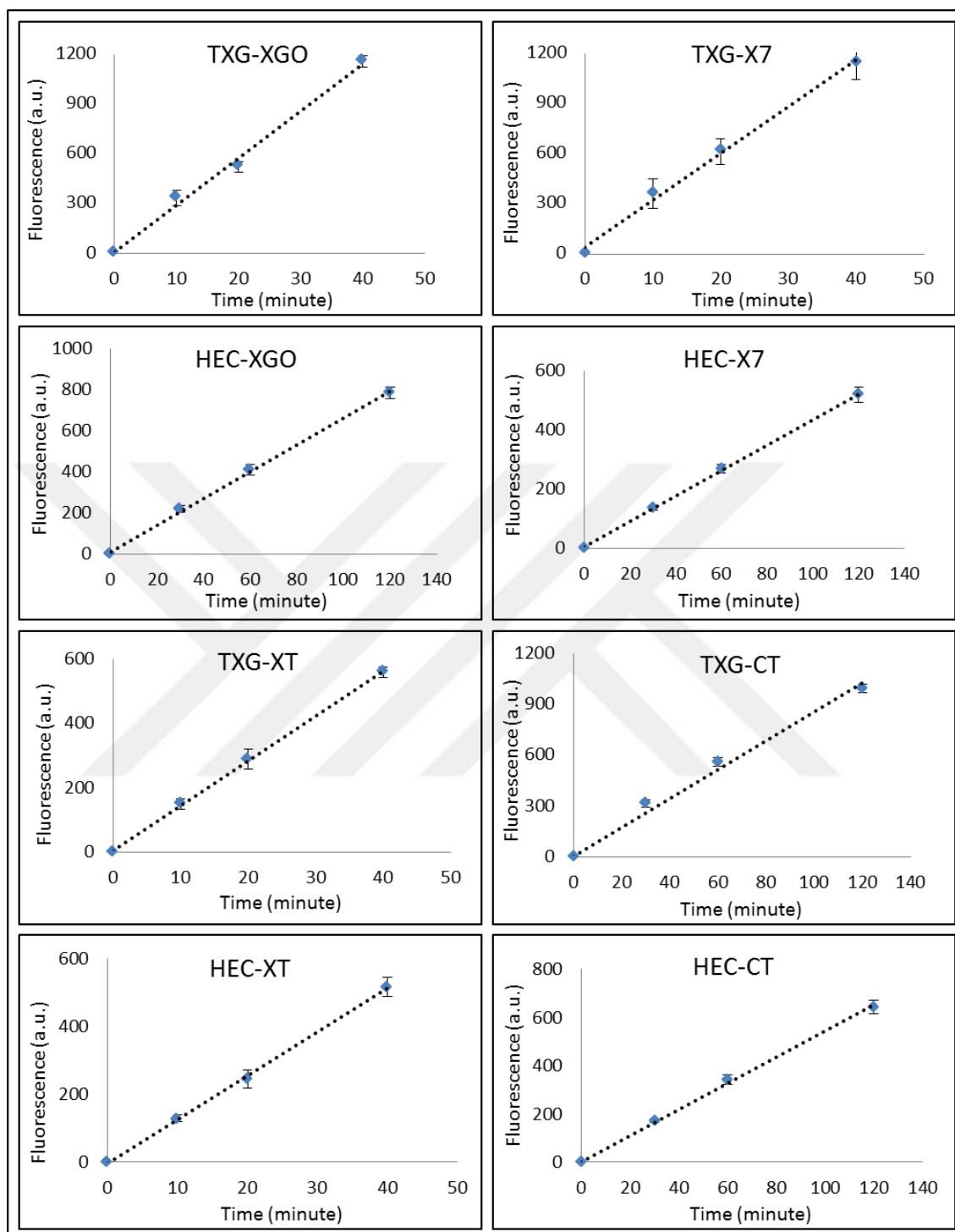


Figure 3.7. The graphs of CaXTH2 enzyme activity on TXG and HEC donor substrates with XGO, X7, XT and CT acceptor substrates based on incubation time and fluorescence (a. u.) value that shows the activity amount on HPLC analysis. Error-bars indicate the variation between the triplicate of results for each time point and substrate couple.

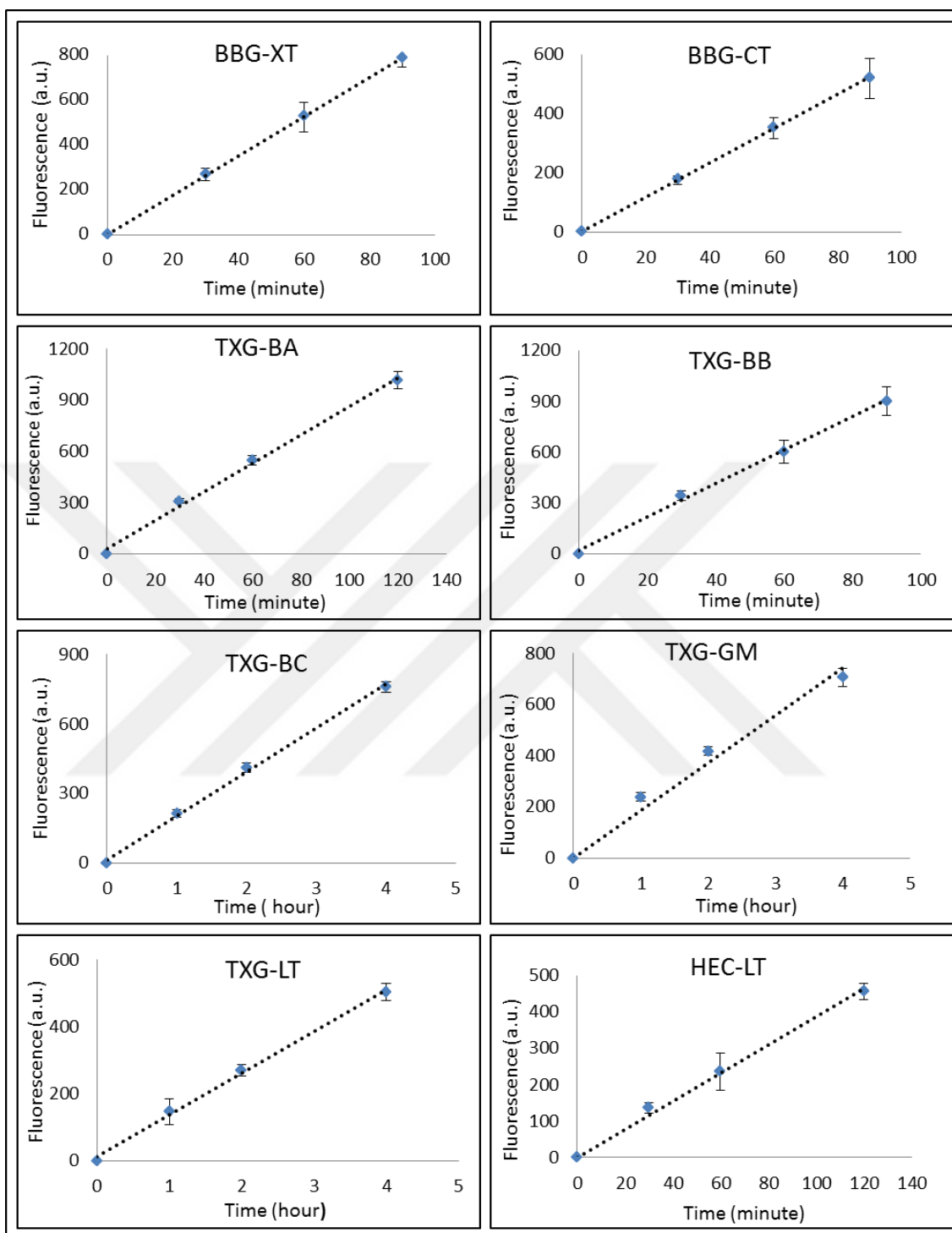


Figure 3.8. The graphs of CaXTH2 enzyme activity on BBG, TXG and HEC donor substrates with BA, BB, BC, GM and LT acceptor substrates based on incubation time and fluorescence (a. u.) value that shows the activity amount on HPLC analysis. Error-bars indicate the variation between the triplicate of results for each time point and substrate couple.

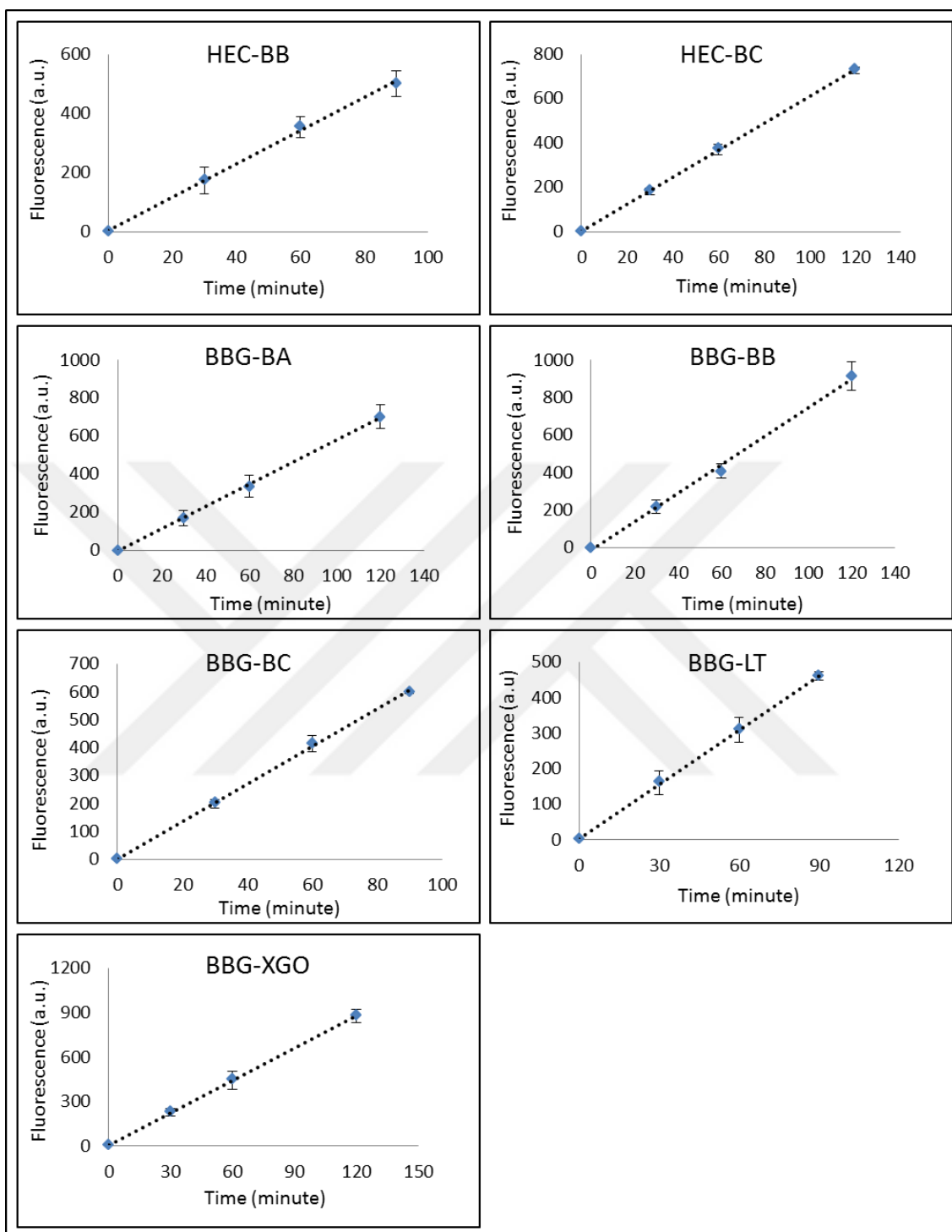


Figure 3.9. The graphs of CaXTH2 enzyme activity on BBG and HEC donor substrates with BA, BB, BC, LT and XGO acceptor substrates based on incubation time and fluorescence (a. u.) value that shows the activity amount on HPLC analysis. Error-bars indicate the variation between the triplicate of results for each time point and substrate couple.

Table 3.3. The activity levels of CaXTH2 enzyme in picokatal/mg value on different substrate couples and as percentages when TXG-XGO substrate couple was set to 100 percent.

<b>Substrate couples</b>	<b>Activity level (picokatal/mg)</b>	<b>Activity level % relative to TXG-XGO</b>
TXG-XGO	2026,9	100
TXG-X7	4121,0	203,3
TXG-XT	3,254	0,1606
TXG-CT	1,842	0,0909
TXG-BA	2,164	0,1068
TXG-BB	3,008	0,1484
TXG-BC	1,654	0,0816
TXG-LT	0,2754	0,0136
TXG-GM	0,3072	0,0152
HEC-XGO	11,67	0,5759
HEC-X7	11,76	0,5803
HEC-XT	1,364	0,0673
HEC-CT	1,015	0,0501
HEC-BB	1,534	0,0757
HEC-BC	1,510	0,0745
HEC-LT	0,1102	0,0054
BBG-XGO	0,6053	0,0299
BBG-XT	0,3866	0,0191
BBG-CT	0,2080	0,0103
BBG-BA	0,2378	0,0117
BBG-BB	0,3820	0,0188
BBG-BC	0,3347	0,0165
BBG-LT	0,1208	0,0060

### 3.1.6. Enzyme Kinetics

After calculating the CaXTH2 enzyme activity levels on different substrate couples in picokatal/mg, enzyme kinetic studies were performed using TXG-X7 donor-acceptor substrate couple on which the enzyme shows the highest activity. In order to obtain the best working concentration of TXG substrate, the reactions were set up using different concentrations of TXG donor substrates varying from 0,05 percent (w/v) to 0,8 percent



(w/v) and X7 acceptor substrate with a constant concentration of 50  $\mu\text{M}$ . Each reaction was set three times for each predetermined time intervals and dilution factors. The reactions were run on HPLC system and specific activity amounts according to TXG donor concentration was determined. After determining the best working TXG donor substrate concentration as 0,3 percent (w/v) for CaXTH2 enzyme, another set of 1-hour reactions were set this time with different concentrations of X7 acceptor substrates varying from 0  $\mu\text{M}$  to 250  $\mu\text{M}$  (0  $\mu\text{M}$ , 5  $\mu\text{M}$ , 10  $\mu\text{M}$ , 15  $\mu\text{M}$ , 30  $\mu\text{M}$ , 50  $\mu\text{M}$ , 70  $\mu\text{M}$ , 100  $\mu\text{M}$ , 150  $\mu\text{M}$ , 200  $\mu\text{M}$ , 250  $\mu\text{M}$ ). Each reaction was set three times and product amounts (fluorescence (a. u.)) which were formed for each X7 concentration were calculated by HPLC system as described before. In order to figure out which X7 substrate concentration was final for the enzyme to produce the maximum product amount, product amount (fluorescence (a. u.)) vs. X7 concentration ( $\mu\text{M}$ ) graph was plotted.

By using a standard fluorescence (a. u.) value of a sample of which the mole amount is known, molarity and the concentrations of the products were calculated. Final concentration of X7 substrate in total volume was determined for each reaction volume which included X7 acceptor substrate with different concentrations. According to those information, reaction rate ( $\mu\text{M}$  product/min),  $1/\text{X7}$  final concentration ( $1/\mu\text{M}$ ) and  $1/\text{reaction rate}$  (min/ $\mu\text{M}$  product) were calculated. Michaelis-Menten (reaction rate ( $\mu\text{M}$  product/min) vs final X7 concentration ( $\mu\text{M}$ )) (Figure 3.10) and Lineweaver-Burke ( $1/\text{reaction rate}$  (min/ $\mu\text{M}$  product) vs  $1/\text{X7}$  concentration ( $1/\mu\text{M}$ )) (Figure 3.11) graphs were plotted. Based on the graph, maximal velocity ( $V_{\text{max}}$ ), Michaelis constant ( $K_{\text{m}}$ ) and turnover number ( $k_{\text{cat}}$ ) values of the enzyme were calculated as 0,0063  $\mu\text{M}/\text{min}$ , 3,6  $\text{min}^{-1}$  and 0,1  $\mu\text{M}$ , respectively.

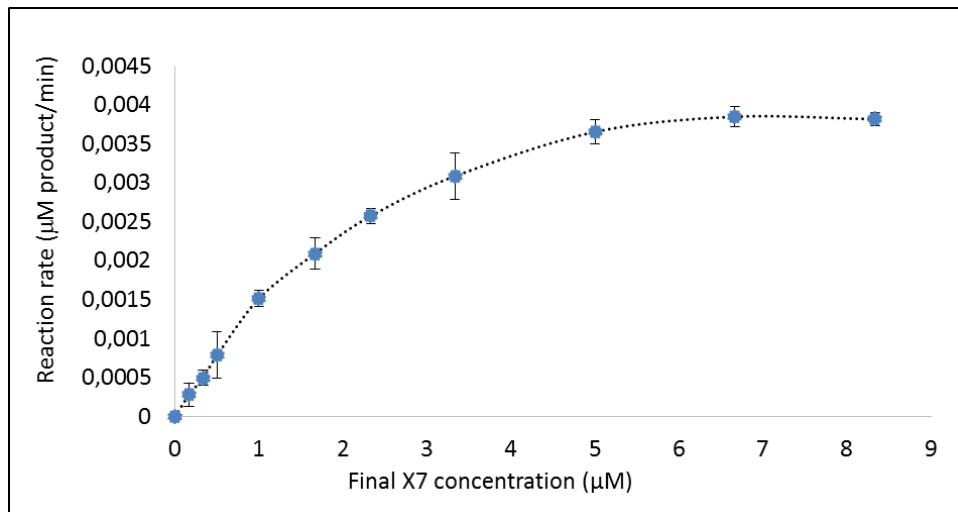


Figure 3.10. Michaelis- Menten (reaction rate ( $\mu\text{M product}/\text{min}$ ) vs final X7 concentration ( $\mu\text{M}$ )) graph of CaXTH2 enzyme.

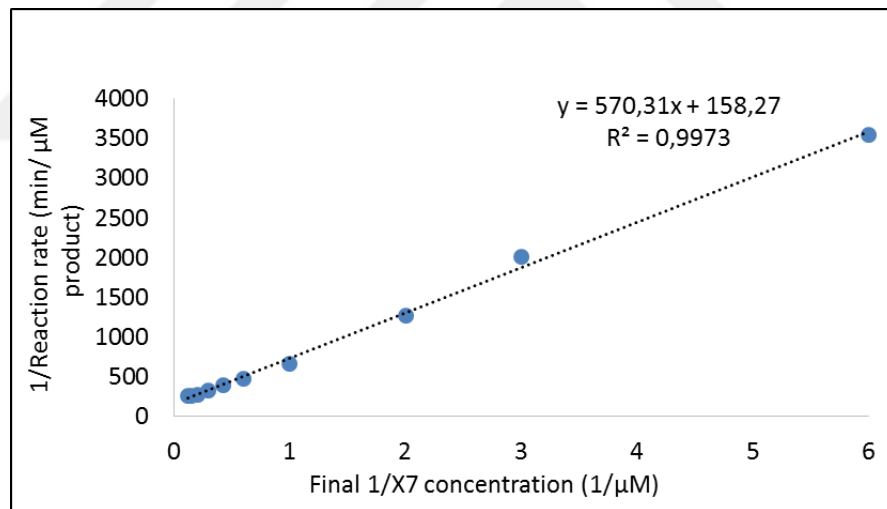


Figure 3.11. Lineweaver- Burke ( $1/\text{Reaction rate (min}/\mu\text{M product)}$ ) vs final  $1/\text{X7 concentration (1}/\mu\text{M)}$ ) graph of CaXTH2 enzyme.

### 3.2. CAPSICUM PLANT GROWTH TRIALS

Capsicum plant growth trials were done with various seeds belong to different regions of Turkey. Since their growth conditions are different from each other, most of them were not germinated in standard laboratory and greenhouse conditions. Their germination rate were different from each other even for the same capsicum varieties at the same growth conditions and the germinated seeds in early trials stopped germination in the next experiments. The inequality of the sizes of germinated seedlings in each plant variety and the decreased number of germinated seeds of different varieties led to the reduction in the number of seeds used per variety for plant growth trials and during salt stress treatments. The seedlings with similar germination rate and phenotypic results were used for growth optimization and salt stress trials.

Before applying salt stress to various capsicum seedlings, trials for the optimization of their germination were carried out. One day before germination, seeds were incubated overnight at  $-20^{\circ}\text{C}$  to speed up the germination process. Also, seed imbibition was carried out before starting the germination process to wake the dormant seeds up in a tube on a rotator with sterile ultra-pure water for  $\sim 20$  hours. For capsicum plant growth optimization trials, different growth media options were tried such as sterile ultra-pure water with 0,5 percent agar, MS medium with 0,5 percent agar, perlite and soil. Since MS medium was one of the richest plant growth media, it was very susceptible to contamination. In order to prevent contamination, surface sterilization method for the seeds was developed including 70 percent EtOH and different concentrations of NaOCl (4 percent stock, Merck) solution. For the optimization of surface sterilization process, ‘Erzurum’ seeds were subjected to 70 percent EtOH and different concentrations of NaOCl (4 percent stock, Merck) solution with different time periods and then surface sterilized seeds were grown on MS with 0,5 percent agar medium in growth cabinet for 11 days. 11-day-old seedling’s root and shoot lengths, root numbers and germination ratios were measured (Figure 3.12) by using a ‘Post-Hoc’ comparison test (Table 3.4). Surface sterilization with 70 percent EtOH incubation for 1.5 minutes and 25 percent NaOCl (4 percent stock, Merck) incubation for 10 minutes was determined as the best method since the highest root-shoot growth and germination rate was observed after that method. It was shown that the least germination

rate and root-shoot length were obtained after 15 percent NaOCl (4 percent stock, Merck) incubation for 10 minutes.

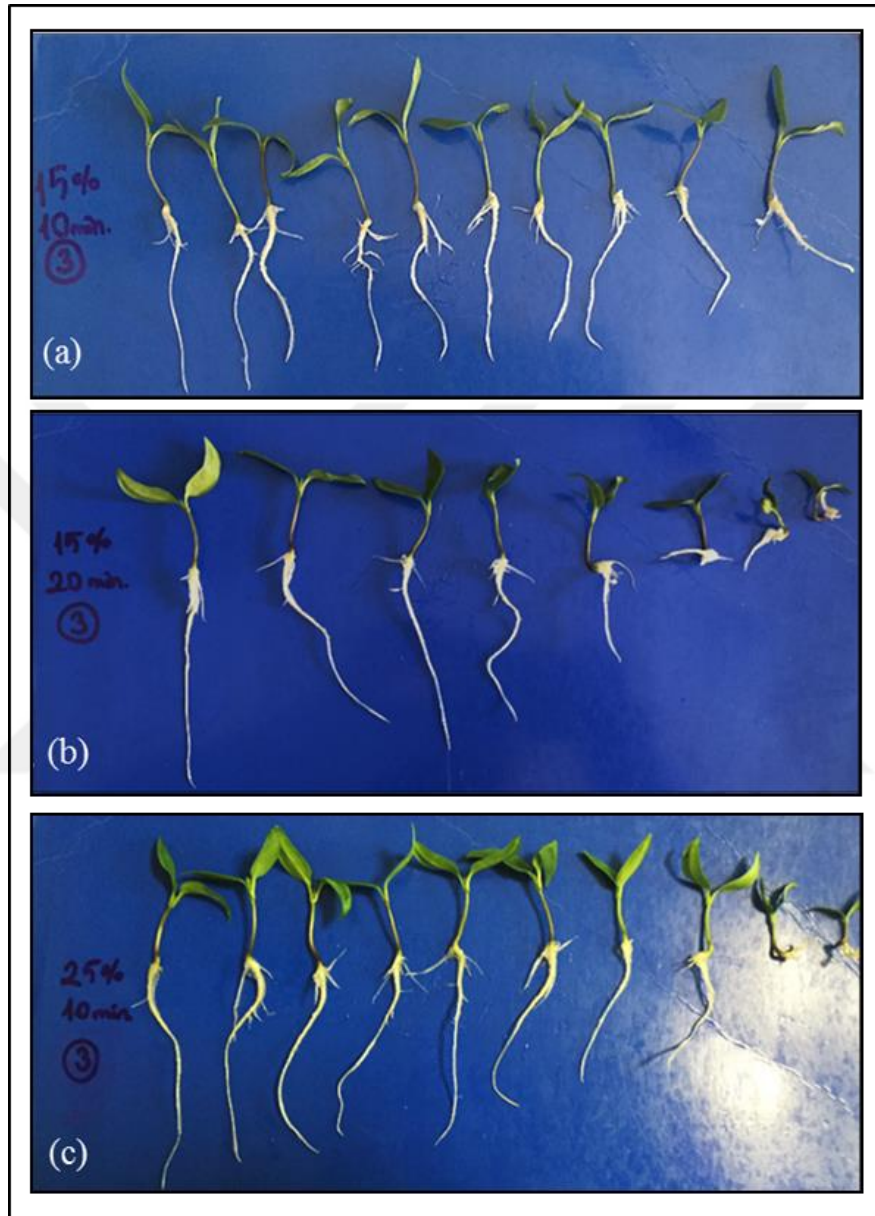


Figure 3.12. Root and shoot length comparison of 11-day-old 'Erzurum' seedlings that were surface sterilized with 70 percent EtOH for 1,5 min and different concentrations of NaOCl (4 percent stock, Merck) at different application periods (a) 15 percent NaOCl for 10 min, (b) 15 percent NaOCl for 20 min, (c) 25 percent NaOCl for 10 min and then grown in MS with 0,5 percent agar medium.

Table 3.4. Comparison of root- shoot lengths, root number and germination percentage with Post-Hoc statistical analysis results of ‘Erzurum’ seedlings grown in MS agar medium and surface sterilized with different concentrations of NaOCl (4 percent stock, Merck) at different time periods.<sup>x</sup>

NaOCl conc. (%)	Incubation time (min)	Primary root length <sup>y</sup> Avg±SD <sup>z</sup> (mm)	Shoot length <sup>y</sup> Avg±SD <sup>z</sup> (mm)	Root number <sup>y</sup> Avg±SD <sup>z</sup>	Germination percentage (%)
15	10	48±2,5 bc	16,3±0,55 a	5,85±0,54 bc	86,6
15	20	51±2,98 b	16,4±0,49 a	6,4±0,54 b	90
25	10	56,2±1,91 a	16,5±0,37 a	7,58±0,46 a	93,3

<sup>x</sup>The results were collected at the end of 11 days incubation. For every trial at least 50 explants were used.

<sup>y</sup>The letters found in every column generate difference ( $P \leq 0.05$ ) according to Post Hoc multiple comparison test. The differences were evaluated vertically.

<sup>z</sup> Avg: Average, SD: Standard Deviation.

### 3.3. SALT STRESS

For the first trial of salt stress on capsicum seedlings, ‘Erzurum’ seeds were surface sterilized and germinated in sterile ultra-pure water (pH 5,8) including 0,5 percent agar in dark for 5 days and germinated seeds were transferred onto same medium this time including different concentrations of NaCl (0 mM, 50 mM, 100 mM) and grown 6 more days in growth cabinet conditions. Phenotypic effects of salt treatment on root and shoot structures of 11-day-old ‘Erzurum’ seedlings were observed and compared for all NaCl concentrations (Figure 3.13). Germination was observed for all 0 mM, 50 mM, 100 mM NaCl concentrations but it was clear that even 50 mM salt concentration was enough to inhibit both root and shoot growth. When the salt concentration was increased to 100 mM, the growth was almost completely inhibited. It was considered that salt concentrations were too high to see the effects of salt stress so reduced salt concentrations were used for further experiments.

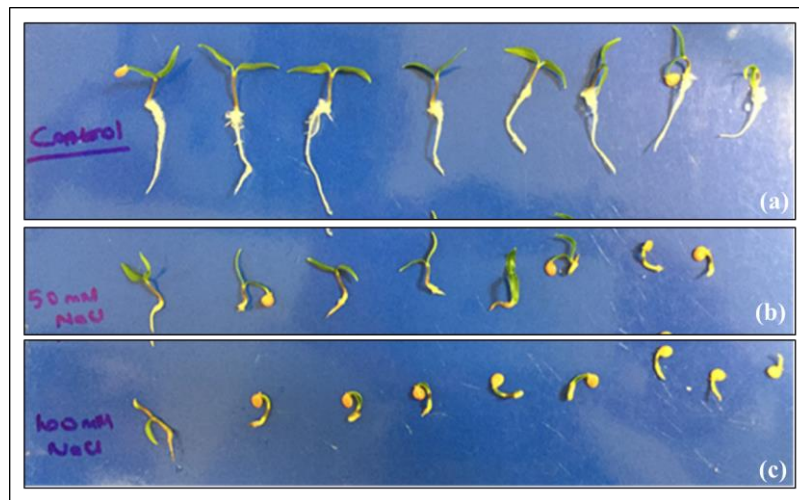


Figure 3.13. Phenotypic comparison of 11-day-old ‘Erzurum’ seedlings grown on 0,5 percent agar including sterile ultra-pure water medium with (a) 0 mM NaCl, (b) 50 mM NaCl, (c) 100 mM NaCl.

Table 3.5. Comparison of root- shoot lengths and root number and Post-Hoc statistical analysis results of ‘Erzurum’ seedlings that were grown on 0,5 percent agar including sterile ultra-pure water medium with 0 mM NaCl, 5 mM NaCl, 10 mM NaCl, 20 mM NaCl, 30 mM NaCl and 40 mM NaCl.<sup>x</sup>

NaCl conc. (mM)	Primary root length <sup>y</sup> Avg±SD <sup>z</sup> (cm)	Shoot length <sup>y</sup> Avg±SD <sup>z</sup> (cm)	Root number <sup>y</sup> Avg±SD <sup>z</sup>
0	2,41± 0,23 ab	0,96±0,07 a	7,00±0,88 a
5	1,85±0,24 bc	0,57±0,05 c	1,69±0,54 bc
10	2,53±0,29 ab	0,80±0,06 ab	3,16±0,85 b
20	3,09±0,66 a	0,72±0,05 b	2,35±0,64 bc
30	0,73±0,12 d	0,64±0,04 bc	1,37±0,26 c
40	0,23±0,04 d	0,40±0,05 d	1,00±0,00 c

<sup>x</sup>The results were collected at the end of 11 days incubation. For every trial at least 50 explants were used.

<sup>y</sup>The letters found in every column generate difference ( $P \leq 0.05$ ) according to Post Hoc multiple comparison test. The differences were evaluated vertically.

<sup>z</sup> Avg: Average, SD: Standard Deviation.

As it was examined that the salt concentration should be less than 50 mM, salt stress was applied again on 0,5 percent agar including sterile ultra-pure water medium with 0 mM, 10 mM, 20 mM, 30 mM, 40 mM NaCl concentration after the seeds were germinated in dark as described before. The phenotypic effects of different salt stress concentrations on 11-day-old ‘Erzurum’ seedlings were observed (Figure 3.14). The root and shoot lengths were measured and the number of roots were counted. The results were analyzed and compared by ‘Post-Hoc’ multiple comparison test (Table 3.5).

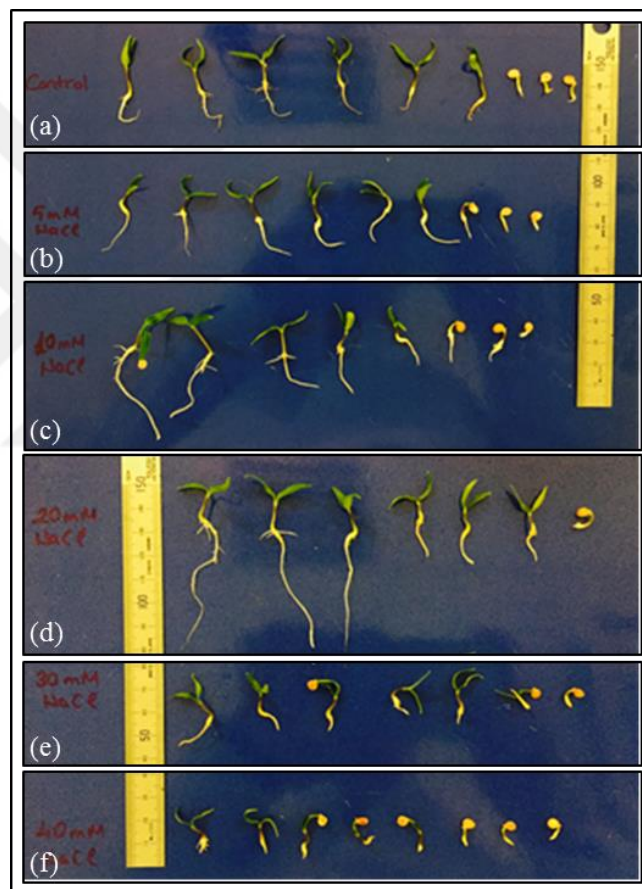


Figure 3.14. Phenotypic comparison of 11-day-old ‘Erzurum’ seedlings grown on 0,5 percent agar including sterile ultra-pure water medium with (a) 0 mM NaCl as control, (b) 5 mM NaCl, (c) 10 mM NaCl, (d) 20 mM NaCl, (e) 30 mM NaCl (f) 40 mM NaCl.

According to the phenotypic and Post-Hoc analysis results, it was shown that until 20 mM NaCl salt concentration the growth of the seedlings was not inhibited, in fact, their root growth increased. However, when the salt concentration was raised to 30 mM and 40 mM



concentration, the results has shown that there was a drastic decrease on root growth of the seedlings. It was clear that the best salt concentration interval to observe the inhibiting effect of salt concentration on plant growth was between 20 mM and 30 mM concentration. In order to observe the effect of salt stress on plants, new salt concentrations were determined as 0 mM- 25 mM- 50 mM NaCl and further experiments were performed on MS medium with 0,5 percent agar using those NaCl concentrations. After surface sterilization and germination of different varieties such as Erzurum, Cila, Aktör, and Samuray seedlings, they were transferred to MS media including 0,5 percent agar with 0 mM NaCl , 25 mM NaCl and 50mM NaCl concentrations as described before (Figure 3.15).

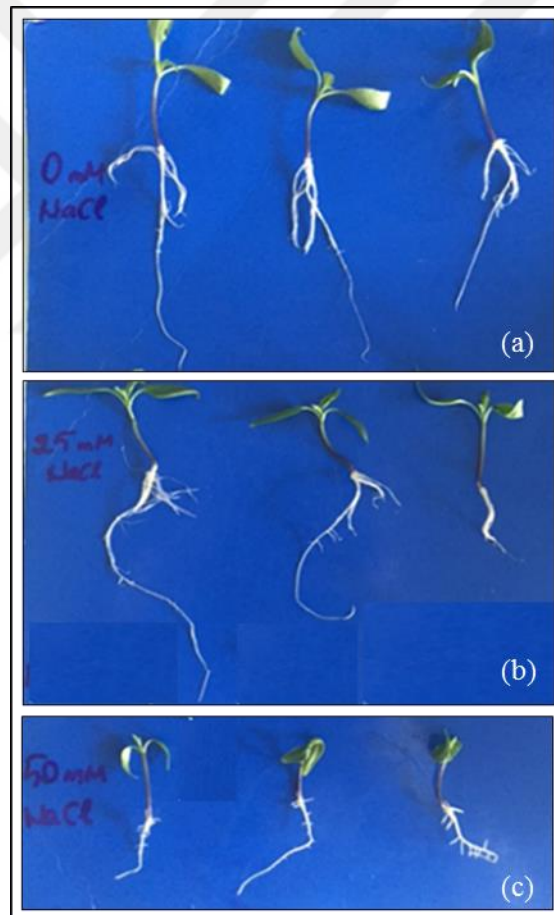


Figure 3.15. Comparison of root- shoot lengths and root numbers of 11-day-old 'Erzurum' seedlings grown on 0,5 percent agar including MS medium with (a) 0 mM NaCl as control, (b) 25 mM NaCl, (c) 50 mM NaCl.



Phenotypic results and Post-Hoc analysis performed on Erzurum seedlings showed that there was a slight decrease on primary root- shoot lengths of 25 mM NaCl grown plants compared to 0 mM NaCl control plants. On the other hand, when the salt concentration was increased to 50 mM, a drastic inhibition was observed on primary root- shoot lengths and root numbers of plants grown in MS with 0,5 percent agar medium. The primary root and shoot lengths of 50 mM NaCl grown seedlings were significantly shorter than the control and 25 mM NaCl grown seedlings. In order to compare the primary root-shoot lengths and root number of seedlings from control and 25 mM NaCl to 50 mM NaCl, Post-Hoc multiple comparison analysis were performed. The analysis results also confirmed the phenotypic inhibition as the salt concentration increased (Table 3.6).

Table 3.6. Comparison of root- shoot lengths and root number and Post-Hoc analysis results of ‘Erzurum’ seedlings that were grown on 0,5 percent agar including MS medium with 0 mM NaCl as control, 25 mM NaCl and 50 mM NaCl.<sup>x</sup>

<b>NaCl conc. (mM)</b>	<b>Primary root length<sup>y</sup> Avg±SD<sup>z</sup> (cm)</b>	<b>Shoot length<sup>y</sup> Avg±SD<sup>z</sup> (cm)</b>	<b>Root number<sup>y</sup> Avg±SD<sup>z</sup></b>
0	71,2±2,53 a	23,1±1,81 a	17,5±1,12 a
25	70,4±5,16 a	22,0±1,48 a	18,8±1,28 a
50	32,3±3,89 b	16,2±1,99 b	10,8±1,81 b

<sup>x</sup>The results were collected at the end of 11 days incubation. For every trial at least 50 explants were used.

<sup>y</sup>The letters found in every column generate difference ( $P \leq 0.05$ ) according to Post Hoc multiple comparison test. The differences were evaluated vertically.

<sup>z</sup> Avg: Average, SD: Standard Deviation.

The salt stress treatment experiment which was performed with 25 mM and 50 mM NaCl salt concentrations on Erzurum variety showed that those determined salt concentrations were enough to see the effect of salt stress on the plants. Other selected varieties such as Cila (Figure 3.16), Aktör (Figure 3.17), Samuray (Figure 3.18) and Seki were subjected to the same salt concentrations using the same procedure as described before. Phenotypically data for seedlings of each variety showed that control and 25 mM NaCl did not inhibit the root lengths of stress treated plants. It was shown that 25 mM NaCl concentration even

increased the root lengths of Cila as 13,6 percent (Table 3.7), Samuray as 22,5 percent (Table 3.8), Aktör as 12,3 percent (Table 3.9) and Seki as 1,4 percent (Table 3.10) compared to the control seedlings. The increase of root length for Seki variety was least among all the other varieties when the NaCl concentration was 25 mM. When the NaCl concentration was increased to 50 mM, there was 17,7 percent reduction in root length of Seki variety compared to control plants. For Aktör variety, there was a 19,7 percent increase in root length of the seedlings even when the salt concentration was 50 mM. On the other hand, when 25 mM NaCl and 50 mM NaCl grown seedlings of Cila and Samuray varieties were compared, 50 mM NaCl grown seedlings demonstrated shorter root lengths than 25 mM NaCl grown ones. Despite the fact that, the root lengths of Cila and Samuray varieties were 0,5 percent and 13 percent longer than the root lengths of control seedlings.

It was shown that salt treatment also affected the shoot lengths of Cila, Samuray, Aktör and Seki varieties in different ways. The shoot lengths of 25 mM NaCl grown seedlings of Cila and Samuray varieties, increased 45 percent and 20,5 percent compared to the control seedlings, respectively. The shoot length of 25 mM NaCl grown Seki variety decreased 16,8 percent while Aktör variety showed a slight decrease as 1,1 percent compared to the control plants. When the salt concentration was increased from 25 mM to 50 mM, there was a significant reduction on the shoot lengths of all varieties except Aktör. At 50 mM NaCl concentration, the shoot lengths of Aktör variety were 0,5 percent less than the control plants. Although the shoot lengths of Cila and Samuray seedlings at 50 mM NaCl concentration were 12,4 percent and 11 percent less than the seedlings grown with 25 mM NaCl concentration, they were still 27 percent and 7,3 percent more than the control seedlings. For Seki variety, there was a reduction on shoot lengths at 25 mM NaCl concentration as 26,5 percent compared to control plants while 11,8 percent reduction compared to 50 mM NaCl concentration.

Germination rate for Cila variety was 85 percent and did not change for all NaCl concentrations. For Samuray variety seedlings grown at 25 mM NaCl concentration the germination rate decreased to 60 percent from 75 percent and increased to 67,2 percent when the salt concentration increased from 25 mM to 50 mM. For Seki variety seedlings grown at 25 mM NaCl concentration the germination rate decreased to 40 percent from 70 percent and increased to 45 percent when the concentration increased to 50 mM. For Aktör variety seedlings the germination rate increased to 100 percent from 95 percent when salt

concentration increased to 25 mM but decreased to 83,3 percent when the salt concentration was increased to 50 mM.

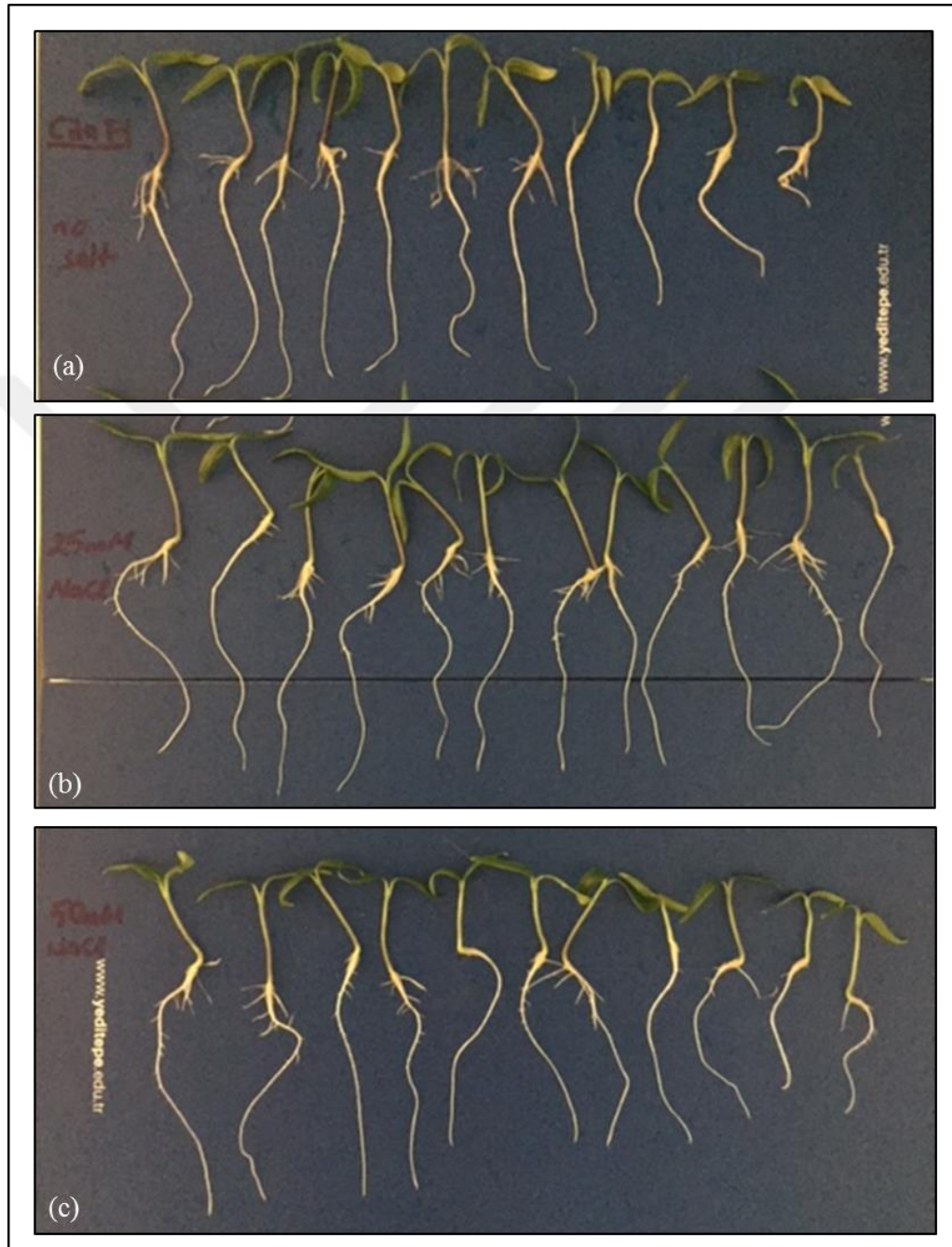


Figure 3.16. Phenotypic comparison of 11-day-old 'Cila' variety seedlings grown in (a) MS with 0,5 percent agar medium with 0 mM NaCl as control, (b) MS with 0,5 percent agar medium with 25 mM NaCl, (c) MS with 0,5 percent agar medium with 50 mM NaCl.

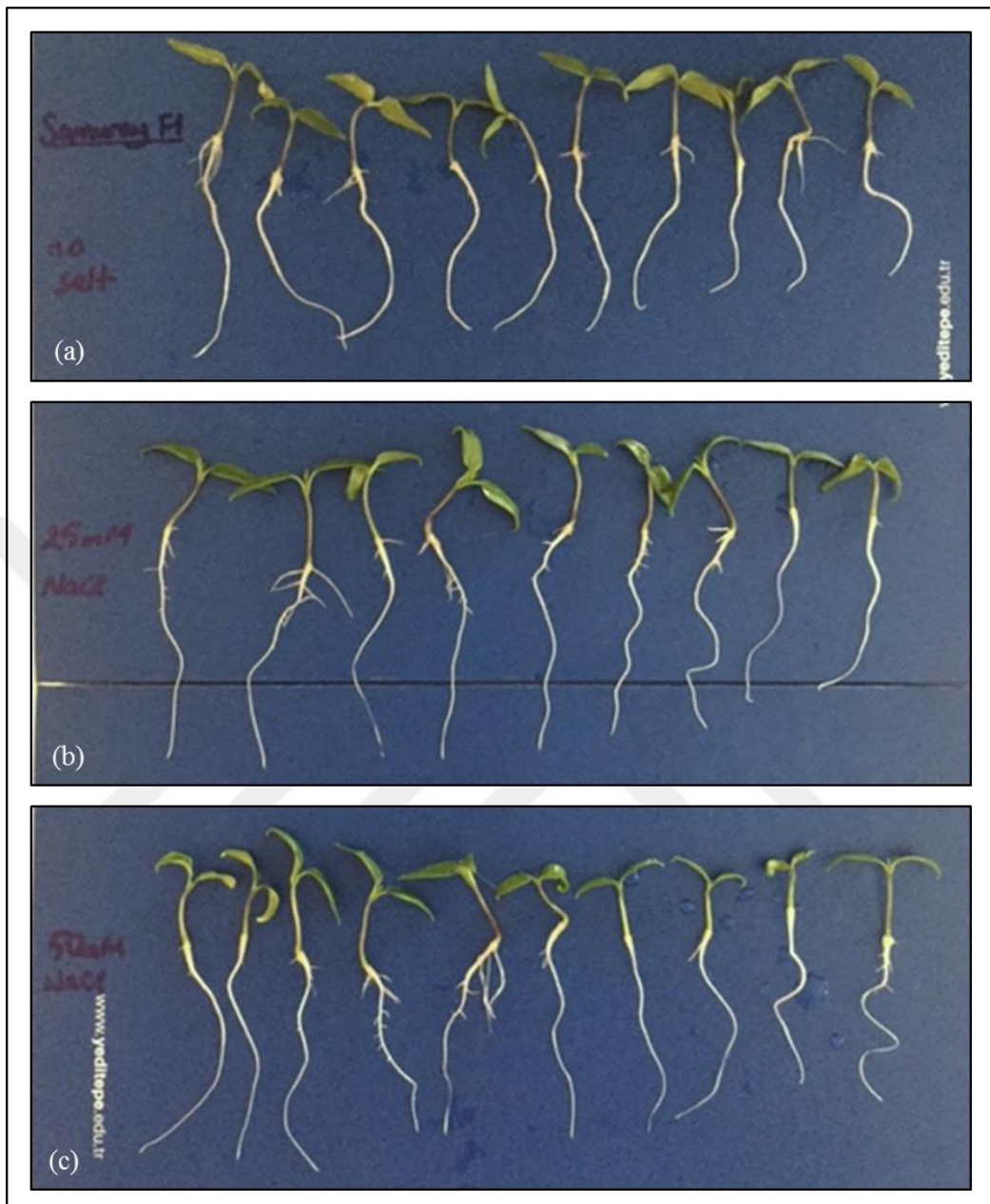


Figure 3.17. Phenotypic comparison of 11-day-old 'Samuray' variety seedlings grown in (a) MS with 0,5 percent agar medium with 0 mM NaCl as control, (b) MS with 0,5 percent agar medium with 25 mM NaCl, (c) MS with 0,5 percent agar medium with 50 mM NaCl.



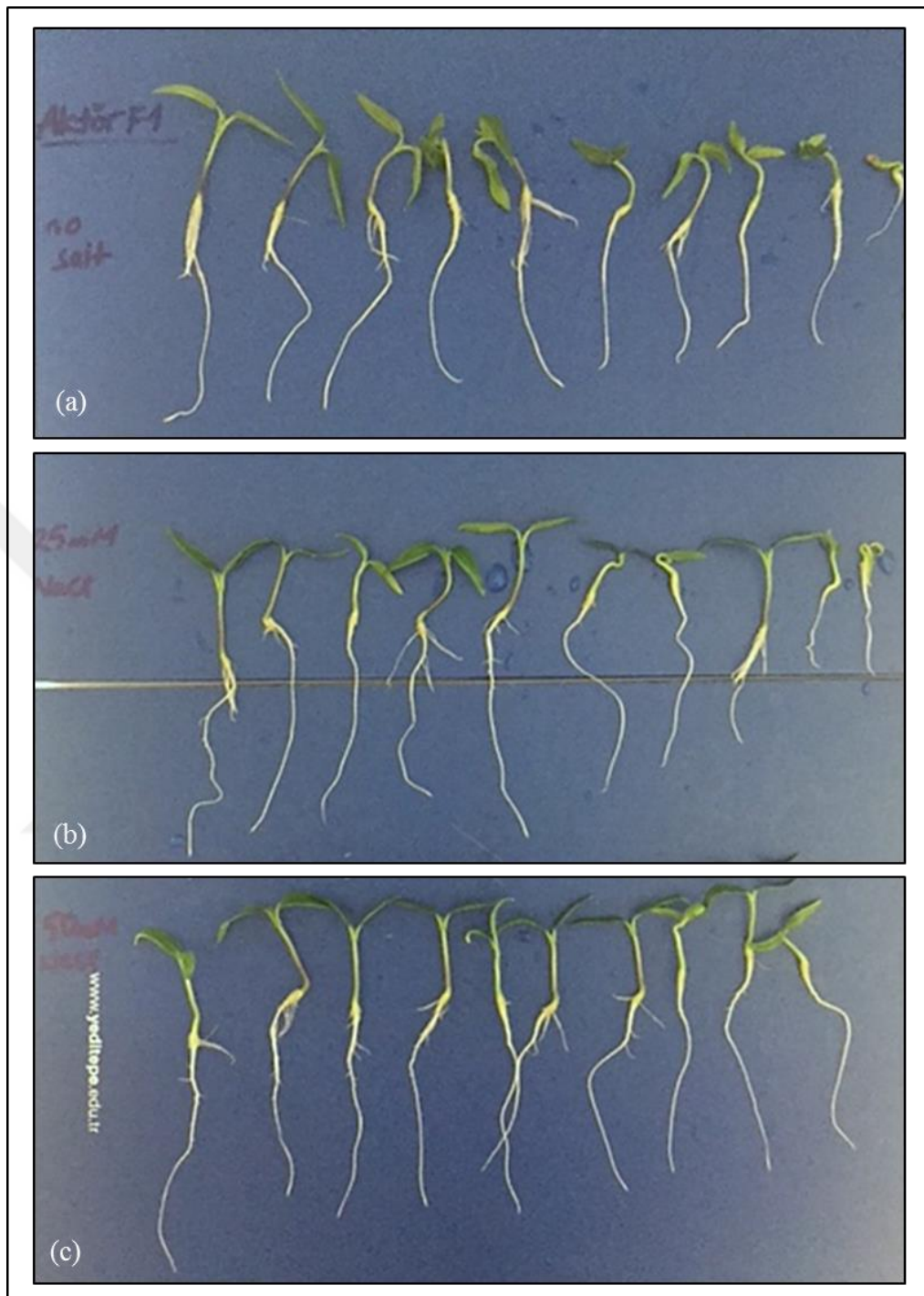


Figure 3.18. Phenotypic comparison of 11-day-old 'Aktör' variety seedlings grown in (a) MS with 0,5 percent agar medium with 0 mM NaCl as control, (b) MS with 0,5 percent agar medium with 25 mM NaCl, (c) MS with 0,5 percent agar medium with 50 mM NaCl.

Table 3.7. The average primary root- shoot lengths and germination rate percentages of 11-day-old 'Cila' variety seedlings in 0 mM NaCl, 25 mM NaCl and 50 mM NaCl concentration.

NaCl concentration (mM)	Primary root length Avg (cm)	Shoot length Avg (cm)	Germination rate percentage (%)
0	7,1	1,8	85
25	8,0	2,6	85
50	7,1	2,3	85

Table 3.8. The average primary root- shoot lengths and germination rate percentages of 11-day-old 'Samuray' variety seedlings in 0 mM NaCl, 25 mM NaCl and 50 mM NaCl concentration.

NaCl concentration (mM)	Primary root length Avg (cm)	Shoot length Avg (cm)	Germination rate percentage (%)
0	6,0	1,5	75
25	7,3	1,8	60
50	6,8	1,6	67,2

Table 3.9. The average primary root- shoot lengths and germination rate percentages of 11-day-old 'Aktör' variety seedlings in 0 mM NaCl, 25 mM NaCl and 50 mM NaCl concentration.

NaCl concentration (mM)	Primary root length Avg (cm)	Shoot length Avg (cm)	Germination rate percentage (%)
0	5,6	1,8	95
25	6,2	1,8	100
50	6,9	1,8	83,33

Table 3.10. The average primary root- shoot lengths and germination rate percentages of 11-day-old ‘Seki’ variety seedlings in 0 mM NaCl, 25 mM NaCl and 50 mM NaCl concentration.

NaCl concentration (mM)	Primary root length Avg (cm)	Shoot length Avg (cm)	Germination rate percentage (%)
0	7,1	1,7	70
25	6,7	1,4	40
50	5,4	1,3	45

Çanakkale and Kahramanmaraş variety seeds were germinated in wet perlite for 3 weeks and then transferred to soil-peat mixture to grow for 3 weeks more in greenhouse conditions as described before. Salt stress treatments were applied by soaking the roots of 6-week-old plants into 200 mM NaCl solution on different time intervals (0 minutes (control), 10 minutes, 30 minutes and 120 minutes). Since taking out the plants from pots and cleaning before soaking method created stress on the plants, phenotypic observations were kept short as possible to see the effect accurately. The effects of salt stress started to be observed with a decrease in the turgor pressure on both varieties after 10 minutes NaCl soaking. This phenotypic alteration was better observed on the plants after 30 minutes NaCl soaking. Still there were no significant alterations in the appearances of 30 minutes NaCl soaking plants and 120 minutes NaCl soaking plants of both Çanakkale (Figure 3.19) and Kahramanmaraş (Figure 3.20) varieties. However, it was also observed that Çanakkale plants were looking more resistant than Kahramanmaraş plants phenotypically. In order to better understand the effect of this salt stress method in gene expression level on plants, QPCR studies were performed with the samples taken from the leaves and roots of the plants.

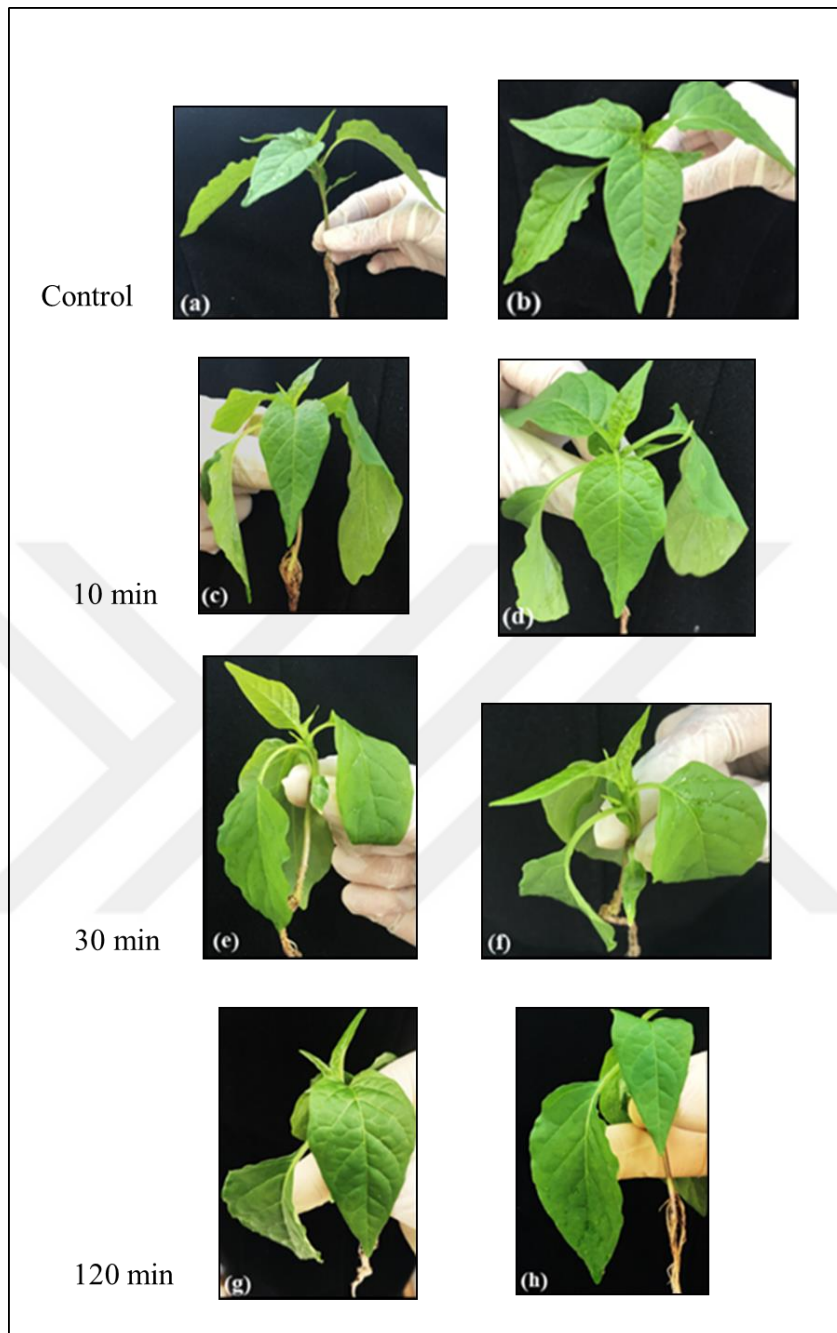


Figure 3.19. Phenotypic comparison of 6-week-old 'Çanakkale' variety plants that the roots were soaked into 200 mM NaCl solution for (a)-(b) 0 min as control, (c)-(d) 10 min, (e)-(f) 30 min, (g)-(h) 120 min.



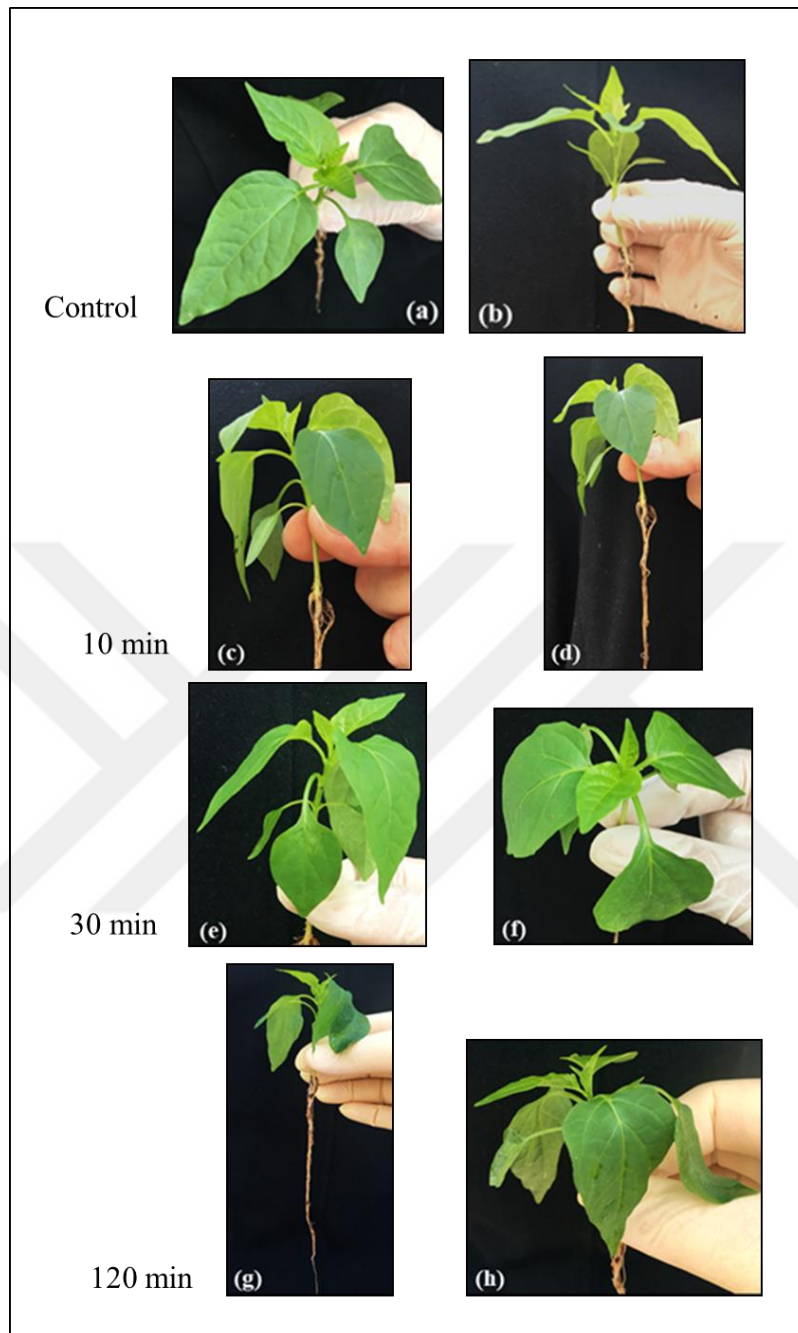


Figure 3.20. Phenotypic comparison of 6-week-old 'Kahramanmaraş' variety plants that the roots were soaked into 200 mM NaCl solution for (a)-(b) 0 min as control, (c)-(d) 10 min, (e)-(f) 30 min, (g)-(h) 120 min.

### 3.4. RNA ISOLATION AND cDNA SYNTHESIS

The root and leaf tissue samples of stress- treated and non-stress treated pepper seedlings were collected to perform RNA isolation using “iNtRON Biotechnology easy-spin (DNA free) Total RNA Extraction Kit” and then cDNA synthesis using “SuperScript® IV First-Strand Synthesis System” (Cat no: 18091050). The concentration of eluted RNAs in ng/μl were measured by “NanoDrop 2000 spectrophotometer (ThermoFisher)” and those values were used to determine the template amount for cDNA synthesis. For the quality and integrity check of RNA isolation, almost 600 ng of eluted RNA were used for 1 percent (w/v) agarose gel electrophoresis for 45 minutes at 90V. In monitored gel images, the samples which showed clear and sharp RNA bands were used for further cDNA synthesis reactions which were used as template for QPCR analysis (Figure 3.21). The concentration values that were measured by OD measurement method were between 100 ng/μl and 500 ng/μl. The A260/A280 ratio which was used to assess RNA purity was between 1,7 and 2,2 for all the RNA samples while A260/A230 ratio was between 1,8 and 2,1. The reason of low A260/A230 ratio might be the phenol contamination remained from the isolation procedure or carbohydrate contamination. All those contaminations were eliminated by normalization factors used during the calculations of QPCR analysis. cDNA samples that were synthesized from intact RNA samples were also run on 1 percent (w/v) agarose gel electrophoresis for 45 minutes at 90V and smear image was observed. Even though the RNA amount used for each cDNA synthesis was almost the same for all, the concentrations of synthesized cDNA of different plant varieties were different.

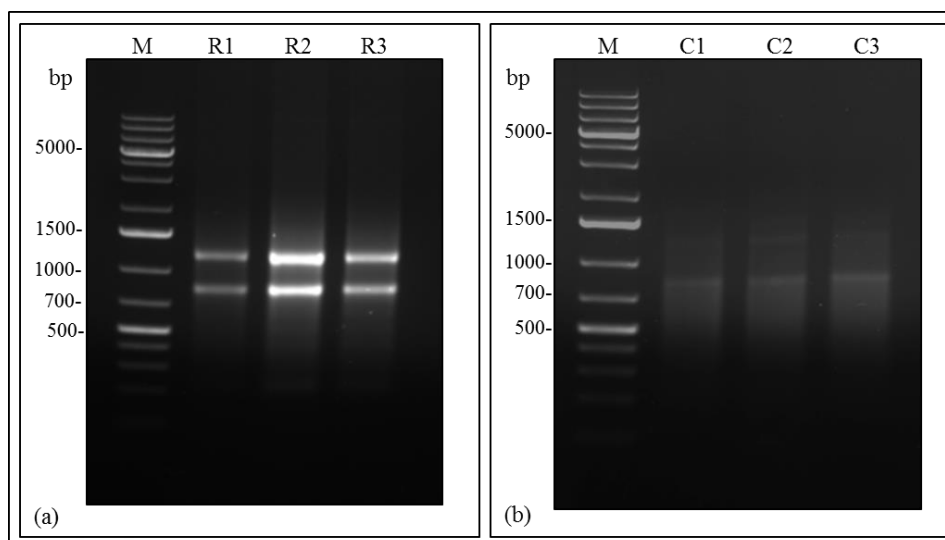


Figure 3.21. 1 percent (w/v) agarose gel electrophoresis results of RNA and cDNA samples obtained from 11-day old salt stress treated ‘Seki’ variety root tissue. (a) The root RNA results of ‘Seki’ that salt stress treated, R1- with 0 mM NaCl as control, R2-with 25 mM NaCl, R3- with 50 mM NaCl. (b) The cDNA results obtained from those root RNA samples of ‘Seki’ that salt stress treated, C1- with 0 mM NaCl as control, C2-with 25 mM NaCl, C3- with 50 mM NaCl. Marker (M): Thermo Scientific GeneRuler 1kb Plus DNA ladder. Bands represented 18S and 28S capsicum rRNA.

### 3.5. GENE EXPRESSION STUDIES

Conventional PCR studies were performed with housekeeping primers which were designed and tested by using “Maximo Taq DNA Polymerase (Geneon)” enzyme. The optimum  $T_m$  values for those reference genes were determined by gradient PCR studies and product samples were checked via 1 percent (w/v) agarose gel electrophoresis. *CaACTIN*, *CaEIF5A2* and *Ca $\alpha$ -TUBULIN* were chosen as reference genes among 6 different housekeeping genes which showed clear bands at expected sizes for further QPCR analysis. Those 3 reference genes primers were then used to obtain template DNAs by conventional PCR and bulked up template DNAs were purified by Varian PLRP-S 1000A 5  $\mu$ m 50x2.1 mm reverse phase column in HPLC to create standards to be used for QPCR and their absorbance was taken in 260 nm (Figure 3.22). The same gradient PCR studies were performed with *CaXTH2* gene and its gene specific primers in order to

determine the optimum  $T_m$  values. In order to obtain higher amounts of gene products, *CaXTH2* gene products that were obtained by PCR were combined with each other. Bulked up reactions containing *CaXTH2* gene products were purified by HPLC as described before.

After collecting the pure products both for reference genes and *CaXTH2* gene, pUC19 vector (500 ng/ $\mu$ l) was digested with HpaII enzyme into known sized 11 fragments and run on HPLC to be used as a marker for standard formation (Figure 3.23). Analyzing the peaks formed of each known sized fragment on chromatogram, the area under the curve values of each fragment was used to calculate the copy number of the genes. For the standardization, serial dilution from  $10^7$  copies/ $\mu$ l to  $10^2$  copies/ $\mu$ l were prepared using reference gene products. Those diluted standards were used as templates at QPCR to prepare calibration curves for genes (Figure 3.24). In order to check whether the reference genes created non-specific products, melt curve analysis were also performed and observed that the products obtained were pure enough to be used for QPCR (Figure 3.25).

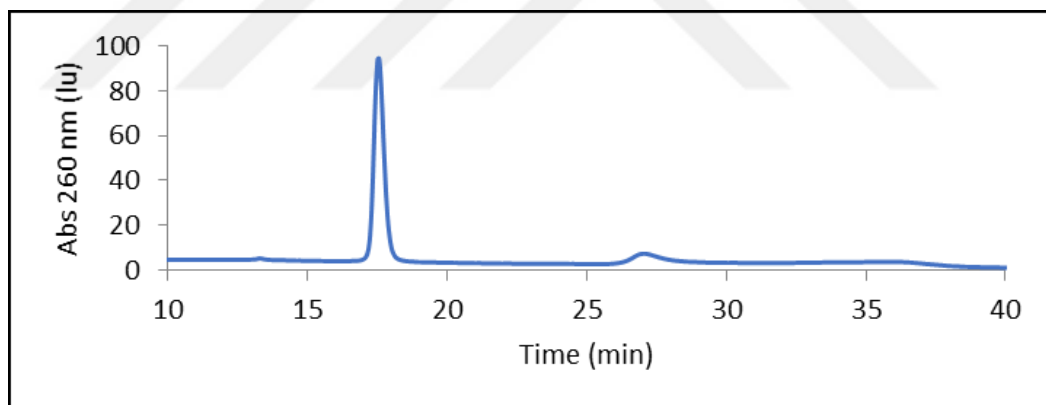


Figure 3.22. The separation of the reference gene *CaActin* at 260 nm using Varian PLRP-S 1000A 5  $\mu$ m 50x2.1 mm reverse phase column in HPLC.

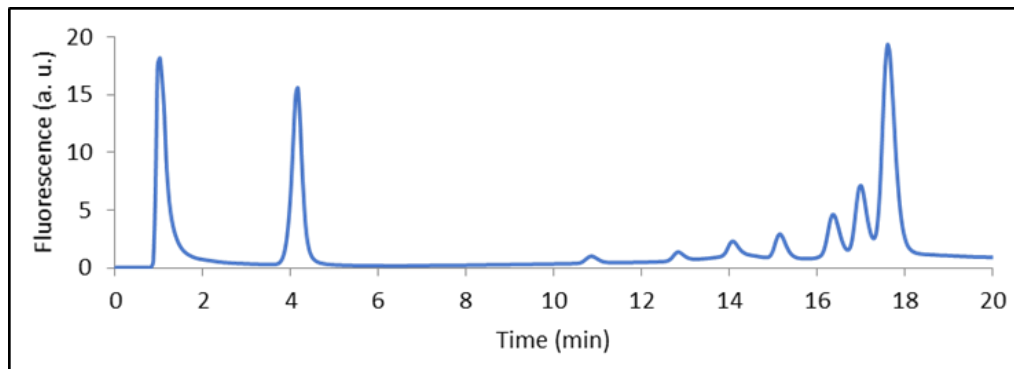


Figure 3.23. HPLC chromatogram image of the separated fragments of pUC19 which was digested with HpaII enzyme.

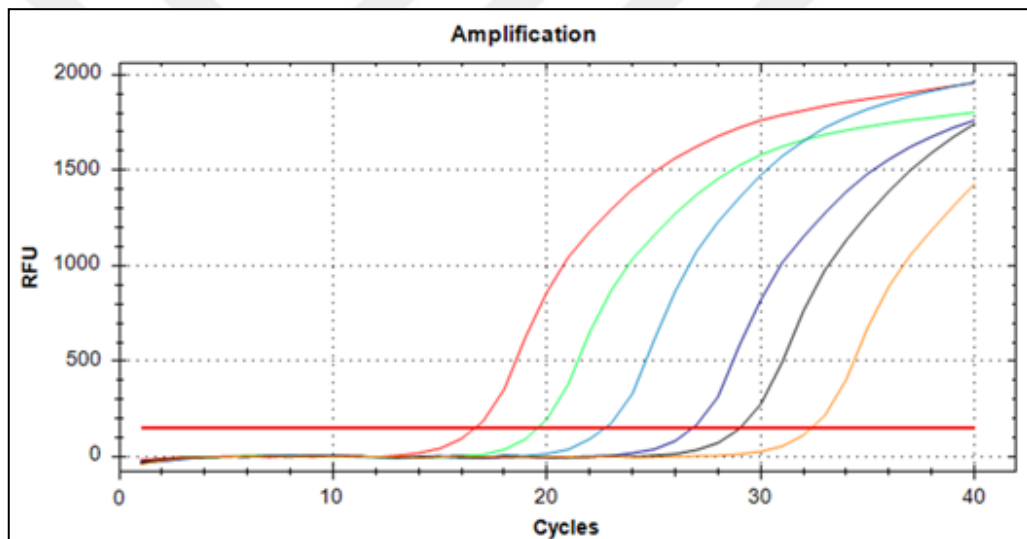


Figure 3.24. Amplification curves of standards from  $10^7$  copies/ $\mu$ l to  $10^2$  copies/ $\mu$ l of *Caa-TUBULIN* formed by performing QPCR with reference gene primers.

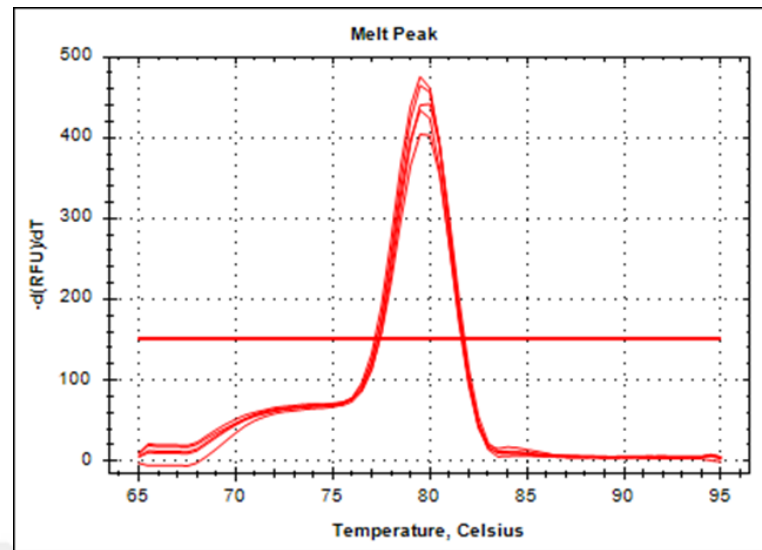


Figure 3.25. Melt curve analysis of standards from  $10^7$  copies/ $\mu\text{l}$  to  $10^2$  copies/ $\mu\text{l}$  of *Ca $\alpha$ -TUBULIN* after performing QPCR with reference gene primers.

The same protocol was carried out with bulked-up *CaXTH2* gene. After determining the total copy number in *CaXTH2* gene product, serial dilution was performed to get  $10^9$  copies/ $\mu\text{l}$  to  $10^2$  copies/ $\mu\text{l}$  standards and using those standards cq vs copy number graphs were created (Figure 3.26). Also melt curve analysis showed that there were no non-specific products generated by the gene specific primers.

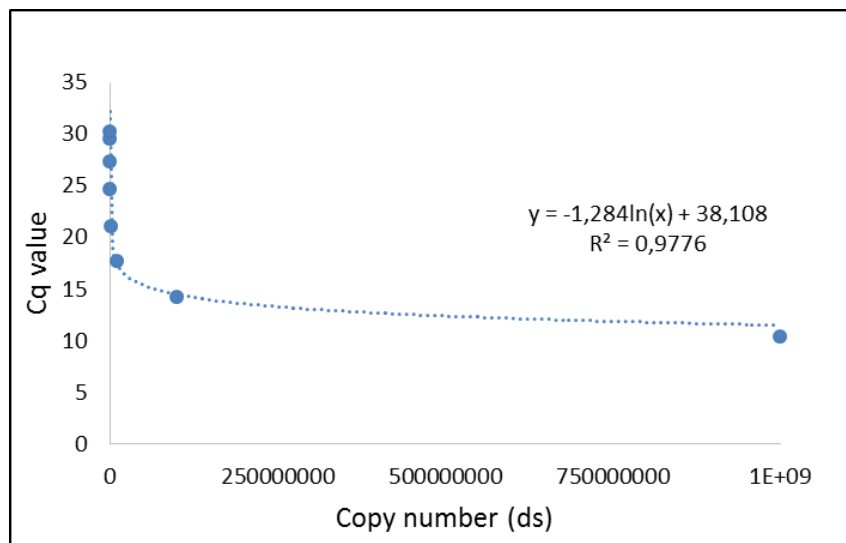


Figure 3.26. Cq vs. copy number graph of *CaXTH2* that was plotted after QPCR with gene specific primers and gene standards ( $10^2$  copies/ $\mu\text{l}$ -  $10^9$  copies/ $\mu\text{l}$ ).

### 3.5.1. Salt Stress Expression Levels for *CaXTH2* Gene

QPCR studies were performed with salt stress-treated tissues and non-treated control tissues to observe the expression level of *CaXTH2* gene on stress treated plants. QPCR studies performed with the root tissues of Aktör and Seki varieties showed that when the NaCl concentration increased to 25 mM and 50 mM, expression level of *CaXTH2* gene was induced. (Figure 3.27).

Those studies with root tissues of the plants showed that the level of increase of gene expression was depended on the variety type. For Aktör variety, the *CaXTH2* gene expression level in 25 mM and 50 mM NaCl salt treated root tissues increased 4-fold and 5,2-fold compared to control samples, respectively. The increase in salt concentration in media that the plants were grown induced the gene expression level also for Seki variety but not as high as Aktör variety. While the *CaXTH2* gene expression level of Seki variety grown in MS medium containing 25 mM NaCl was 1,7-fold higher, 50 mM NaCl containing MS medium grown Seki variety was 3,6-fold higher than the control plants of Seki.

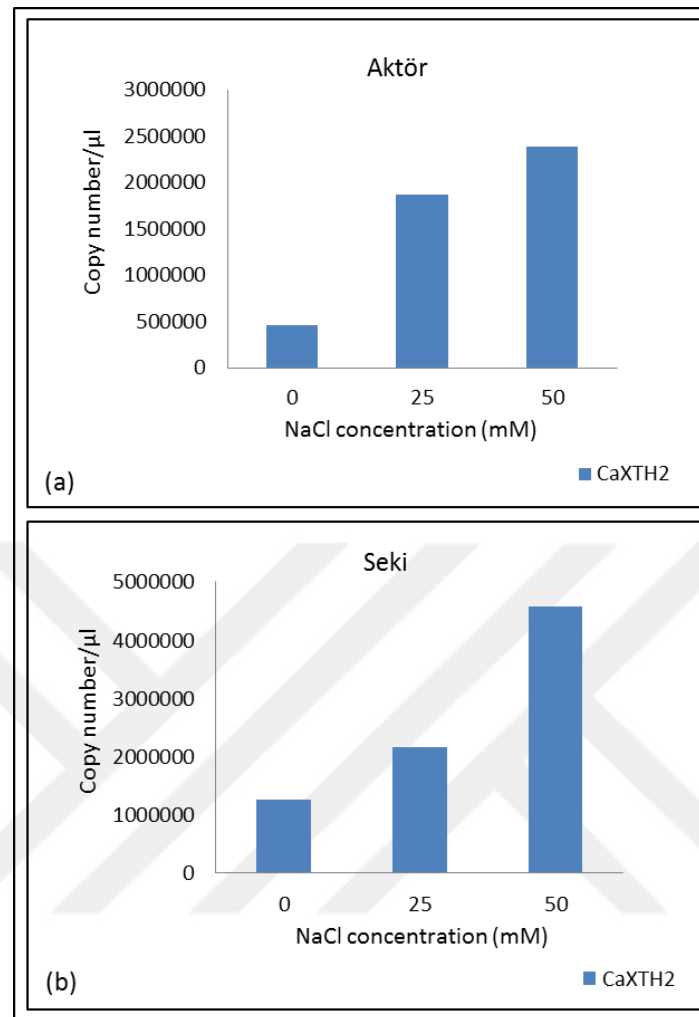


Figure 3.27. Graphs showing the copy numbers of *CaXTH2* gene in root tissues of 11-day-old 0 mM- 25 mM and 50 mM NaCl containing MS medium grown (a) Aktör and (b) Seki variety.

Same salt stress studies and QPCR analysis were performed for Cila and Samuray varieties. While the gene expression level of 25 mM NaCl containing MS agar grown Cila variety was 3,9- fold higher, 50 mM NaCl containing MS agar grown Cila variety was 1,4- fold higher than the no salt control plants. For the first time, only for Cila variety the increase in expression level dropped 2,4-fold when the NaCl concentration was increased from 25 mM to 50 mM (Figure 3.28). Also for Samuray variety, the expression levels were induced with increased salt concentrations as the other varieties. The *CaXTH2* gene expression levels were 1,6-fold and 1,8-fold higher when the NaCl concentration increased to 25 mM and 50 mM, respectively.



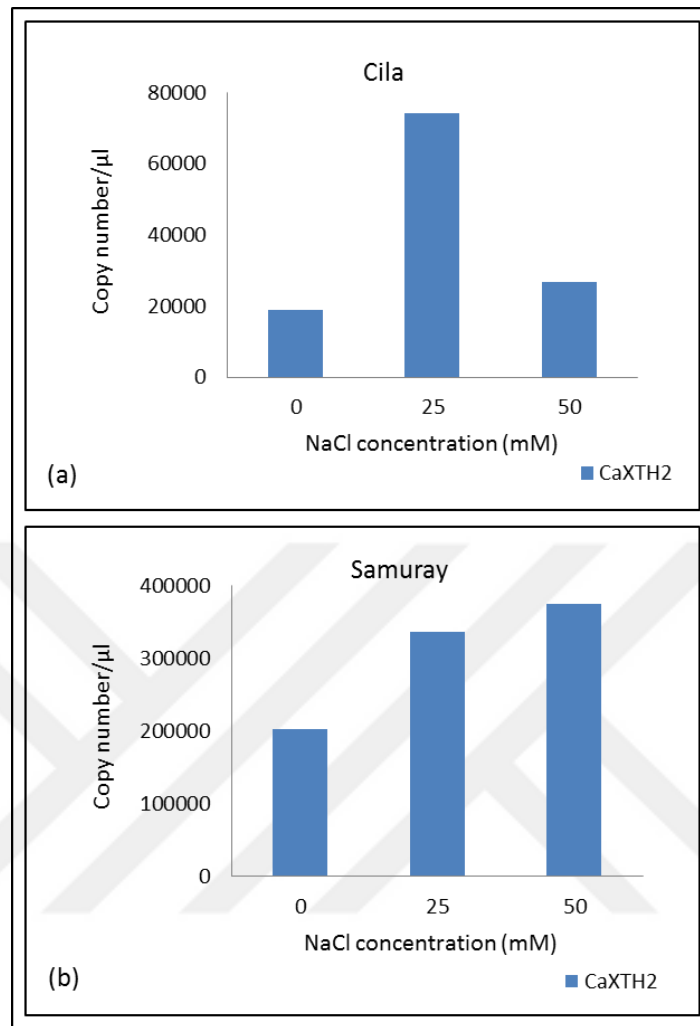


Figure 3.28. Graphs showing the copy numbers of *CaXTH2* gene in root tissues of 11-day-old 0 mM- 25 mM and 50 mM NaCl containing MS medium grown (a) Cila and (b) Samuray variety.

Table 3.11. Copy numbers of *CaXTH2* gene in root tissues of Aktör, Seki, Cila and Samuray seedlings that were grown on MS agar containing 0 mM, 25 mM and 50 mM NaCl.

NaCl conc. (mM)	Copy number of <i>CaXTH2</i> for Aktör	Copy number of <i>CaXTH2</i> for Seki	Copy number of <i>CaXTH2</i> for Cila	Copy number of <i>CaXTH2</i> for Samuray
0	$0.458 \times 10^6$	$1.26 \times 10^6$	$0.0188 \times 10^6$	$0.203 \times 10^6$
25	$1.87 \times 10^6$	$2.16 \times 10^6$	$0.0742 \times 10^6$	$0.337 \times 10^6$
50	$2.39 \times 10^6$	$4.57 \times 10^6$	$0.0268 \times 10^6$	$0.375 \times 10^6$

All of four varieties showed induced gene expression level when the NaCl concentration increased. Among all varieties, only the gene expression level in the roots of Cila variety decreased when the NaCl concentration was increased from 25 mM to 50 mM (Table 3.11).

A different salt stress treatment was performed for more mature plants of Çanakkale and Kahramanmaraş varieties. 6-week-old soil-peat mixture grown plants were soaked into 200 mM NaCl solution for different time intervals (0 min as control- 10 min- 30 min- 120 min). QPCR method was applied to collected root and leaf tissues of control and salt stress treated plants and their gene expression levels were calculated. For Çanakkale variety, *CaXTH2* gene expression levels were induced 2-fold and 1,5-fold for root and leaf tissues, respectively when exposed to salt stress for 10 minutes. On the other hand, when the salt stress exposure time increased to 30 minutes, the expression levels of *CaXTH2* gene decreased both for root and leaf tissues compared to control plants. After 120 minutes of exposure to 200 mM NaCl solution, the expression levels were decreased even more for both root and leaf tissues (Figure 3.29). When the exposure time increased from 30 minutes to 120 minutes, the copy number of *CaXTH2* gene decreased even more (Table 3.12).

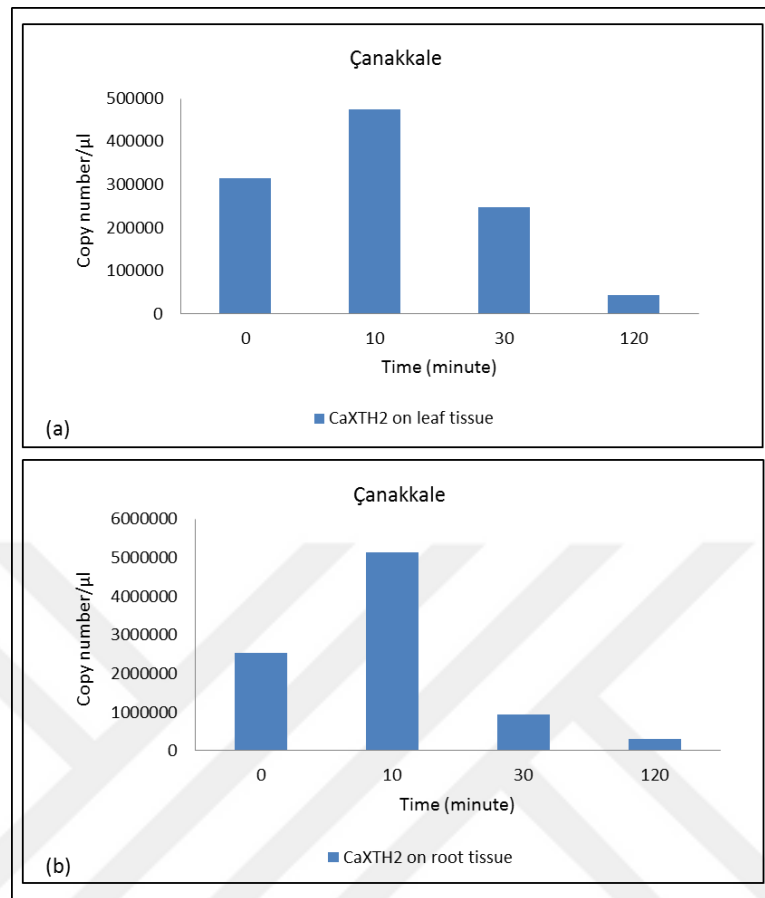


Figure 3.29. Copy numbers of *CaXTH2* gene from (a) leaf and (b) root tissues of Çanakkale variety whose roots were soaked into 200 mM NaCl solution for 0 min as control, 10 min, 30 min and 120 min.

Table 3.12. Copy numbers of *CaXTH2* gene from the leaf and root tissues of 6-week-old Çanakkale seedlings whose roots were soaked into 200 mM NaCl solution for different time intervals (0 min as control-10 min-30 min-120 min).

Time (minute)	Copy number of <i>CaXTH2</i> for leaf tissue	Copy number of <i>CaXTH2</i> for root tissue
0	$0.315 \times 10^6$	$2.52 \times 10^6$
10	$0.475 \times 10^6$	$5.14 \times 10^6$
30	$0.248 \times 10^6$	$0.931 \times 10^6$
120	$0.0429 \times 10^6$	$0.309 \times 10^6$

The leaf samples of Kahramanmaraş variety showed decreased gene expression levels after exposure to 10 minutes of stress application. Copy number of *CaXTH2* gene decreased 3,6-fold after exposure to 10 minutes of salt stress compared to control leaf tissues. A drastic drop as 15,2-fold on copy number of leaf tissues was observed after 30 minutes exposure to 200 mM NaCl solution for Kahramanmaraş variety (Figure 3.30). While the decrease in copy number of the gene continued when the exposure time reached to 120 minutes, it was not as strong as it was after 10 minutes and 30 minutes of exposure.

On the root tissue samples of Kahramanmaraş variety, *CaXTH2* gene expression increased 1,4-fold when the salt stress exposure time reached to 10 minutes. However, compared to control tissue samples a 6,8-fold and 19,3-fold decrease on copy numbers were observed on root tissue samples when the salt stress exposure time reached to 30 minutes and 120 minutes, respectively (Table 3.13).

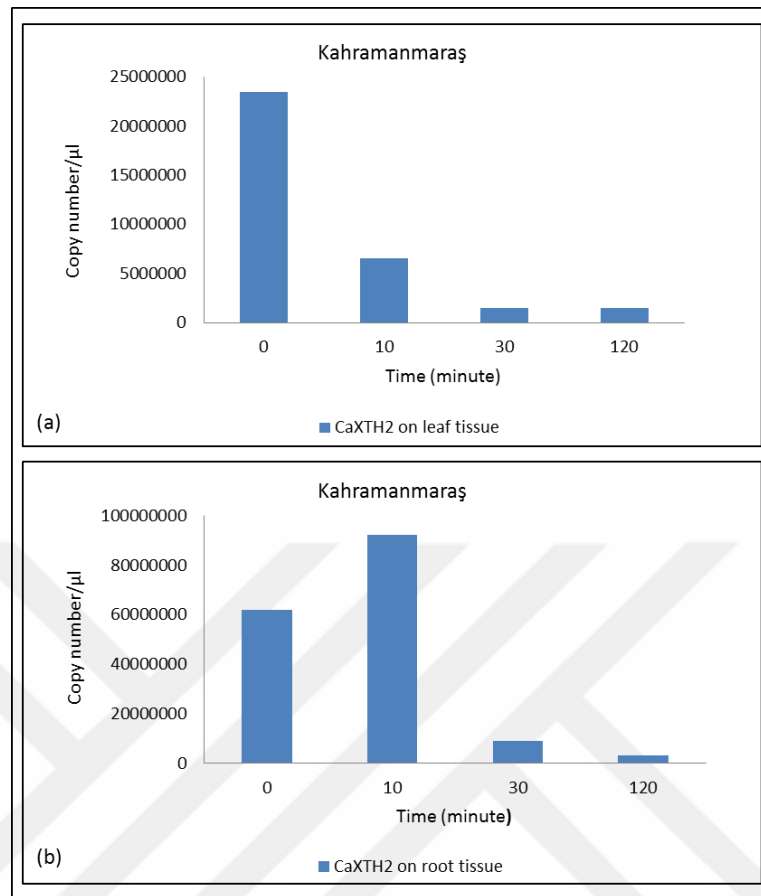


Figure 3.30. Copy numbers of *CaXTH2* gene from (a) leaf and (b) root tissues of Kahramanmaraş variety whose roots were soaked into 200 mM NaCl solution for 0 min as control, 10 min, 30 min and 120 min.

Table 3.13. Copy numbers of *CaXTH2* gene from the leaf and root tissues of 6-week-old Kahramanmaraş seedlings whose roots were soaked into 200 mM NaCl solution for different time intervals (0 min as control-10 min-30 min-120 min).

Time (minute)	Copy number of <i>CaXTH2</i> for leaf tissue	Copy number of <i>CaXTH2</i> for root tissue
0	23.5 x 10 <sup>6</sup>	61.8 x 10 <sup>6</sup>
10	6.59 x 10 <sup>6</sup>	92.2 x 10 <sup>6</sup>
30	1.54 x 10 <sup>6</sup>	9.11 x 10 <sup>6</sup>
120	1.48 x 10 <sup>6</sup>	3.21 x 10 <sup>6</sup>

## 4. DISCUSSION

In this study, codon optimized *CaXTH2* gene was transformed to *E.coli* and amplified, then it was heterologously expressed in yeast *Pichia pastoris*. Enzyme production was carried out in BMMY medium with 5 days of methanol induction of *AOX1* (Alcohol oxidase 1) promoter and the colony that is producing the most active enzyme was selected via SDS-PAGE, Western blotting and HPLC activity analysis. Although there were protein bands of more than one colonies on SDS-PAGE and Western blotting results, the 2<sup>nd</sup> colony, CaXTH2-2 was chosen as the mostly produced protein since it has the sharpest protein band at expected size. SDS-PAGE and Western analysis were performed to detect the presence of the protein which the molecular size is known. The protein band size of CaXTH2-2 was ~35-40 kDa instead of ~33,88 kDa which is the predicted size of the CaXTH2 protein and also there were smear-like banding patterns on the gel image. Both supported the idea that they might be due to the glycosylation of the proteins since it is known that CaXTH2 has two potential glycosylation site that are both likely to be glycosylated according to the NetNGlyc web program. Also, the other reason of the smear-like banding pattern might be the large number of hydrophobic amino acids of XTH proteins that affect the mobility of proteins on SDS-PAGE gels. The presence of 6xHis-tagged protein was approved by Western blotting and to be able to select the most active enzyme producing colony, enzyme activity analysis were performed via HPLC method using TXG-XGO substrate couple. As a result of all the analysis, CaXTH2-2 was chosen as the most active enzyme producing colony. The heterologous gene expression in *P. pastoris* and large scale production of the gene products were also performed for other two homolog genes *CaXTH1* and *CaXTH3* by the laboratory project assistant Dr. Burcu Gür. CaXTH1 and CaXTH3 enzyme activity and enzyme kinetics results were compared with CaXTH2 results.

Large scale production was achieved with CaXTH2-2 enzyme again via methanol induction of *AOX1* promoter. The proteins that were produced were first precipitated and then purified via performing ammonium sulfate precipitation, dialysis, affinity chromatography and size- exclusion chromatography methods, respectively. Polishing was applied for further purification of CaXTH2 enzyme. Purified enzyme was concentrated and protein concentration was measured by Bradford assay as 2,723 mg/ml. These enzymes are

usually located in the plant apoplast which has a slightly acidic pH varying between 5.0 to 6.0 [39]. The optimum working pH of CaXTH2 enzyme was determined as pH 6.0 and all the substrates used for activity analysis were prepared at pH 6.0.

In order to test the activity levels of the enzyme on variety of carbohydrate molecules, different donor and acceptor substrate couples were selected. Since native xyloglucan structures as substrate form cannot be obtained, varying polysaccharides found in substrate form such as TXG, HEC, BBG were chosen to test the enzyme activity with xyloglucan and other plant cell wall carbohydrate molecules. TXG, tamarind seed xyloglucan consists of XXXG, XXLG, XLXG and XLLG xyloglucan subunits which is similar to native capsicum xyloglucan [57]. The activity levels of CaXTH2 enzyme on different substrate couples were determined by the HPLC analysis and the specific activity results obtained in picokatal/mg units were compared to better understand the working mechanism of capsicum XTH enzymes on cell wall polysaccharides. Also, CaXTH1 and CaXTH3 enzyme activity levels on different substrate couples were determined and the enzyme activity experiments were conducted by Dr. Burcu Gür and compared with CaXTH2. CaXTH2 enzyme showed the highest activity with TXG as donor and with X7 and XGO as acceptor substrates. The highest specific activity was shown with TXG-X7 substrates with a value of 4121,0 picokatal/mg and following highest specific activity was with TXG-XGO substrates with a value of 2026,9 picokatal/mg. When HEC-X7 substrate couple was used, the enzyme had the next highest activity which was almost 0,3 percent less than the activity with TXG-X7 couple. Those activity results with X7 acceptor oligosaccharide brings to mind that the enzyme is better at catalyzing the reaction for a specific substrate and tends to accommodate that specific substrate in its active site more. The following highest activities were 817,22 picokatal/mg for CaXTH3 and 557,87 picokatal/mg for CaXTH1 enzymes on TXG-X7 substrate couple. Activities of the enzymes on the TXG-XGO substrate couple level was significantly lower than the activities on the TXG-X7 substrate couples. The values for TXG-XGO activity were 365,23 picokatal/mg, 2026,9 picokatal/mg and 494,36 picokatal/mg for CaXTH1, CaXTH2 and CaXTH3 enzymes, respectively (Table 4.1). As it was mentioned, the enzyme activity on TXG-XGO substrate couple was lower than the activity on TXG-X7. Enzyme prefers the X7 as acceptor oligosaccharide since it consists of only XXXG while XGO contains other xyloglucan subunits- XXXG, XXLG, XLXG and XLLG [58]. It was demonstrated that, xyloglucan

molecules in capsicum cell wall mainly consists of XXGG and XSGG structures which had no substitution on third glucosyl residue. Since there is further substitution on the third glycosyl residue of XXLG and XLLG structures, pepper XTH enzymes most probably do not work on those oligosaccharides. On the other hand, XLXG is more likely to behave as a native substrate for pepper XTH enzymes as there is no substitution on its third glycosyl residue. Capsicum xyloglucan structures include xylosyl residue further substituted with L-Arabinofuranosyl side chains however, they do not include residues substituted with L-fucosyl side chains [34].

Table 4.1. CaXTH1, CaXTH2 and CaXTH3 enzymes as paired with substrates showing the highest activity.

<b>Enzyme</b>	<b>The highest activity showing substrate couple</b>	<b>Activity level (picokatal/mg)</b>
CaXTH1	TXG-X7	557,87
	TXG-XGO	365,23
CaXTH2	TXG-X7	4121,04
	TXG-XGO	2026,9
CaXTH3	TXG-X7	817,22
	TXG-XGO	494,36

Tamarind seed xyloglucan, TXG, was the most efficient donor polysaccharide for the XTH enzymes studied since it is the only commercially available carbohydrate which has structure similarities with pepper native xyloglucan structures [58]. When TXG-XGO activity percentage was taken as 100 percent, TXG-X7 activity percentage for CaXTH2 enzyme is 200 percent which showed that the enzyme was selective on substrates and showed faster activity on X7 substrate. The activities on all other substrate couples were less than 1 percent of the activity on TXG-XGO and TXG-X7. Only the relative enzyme activity levels of HEC-XGO and HEC-X7 substrate couples were the next highest activities as their activity percentage being close to 1 percent. Barley  $\beta$ -glucan (BBG),



which is obtained from monocot barley plants used as donor substrate. Since capsicum plants are dicot and they do not have  $\beta$ -glucans, the enzyme activity was low with BBG donor substrate. The CaXTH2 enzyme activity with the other acceptor oligosaccharides XT, CT, LT, BA, BB, BC and GM was also very low compared to XGO and X7 substrates which might be because of the lack of substitution on their structure. All the enzyme activities for the rest of the substrates were less than 1 percent of the activity on TXG-XGO. It must be considered that even if XTH enzymes prefer to work on xyloglucan polysaccharides they have the ability to bind to different substrates found in the cell wall. During the transglycosylase activity, the enzyme can cross-link the cleaved xyloglucan to other polysaccharide chains with non-reducing end which can be BBG, cellulose or xylan.

Enzyme kinetic studies were performed for CaXTH2 using TXG-X7 donor-acceptor substrate couple on which the enzyme shows the highest activity in order to understand better the working dynamics and the catalytic activity of the enzyme. Using different concentrations of TXG and X7 substrates enzyme activity reactions were carried out and analyzed by HPLC as were performed before. Maximum velocity ( $V_{max}$ ), Michaelis constant ( $K_m$ ) and turnover number ( $k_{cat}$ ) values of the enzyme were calculated on TXG-X7 substrate couple.  $V_{max}$  is the maximum velocity that the enzyme is saturated by the substrates.  $K_m$  is the substrate concentration when the enzyme achieved the half of the maximum velocity ( $V_{max}$ ). If the  $K_m$  value of the enzyme is high that means the affinity of the enzyme for its substrate is low and in order to achieve  $V_{max}$ , it needs higher substrate concentration.

Table 4.2. Kinetic parameters of CaXTH1, CaXTH2 and CaXTH3 enzymes.

Enzyme	$V_{max}$ ( $\mu\text{M}/\text{min}$ )	$K_m$ ( $\mu\text{M}$ )	$k_{cat}$ ( $\text{min}^{-1}$ )	$k_{cat}/K_m$ ( $\text{min}^{-1}\mu\text{M}^{-1}$ )
CaXTH1	0,014	5,84	2,64	0,452
CaXTH2	0,0063	0,1	3,6	36
CaXTH3	0,046	2,48	41,85	16,88

When the  $K_m$  values were compared, it can be seen that CaXTH2 enzyme had the lowest  $K_m$  value which means CaXTH2 had the highest affinity for the substrate couple that was used. CaXTH3 and then CaXTH1 followed in order. Although the substrate affinity of

CaXTH3 is less than CaXTH2, it has shown the highest turnover rate ( $k_{cat}$ ) that means the number of substrate molecules turned into products per minute was the highest for this enzyme. The highest  $K_m$  value belongs to CaXTH1 enzyme, so it had the lowest affinity for substrate and also the lowest  $k_{cat}$  value. The catalytic efficiency of the enzymes were measured by  $k_{cat}/K_m$  ratio. According to the results, CaXTH2 had the highest ratio which means it demonstrated the best catalytic activity. Catalytic efficiency was followed by CaXTH3 with  $k_{cat}/K_m$  ratio as  $16,88 \text{ min}^{-1}\mu\text{M}^{-1}$ , which was half of CaXTH2 activity. Maximum velocity ( $V_{max}$ ) value was shown to be highest for CaXTH3 enzyme. The lowest catalytic activity was shown for CaXTH1 enzyme as it has the lowest affinity to the substrate couple and the number of substrate molecules that was turned into product is the lowest among others.

Plant growth optimization studies were performed on various pepper seeds from different regions of Turkey to determine the optimal germination and growth conditions for salt stress applications. During the optimization studies, it was observed that the germination rate and the growth ratios of the different varieties were different from each other. Even if the same growth conditions both in laboratory and greenhouse were applied to the same variety, some seeds were not germinated at all while some were germinated. This led to the usage of reduced number of varieties which achieved the best and similar germination rate and growth ratio in optimized conditions for salt stress applications. As soon as the growth conditions were optimized for the plants, grown seedlings of different varieties were exposed to salt stress both in agar and soil. QPCR studies were carried out with the RNA samples of control and stress treated tissues of Cila, Aktör, Seki, Samuray, Çanakkale and Kahramanmaraş varieties.

First salt stress optimization trials were performed with Erzurum variety on agar medium. Germinated seeds were grown in the presence of 0 mM, 50 mM and 100 mM NaCl concentrations and it was observed phenotypically that even 50 mM NaCl inhibited the growth of the seedlings. Second salt stress trials were performed with Erzurum variety, this time with lower NaCl concentrations and up to 20 mM NaCl concentration there were no inhibiting effect on germination or growth of the seedlings. However, a significant decrease on the root lengths of the seedlings were observed when the NaCl concentration increased to 30 mM. As a result of the salt stress optimization experiments, 25 mM NaCl concentration was determined as the starting concentration to see the first effect of NaCl on

plants whereas 50 mM NaCl concentration was determined as the upper limit to observe the inhibition effect of salt. After determining the NaCl concentrations as 25 mM and 50 mM, salt stress trials were performed in MS agar medium with the seedlings of Erzurum variety. The results showed that only after the salt concentration reached to 50 mM NaCl, a drastic drop as 50 percent and 30 percent in root and shoot lengths of the seedlings were observed, respectively.

Further salt stress trials were performed using the seedlings of Cila, Samuray, Aktör and Seki varieties in MS agar medium containing the same salt concentrations (0 mM- 25 mM- 50 mM NaCl). The root- shoot lengths and germination rate of all the stress- treated 11-day-old seedlings were first phenotypically compared and then QPCR was carried out with the cDNAs from the root samples of control and stress- treated Cila, Samuray, Aktör and Seki variety seedlings to observe their *CaXTH2* gene expression.

Phenotypic observation showed that Cila and Samuray varieties demonstrated improved root lengths compared to control group plants at both 25 mM and 50 mM NaCl concentrations. Aktör variety on the other hand, did not show any significant increase in the root lengths until the salt concentration reached 50 mM. Seki variety revealed decreased root lengths as the salt concentration increased but this decrease was not significant until the salt concentration reached 50 mM. Since inhibition of shoot and root lengths is a clear sign of the effects of the stress, it is possible to say that Seki variety showed susceptibility to salt stress conditions more than any other variety included in this study. Root length increase under stress conditions can also indicate that the plant is being affected from stress conditions and trying to cope with it. Abiotic stresses, like cold and salinity will eventually lead to an osmotic stress as they would reduce the amount of water that is available for the plant's use. The increase in root lengths, in the initial stages of salt stress, was considered as a result of pepper plants growing their roots deeper to be able to reach water rich zones. In that case, it can be said that Cila and Samuray varieties started to be affected from stress conditions at a lower salt concentration level compared to Aktör variety. Therefore Aktör variety was phenotypically considered to be the most tolerant variety among all. Shoot lengths of the varieties according to different salt concentrations revealed the same pattern as the root lengths.

When the expression levels of *CaXTH2* gene under salt stress were observed, different expression patterns were found for different varieties. *CaXTH2* gene expression level in

Cila variety showed the highest increase at 25 mM NaCl concentration when the root and shoot lengths were also the longest. While the root- shoot lengths and copy numbers of *CaXTH2* gene decreased simultaneously, when the salt concentration increased from 25 mM to 50 mM, the expression of *CaXTH2* was still upregulated at 50 mM NaCl compared to the control seedlings. The induction level in the copy number of Samuray variety was not as high as it was in Cila variety even if the copy number values of Samuray variety were higher in number. Unlike Cila variety, the copy numbers of the gene in Samuray increased with the increasing salt concentration. However, it was phenotypically observed that the Samuray exhibited shorter root and shoot lengths when the salt concentration was increased to 50 mM, even though the copy number of the gene increased.

The *CaXTH2* gene expression levels for Aktör variety was extreme at 25 mM NaCl and 50 mM NaCl concentrations. Root lengths and the gene copy numbers increased simultaneously with increasing salt concentration while the shoots exhibited almost no difference on their lengths. In Seki variety, inhibited root growth was observed when the salt concentration reached to 50 mM from 25 mM and also shoot lengths had become shorter with the increasing salt concentration. However, the gene expression levels of *CaXTH2* in the root tissues of Seki showed increasing pattern as the salt concentration increased. Upregulation of *CaXTH2* gene did not correlate with any improvement in root growth.

Based on the applied salt concentration and pepper variety, distinct *CaXTH2* gene expression patterns were shown. For all the varieties, increased expression levels of the gene was observed compared to their control groups under increased salt concentrations. The upregulation of the gene and increase in root lengths were observed simultaneously, for Cila, Samuray and Aktör variety. As a response to salt stress, *CaXTH2* gene is upregulating under stress conditions. When the salt concentration was increased to 25 mM, the gene expression for the root tissues of Cila and Aktör increased rapidly together with their root lengths. This might be explained as a fast and early response to salt stress. On the other hand, while the root length of Seki variety decreased drastically when the salt concentration reached to 50 mM NaCl, the gene expression level in the root tissues increased. The reason might be that Seki is starting to show susceptibility causing general inhibition of the metabolism and Capsicum genes are not enough to provide tolerance or response mechanism. Maybe these genes are co-expressed with other genes that take role

in stress response mechanisms therefore *CaXTH* genes only are not enough to create a response or tolerance but they are involved in a more complex mechanism. All those results one again demonstrated that XTH enzymes have role in cell elongation by being responsible both for loosening and strengthening processes in the cell wall. The ability of cross-linking different cell-wall polysaccharides might increase the rigidity of the wall which helps to give resistance to the plant under stress conditions. Since stress tolerance is a very complex mechanism and different varieties have different genetic patterns, it is not easy to create correlation between the gene expression levels and the phenotypic features of the varieties.

Salt stress studies were also performed with Çanakkale and Kahramanmaraş varieties which were older grown in soil-peat mixture in the greenhouse. This time salt stress treatment method was soaking the roots of 6-week-old plants into 200 mM NaCl containing solution at different time intervals; 0 minutes as control, 10 minutes, 30 minutes and 120 minutes. Before the salt soaking method was applied, the roots were taken out of the soil-peat mixture and cleaned with water and also phenotypically observed after salt treatment. Since those processes might create additional stress on the plants, phenotypic observations were kept as short as possible. After the plants were treated with salt stress, both root and leaf tissue samples were collected. QPCR was carried out with the cDNAs of collected root and leaf samples. There were no significant phenotypic changes for both varieties. Although some phenotypic changes such as withering was observed as the soaking time was increased, both plant varieties were looking healthy. For Çanakkale variety, *CaXTH2* expression levels at 10 minutes of soaking were upregulated both in root and leaf tissues. For Kahramanmaraş variety, it was observed that copy numbers of *CaXTH2* gene in both tissues decreased with the increasing soaking time to 200 mM NaCl. Although, the gene was upregulated only in the root tissues after 10 minutes of soaking, the gene copy numbers continued to decrease when the soaking time was increased to 30 minutes or 120 minutes in both tissues. While Çanakkale variety showed increased gene expression pattern at initial stress conditions, Kahramanmaraş variety showed decreased gene expression pattern. It might be explained as Çanakkale variety give faster response to salt stress than Kahramanmaraş variety. As the salt stress exposure time increased, decreased gene expression levels might be the sign of the metabolic inhibition of the plants. In order to be adapted to the stress conditions, plants might be closing their stomata

to prevent the loss of water or they might be increasing the cross-linking ability of cell wall modifying enzymes to strengthening the cell wall for resistance to stress conditions. Based on the previous findings of another study group, Kahramanmaraş was considered to be a stress susceptible variety [59]. According to the phenotypic results of both varieties after 120 minutes soaking, Kahramanmaraş plants looked like their leaves were more withered compared to Çanakkale plants, meaning that it was late for a response to the stress. This result supported the idea that Kahramanmaraş variety being more susceptible to stress than Çanakkale variety. The copy numbers of the *CaXTH2* gene in both non-stressed tissues of Kahramanmaraş variety were extremely higher than the copy numbers in non-stressed tissues of Çanakkale variety. This supported the idea that less tolerant plants store more of the *XTH* genes as a precaution since they do not have rapid stress response mechanism.

## 5. CONCLUSION

Large *XTH* gene families that are found in all land plants each gene encodes a cell wall enzyme, catalyzing the cell wall polysaccharides such as xyloglucan. Assuming that one enzyme works on one type of xyloglucan substrate in the cell wall, the existence of different types of xyloglucan structures create the need for different varieties of *XTH* genes. *XTH* gene family members have different abilities with different promoters and important roles which are not yet enlightened completely such as tissue specific regulations, hormonal, and stress control in plants. In order to get more insights about how those genes function, characterization of a *XTH* enzyme within pepper plants and *XTH* gene expression levels under abiotic stress conditions was investigated in this study. One of the Capsicum endotransglycosylase/hydrolase enzyme, CaXTH2, was produced heterologously in *Pichia pastoris* and the purified enzyme was characterized by using different polysaccharides as the representatives of the cell wall substrates. Also, *CaXTH2* gene expression on different pepper varieties under salt stress was examined.

The CaXTH2 enzyme showed its highest activity when xyloglucan polysaccharide and oligosaccharide were used as donor and acceptor substrates since capsicum enzymes have specific substrate preferences. Also, heterotransglycosylase enzyme activity which was less than 1 percent of the activity level with TXG-XGO substrates was detected when XT and CT were used as acceptor oligosaccharides. An adequate amount of enzyme activity which was around 0,5 percent of the activity level of TXG-XGO substrates was observed when HEC was used as donor polysaccharide with xyloglucan oligosaccharides XGO and X7. Accordingly, the enzyme activity results bring to mind that CaXTH2 enzyme is highly specific to xyloglucan but also it has heterotransglycosylation activity which is much reduced. The efficiency of the enzyme activity on different cell wall polysaccharides also depends on the availability of sugars in the cell wall. The distinct preference of CaXTH2 for X7 over XGO/galactosylated acceptor molecules is a new finding. It opens up new possibilities for studying different xyloglucan substitution patterns in addition to studies on substrate binding, particularly in the '+'-subsite binding region.

Since the ability of the *XTH* enzyme to cross-link different carbohydrate molecules in the wall might be correlated with the other roles of the enzyme in stress response, the

expression levels of *XTH* genes under salt stress was investigated in this study. *CaXTH2* gene expression studies has shown that the level of expression is more in susceptible plants without any stress conditions but also the gene is upregulated as a fast and early response in plants that are tolerant under salt stress. The upregulation of *CaXTH2* gene did not mean stress response all the time for all varieties unless they have available polysaccharides that the enzyme works on. This enzyme might make cross-linkage between other cell wall polysaccharides and strengthen the wall which makes it more tolerant to stress. Since stress response and tolerance mechanisms are very complex, the results of this study are not enough to interpret whether the XTH enzymes in pepper have influence in stress tolerance and that they are part of an even more complex mechanism.

In future studies, the role of XTH enzymes in other plant species and the expression of those genes in different tissues of variable plants under abiotic stress conditions should be examined to better understand their working mechanism under stress. Also, molecular docking/modelling and protein structure crystallization processes can be studied to gain more information about the enzyme- substrate interactions and the structure itself.



## REFERENCES

1. Zhigila DA, AbdulRahaman AA, Kolawole OS, Oladele FA. Fruit morphology as taxonomic features in five varieties of *Capsicum Annuum* L. Solanaceae. *Journal of Botany*. 2014;1-6.
2. Silva LR, Azevedo J, Pereira MJ, Valentao P, Andrade PB. Chemical assessment and antioxidant capacity of pepper (*Capsicum annuum* L.) seeds. *Food Chem Toxicology*. 2013;53:240-248.
3. Barceloux DG. Pepper and capsaicin (*Capsicum* and piper species). *Disease-a-Month*. 2009;55(6):380-390.
4. Chillies and Peppers (Green) Harvested Area [cited 2016 9 November]. Available from: <http://chartsbin.com/view/41158>.
5. Loizzo MR, Pugliese A, Bonesi M, Menichini F, Tundis R. Evaluation of chemical profile and antioxidant activity of twenty cultivars from *Capsicum annuum*, *Capsicum Baccatum*, *Capsicum Chacoense* and *Capsicum Chinense*: A comparison between fresh and processed peppers. *LWT - Food Science and Technology*. 2015;64(2):623-631.
6. Kothari SL, Joshi A, Kachhwaha S, Ochoa-Alejo N. Chilli peppers--A review on tissue culture and transgenesis. *Biotechnology Advances*. 2010;28(1):35-48.
7. Livingstone KD, Lackney VK, Blauth JR, van Wijk R, Jahn MK. Genome mapping in *Capsicum* and the evolution of genome structure in the Solanaceae. *Genetics*. 1999;152(3):1183-1202.
8. Choi JY, Seo YS, Kim SJ, Kim WT, Shin JS. Constitutive expression of CaXTH3, a hot pepper xyloglucan endotransglucosylase/hydrolase, enhanced tolerance to salt and drought stresses without phenotypic defects in tomato plants (*Solanum Lycopersicum* Cv. Dotaerang). *Plant Cell Reports*. 2011;30(5):867-877.

9. Zhou Y, Shao HB. The responding relationship between plants and environment is the essential principle for agricultural sustainable development on the globe. *Comptes Rendus Biologies*. 2008;331(4):321-328.
10. Kosova K, Vitamvas P, Prasil IT, Renaut J. Plant proteome changes under abiotic stress--Contribution of proteomics studies to understanding plant stress response. *Journal of Proteomics*. 2011; 74(8):1301-1322.
11. Roy SJ, Tucker EJ, Tester M. Genetic analysis of abiotic stress tolerance in crops. *Current Opinion in Plant Biology*. 2011;14(3):232-239.
12. Sasidharan R, Voesenek LACJ, Pierik R. Cell wall modifying proteins mediate plant acclimatization to biotic and abiotic stresses. *Critical Reviews in Plant Sciences*. 2011;30(6):548-562.
13. Cho SK, Kim JE, Park JA, Eom TJ, Kim WT. Constitutive expression of abiotic stress-inducible hot pepper CaXTH3, which encodes a xyloglucan endotransglucosylase/hydrolase homolog, improves drought and salt tolerance in transgenic Arabidopsis plants. *FEBS Letters*. 2006;580(13):3136-3144.
14. Cosgrove DJ. Growth of the plant cell wall. *Nature Reviews Molecular Cell Biology*. 2005;6(11): 850.
15. Reiter WD. Biosynthesis and properties of the plant cell wall. *Current Opinion in Plant Biology*. 2002;5(6):536-542.
16. Keegstra K. Plant cell walls. *Plant Physiology*. 2010;154(2):483-486.
17. Somerville C, Bauer S, Brininstool G, Facette M, Hamann T, Milne J, Osborne E, Paredez A, Persson S, Raab T, Vorwerk S, Youngs H. Toward a systems approach to understanding plant cell walls. *Science*. 2004;306(1):2206-2211.
18. Yokoyama R, Nishitani K. Genomic basis for cell- wall diversity in plants. A comparative approach to gene families in rice and Arabidopsis. *Plant and Cell Physiology*. 2004;45(9):1111-1121.
19. Reid JG. Cementing the wall: Cell wall polysaccharide synthesizing enzymes. *Current Opinion in Plant Biology*. 2000;3(6):512-516.

20. Pauly M, Keegstra K. Biosynthesis of the plant cell wall matrix polysaccharide xyloglucan. *Annual Review of Plant Biology*. 2016;67:235-259.
21. Lerouxel O, Cavalier DM, Liepman AH, Keegstra K. Biosynthesis of plant cell wall polysaccharides – A complex process. *Current Opinion in Plant Biology*. 2006;9(6):621-630.
22. Brown Jr RM, Saxena IM, Kudlicka K. Cellulose biosynthesis in higher plants. *Trends in Plant Science*. 1996;1(5):149-156.
23. Carpita NC, Gibeaut DM. Structural models of primary cell walls in flowering plants: Consistency of molecular structure with the physical properties of the walls during growth. *Plant Journals*. 1993;3(1):1-30.
24. Levy I, Shani Z, Shoseyov O. Modification of polysaccharides and plant cell wall by endo-1,4-beta-glucanase and cellulose-binding domains. *Biomolecular Engineering*. 2002;19(1):17-30.
25. Yapo BM. Pectic Substances: From simple pectic polysaccharides to complex pectins- A new hypothetical model. *Carbohydrate Polymers*. 2011;86(2):373-385.
26. Mohnen D. Pectin structure and biosynthesis. *Current Opinions in Plant Biology*. 2008;11(3):266-277.
27. Pauly M, Gille S, Liu L, Mansoori N, de Souza A, Schultink A, Xiong G. Hemicellulose biosynthesis. *Planta*, 2013;238(4):627-642.
28. Dhugga KS. Biosynthesis of non-cellulosic polysaccharides of plant cell walls. *Phytochemistry*. 2012;74:8-19.
29. Van Zyl WH, Rose SH, Trollope K, Görgens JF. Fungal  $\beta$ -mannanases: Mannan hydrolysis, heterologous production and biotechnological applications. *Process Biochemistry*. 2010;45(8):1203-1213.
30. Lazaridou A, Biliaderis C. Molecular Aspects of Cereal  $\beta$ -glucan functionality: physical properties, technological applications and physiological effects. *Journal of Cereal Science*. 2007;46(2):101-118.

31. Fincher GB. Revolutionary times in our understanding of cell wall biosynthesis and remodeling in the grasses. *Plant Physiology*. 2009;149(1):27-37.
32. Lima DU, Loh W, Buckeridge MS. Xyloglucan-cellulose interaction depends on the sidechains and molecular weight of xyloglucan. *Plant Physiology and Biochemistry*, 2004;42(5): 389-394.
33. Frankova L, Fry SC. Trans- $\alpha$ -xylosidase, a widespread enzyme activity in plants, introduce (1 $\rightarrow$ 4)- $\alpha$ -D-xylobiose side-chains into xyloglucan structures. *Phytochemistry*. 2012;78(1):29-43.
34. Hoffman M, Jia Z, Peña MJ, Cash M, Harper A, Blackburn AR, Darvill A, York WS. Structural analysis of xyloglucans in the primary cell walls of plants in the subclass Asteridae. *Carbohydrate Research*. 2005;340(11):1826-1840.
35. Tuomivaara ST, Yaoi K, O'Neill MA, York WS. Generation and structural validation of a library of diverse xyloglucan-derived oligosaccharides, including an update on xyloglucan nomenclature. *Carbohydrate Research*. 2015;402:56-66.
36. Davis J, Brandizzi F, Liepman AH, Keegstra K. Arabidopsis mannan synthase CSLA9 and glucan synthase CSLC4 have opposite orientations in the golgi membrane. *The Plant Journal*. 2010;64(6):1028-1037.
37. Liu YB, Lu SM, Zhang JF, Liu S, Lu YT. A Xyloglucan endotransglucosylase/hydrolase involves in growth of primary root and alters the deposition of cellulose in Arabidopsis. *Planta*. 2007;226(6):1547-1560.
38. Nishitani K. Division of roles among members of the *XTH* gene family in plants. *Plant Biosystems*. 2005;139(1):98 – 101.
39. Rose JK, Braam J, Fry SC, Nishitani K. The XTH family of enzymes involved in xyloglucan endotransglucosylation and endohydrolysis: Current perspectives and a new unifying nomenclature. *Plant Cell Physiology*. 2002;43(12):1421-1435.
40. Eklöf JM, Brumer H. The *XTH* Gene Family: An update on enzyme structure, function, and phylogeny in xyloglucan remodeling. *Plant Physiology*. 2010;153(2):456-466.

41. Maris A, Kaewthai N, Eklöf JM, Miller JG, Brumer H, Fry SC, Verbelen J, Vissenberg K. Differences in enzymic properties of five recombinant xyloglucan endotransglycosylase/hydrolase (XTH) proteins of *Arabidopsis thaliana*. *Journal of Experimental Botany*. 2010;62(1):261-271.
42. Vaaje-Kolstad G, Farkas V, Hrmova M, Fincher GB. Xyloglucan xyloglucosyl transferases from barley (*Hordeum vulgare* L.) bind oligomeric and polymeric xyloglucan molecules in their acceptor binding sites. *Biochimica et Biophysica Acta*. 2010;1800(7):674-684.
43. Takeda T, Furuta Y, Awano T, Mizuno K, Mitsuishi Y, Hayashi T. Suppression and acceleration of cell elongation by integration of xyloglucans in pea stem segments. *Proceedings of the National Academy of Sciences*. 2002;99(13):9055-9060.
44. Nishitani K, Tominaga R. Endo-xyloglucan transferase, a novel class of glycosyltransferase that catalyzes transfer of a segment of xyloglucan molecule to another xyloglucan molecule. *The Journal of Biological Chemistry*. 1992;267(29):21058-21064.
45. Cantarel BL, Coutinho PM, Rancurel C, Bernard T, Lombard V, Henrissat B. The carbohydrate-active enzymes database (CAZy): An expert resource for glycogenomics. *Nucleic Acids Research*. 2009;37(database):233-238.
46. Eklof JM, Shojania S, Okon M, McIntosh LP, Brumer H. Structure-function analysis of a broad specificity *Populus trichocarpa* endo-beta-glucanase reveals an evolutionary link between bacterial licheninases and plant XTH gene products. *Journal of Biological Chemistry*. 2013;288(22):15786-15799.
47. Kaewthai N, Harvey AJ, Hrmova M, Brumer H, Ezcurra I, Teeri TT, Fincher GB. Heterologous expression of diverse barley XTH genes in the yeast *Pichia pastoris*. *Plant Biotechnology*. 2010;27(3):251-258.
48. Potvin G, Ahmad A, Zhang Z. Bioprocess engineering aspects of heterologous protein production in *Pichia pastoris*: A review. *Biochemical Engineering Journal*. 2012;64:91-105.

49. Cereghino GP, Cereghino JL, Ilgen C, Cregg JM. Production of recombinant proteins in fermenter cultures of the yeast *Pichia pastoris*. *Current Opinions in Biotechnology*. 2002;13(4):329-332.
50. Daly R, Hearn MTW. Expression of heterologous proteins in *Pichia pastoris*: A useful experimental tool in protein engineering and production. *Journal of Molecular Recognition*. 2005;18(2):119-138.
51. Wang Y, Wang Z, Xu Q, Du G, Hua Z, Liu L, Li J, Chen J. Lowering induction temperature for enhanced production of polygalacturonate lyase in recombinant *Pichia pastoris*. *Process Biochemistry*. 2009;44(9):949-954.
52. Fregel R, Rodriguez V, Cabrera VM. Microwave improved *Escherichia coli* transformation. *Letters in Applied Microbiology*. 2008;46(4):498-499.
53. Li X, Sui X, Zhang Y, Sun Y, Zhao Y, Zhai Y, Wang Q. An improved calcium chloride method preparation and transformation of competent cells. *African Journal of Biotechnology*. 2010;9(50):8549-8554.
54. Lin-Cereghino J, Wong WW, Xiong S, Giang W, Luong LT, Vu J, Johnson SD, Lin-Cereghino GP. Condensed protocol for competent cell preparation and transformation of the methylotrophic yeast *Pichia pastoris*. *Biotechniques*. 2005;38(1):44, 46, 48.
55. Park J-A, Cho SK, Kim JE, Chung HS, Hong J-P, Hwang B, Hong CB, Kim WT. Isolation of cDNAs differentially expressed in response to drought stress and characterization of the *Ca-Lea11* gene encoding a new family of atypical LEA-like protein homologue in hot pepper (*Capsicum Annuum* L. cv. Pukang). *Plant Science*. 2003;165(3):471-481.
56. Burton RA, Shirley NJ, King BJ, Harvey AJ, Fincher GB. The *CesA* gene family of barley. Quantitative analysis of transcripts reveals two groups of co-expressed genes. *Plant Physiology*. 2004;134(1):224-236.
57. Tuomivaara ST, Yaoi K, O'Neill MA, York WS. Generation and structural validation of a library of diverse xyloglucan-derived oligosaccharides, including an update on xyloglucan nomenclature. *Carbohydrate Research*. 2015;402:56-66.

58. Marry M, Cavalier DM, Schnurr JK, Netland J, Yang Z, Pezeshk V, York WS, Pauly M, White AR. Structural characterization of chemically and enzymatically derived standard oligosaccharides isolated from partially purified tamarind xyloglucan. *Carbohydrate Polymers*. 2003;51(3):347-356.
59. Esra K, İşlek C, Üstün AS. Effect of Cold on Protein, Proline, Phenolic Compounds and Chlorophyll Content of Two Pepper (*Capsicum Annuum* L.) Varieties. *Gazi University Journal of Science*. 2010;23(1):1-6.

